Characterization of the role of alpha-arylphorin in the *Heliothis virescens* midgut response to Cry1Ac toxin from *Bacillus thuringiensis*

A Dissertation Presented for the

Doctor of Philosophy

Degree

The University of Tennessee, Knoxville

Jerreme Jamael Jackson

May 2015

Copyright © 2015 by

Jerreme Jamael Jackson and Juan Luis Jurat-Fuentes

All rights reserved.

Acknowledgements

The completion of this dissertation would not have been possible, had it not been for the contributions of numerous people, some of which I'd like to mention here.

First, I would like to thank my major professor, Juan Luis Jurat-Fuentes, a passionate entomologist, gifted teacher, and exceptional person. Without having any prior experience working with insects, Juan accepted me into his laboratory at the end of my first year of graduate school, taught me important principals of insect physiology, and equipped me with the technical training necessary to begin exploring the intricacies of my project. He balanced open recognition of my maturation as a scientist with experimental challenges and always encouraged me to strive for excellence. My experiences in the Jurat-Fuentes lab have been, fun, intellectually stimulating, and given me the enthusiasm to pursue a career in academic research.

I would also like to thank my committee members, Drs. Albrecht von Arnim, Ranjan Ganguly, and Debra Miller, for all of the guidance and insight you provided during the course of my research. Each of you always seemed to be in your office when I showed up unexpectedly with questions. I am appreciative of the financial support that Dr. von Arnim and the Genome Science and Technology (GST) graduate program provided during my studies, particularly for my first overseas trip to Trabzon, Turkey to present my research at the Society of Invertebrate Pathology. This opportunity and others that followed allowed me to network with aspiring and prominent scientists from all over the world. To Dr. Ganguly, thank you for helping me identify my own strengths. Often times, doctoral students lose sight of their own incremental improvements while in pursuit of the degree. You reminded me to occasionally look in the rear view mirror. To Dr. Debra Miller, thank you for the countless hours you spent sitting with me at the teaching microscope. I have a heightened appreciation for pathology and the power of immunohistochemistry. Your knowledge of and ability to teach all aspects of intestinal

physiology helped me piece together a compelling story. A special thanks also goes out to Dr. Omaththage Perera for the work you performed on sequencing the custom transcriptome of the tobacco budworm, which I relied upon heavily throughout my research, as well as advising me on how to perform gene expression analysis.

To Dr. Cynthia Peterson (now at LSU) and Dr. Sekeenia Haynes, I would like to say thanks for providing me with the opportunity to participate in PEER (Program for Equity and Excellence in Research). It goes without saying that PEER activities have contributed tremendously to my professional development outside of the laboratory. To Dr. John Koontz, it has been a great pleasure getting to know you and my only wish would be that other students (especially those who see you at TRecs) would get to know you as well. You're a brilliant biochemistry teacher who cares deeply for his students. To the Jurat-Fuentes laboratory members, past and present, it has been a blast working and learning with each of you along the way. I wish you all continued success in your research projects as well as in whatever endeavors you choose to undertake in the future. I would also like to thank close friends Dr. Dan Close, Dr. Migun Shakya, Myles Baker and Bryan Norrod, who each helped me balance the challenges of graduate school at various times.

I owe my parents, Marvin and Joyce Reese, a tremendous amount of gratitude, because they've always encouraged me to set high expectations and commit to meeting them. I would've never made it this far if you hadn't instilled in me the belief that I was capable of accomplishing great things. I cannot thank you enough for all that you have done for me, but just know that the impacts of your support are immeasurable.

Lastly, I want to thank my wife Amanda for exhibiting great patience and understanding of the challenges facing me since day 1. Your unwavering support and unconditional love played an integral part in getting me to this point. Thanks for believing in me.

Abstract

Homeostasis of the intestinal epithelium in *Heliothis virescens* is mediated by the proliferation and differentiation of multipotent intestinal stem cells (ISCs) that lie quiescent and adjacent to the basal lamina. In response to extrinsic and intrinsic signals received during larval development, ISC proliferation and differentiation promotes epithelial growth and expansion or regeneration following enterocyte damage and expulsion into the lumen. We tested the *in vivo* mitogen effects of purified α [alpha]-arylphorin on the *H. virescens* intestinal epithelium and observed dose-dependent ISC proliferation resulting in distinct morphological changes. To follow up, we assayed how these changes affected the intestinal epithelium response to Cry1Ac toxin from *Bacillus thuringiensis*. Histological examination of intestinal tissues prepared from Cry1Ac exposed larvae and *in vitro* binding experiments supported two distinct mechanisms whereby ingestion of α-arylphorin reduced Cry1Ac toxicity in *H. virescens* larvae.

To characterize the role of alkaline phosphatase as a Cry toxin receptor in the *H. virescens* larval midgut, we used mechanistically distinct double-stranded RNA (dsRNA) delivery strategies to activate RNA-interference (RNAi) machinery and induce transient silencing of midgut alkaline phosphatase (HvmALP) prior to exposing larvae to Cry1Ac toxin. Quantitative and qualitative analyses of gene and protein expression supported that hemocoelic microinjections resulted in the largest reduction in HvmALP protein expression and, furthermore, that bypassing physiological barriers such as the intestinal epithelium may enhance the efficiency of target gene silencing.

Table of contents

Introduction 1

Chapter 1 A review on the regulation of midgut stem cell behavior in insects 3

Abstract 5

1.1 Introduction 5

1.2 Factors regulating midgut stem cell proliferation 9

1.2.1 Mitogens identified in *Drosophila* 9

1.2.2 Ecdysone and 20-Hydroxyecdysone 11

1.2.3 Alpha-arylphorin (α-Arylphorin) 13

1.2.4 Insulin-like peptides 15

1.2.5 Midgut peptides 16

1.2.6 Calcium (Ca^{2+}) 16

1.2.7 Platelet-derived growth factor 17

1.2.8 Albumax II 17

1.3 Regulation of midgut stem cell proliferation 18

1.4 Factors regulating midgut stem cell differentiation 20

1.4.1 Midgut Differentiation Factor 1 (MDF-1) 20

1.4.2 Midgut Differentiation Factor 2 (MDF-2) 22

1.4.3 Midgut Differentiation Factors 3 and 4 (MDF-3 and -4) 23

1.4.4 Ecdysone and 20-Hydroxyecdysone 23

1.4.5 Perlecan 24

1.4.6 Integrin β1-like protein 24

1.5 Regulation of midgut stem cell differentiation 25

1.6 Midgut response to pathogens 27

1.7 Conclusions 30

Appendix....33

Chapter 2 Mitogenic α-arylphorin in circulating hemolymph activates intestinal stem cell proliferation....34

Abstract....36

2.1 Introduction....36

2.2 Materials and methods....39

2.2.1 Insects....39

2.2.2 Purification and proteomic analysis of α-arylphorin....39

2.2.3 Sequence analysis....40

2.2.4 Electrophoresis and Western blotting....41

2.2.5 Preparation of primary midgut cell cultures....41

2.2.6 *In vitro* cell proliferation assays....42

2.2.7 Arylphorin feeding bioassay....43

2.2.8 EdU incorporation and preparation of histological midgut sections....43

2.2.9 Preparation of *H. virescens* midgut cDNA....44

2.2.10 Cloning of *H. virescens* arylphorin....45

2.2.11 dsRNA preparation and RNA interference (RNAi)....45

2.2.12 Real-time quantitative PCR (RT-qPCR)....47

2.3 Results....48

2.3.1 α-Arylphorin circulation in hemolymph of *H. virescens* larvae....48

2.3.2 Identification of proteins partially purified from *H. virescens* hemolymph....49

2.3.3 α-Arylphorin bioactivity on *H. virescens* primary intestinal stem cell cultures....50

2.3.4 α-Arylphorin induces dose-dependent midgut stem cell proliferation *in vivo*....50

2.3.5 Identification of α-arylphorin expressed in the *H. virescens* midgut....51

2.3.6 Developmental effects of α-arylphorin silencing on *H. virescens* larvae....51

2.4 Discussion....52
Appendix....59
Chapter 3 Dose-dependent mitogenic effect of arylphorin during midgut healing in response to Cry1Ac intoxication in *Heliothis virescens* larvae....72
Abstract....74
3.1 Introduction....74
3.2 Materials and methods....77
3.2.1 Insects....77
3.2.2 Purification and proteomic analysis of α-arylphorin....77
3.2.3 α-Arylphorin feeding bioassays....78
3.2.4 Preparation of histological midgut sections....78
3.2.5 Bacterial toxin purification and labeling of Cry1Ac and arylphorin....80
3.2.6 Electrophoresis, ligand, and lectin blotting of BBMV and α-arylphorin....80
3.2.7 Preparation of brush border membrane vesicles (BBMV)....82
3.2.8 Cry1Ac competition binding assays....82
3.2.9 Digestion of α-arylphorin with peptide-N-glycosidase F....83
3.2.10 Preparation of double stranded RNA (dsRNA)....84
3.2.11 Silencing of α-arylphorin expression by RNA interference (RNAi)....85
3.2.12 Real-time quantitative PCR (RTqPCR)....85
3.3 Results....86
3.3.1 Ingesting α-arylphorin reduces *H. virescens* mortality upon exposure to Cry1Ac....86
3.3.2 Histopathology of Cry1Ac intoxication in *H. virescens* larvae fed α-arylphorin....87
3.3.3 Cry1Ac binds specifically to α-arylphorin purified from *H. virescens* hemolymph....88
3.3.4 Cry1Ac recognizes an N-linked glycan moiety in *H. virescens* α-arylphorin....89

3.4 Discussion....90

Appendix....94

Conclusions and outlook 101

List of references....104

Appendix 1 Development of an RNA interference protocol for silencing gene expression in *Heliothis virescens* 120

Abstract....121

A1.1 Introduction....122

A1.2 Materials and methods....123

A1.2.1 Insects 123

A1.2.2 Bacterial toxin purification 123

A1.2.3 Preparation of double stranded RNA (dsRNA) 124

A1.2.4 RNA interference (RNAi) of alkaline phosphatase (HvmALP)....125

A1.2.5 Preparation of midgut total RNA (tRNA) and protein 125

A1.2.6 Preparation of brush border membrane vesicles (BBMV)....126

A1.2.7 Electrophoresis and Western blotting....126

A1.2.8 Real-time quantitative PCR (RTqPCR)....127

A1.3 Results 128

A1.3.1 RNAi reduces HvmALP expression in *H. virescens* larvae but not Cry1Ac toxicity 128

A1.3.2 Quantification of mALP expression in *H. virescens* 129

A1.3.3 Microinjection of dsALP reduces mALP expression in *H. virescens* 129

A1.3.4 Discussion 130

Appendix: tables and figures....133

Vita....139

List of tables

Table 1: Proteins identified in partially purified α-arylphorin (fraction pool F3).....60

Table 2: Primers used for cloning α-arylphorin, *in vitro* synthesis of dsArylphorin, and RT-qPCR 71

Table 3: Primers used for *in vitro* synthesis of dsArylphorin and RT-qPCR 100

Table 4: Primers used for *in vitro* synthesis of dsALP and RT-qPCR 133

List of figures

Figure 1: Integrative model for stem cell proliferation and differentiation in the insect midgut epithelium.....33

Figure 2: Identification of α-arylphorin-induced proliferation of *H. virescens* midgut stem cell cultures using light microscopy 59

Figure 3: Protein sequence alignment of arylphorins from *H. virescens* larvae.....61

Figure 4: A phylogenetic tree generated by MEGA alignment of hexamerin amino acid sequences.....62

Figure 5: Bioactivity of purified α-arylphorin on primary midgut stem cell cultures from *H. virescens* larvae 64

Figure 6: Purified α-arylphorin induces dose-dependent ISC proliferation *in vivo* in *H. virescens* larvae 66

Figure 7: Amplification of full-length α-arylphorin cDNA from *H. virescens* midgut tissue 70

Figure 8: Ingestion of purified α-arylphorin induces dose-dependent reductions in mortality of *H. virescens* larvae exposed to Cry1Ac toxin 94

Figure 9: Morphological response of *H. virescens* midgut epithelium to Cry1Ac exposure following the ingestion of different α-arylphorin titers.....95

Figure 10: Binding of Cry1Ac and α-arylphorin to *H. virescens* BBMV 96

Figure 11: α-Arylphorin reduces Cry1Ac binding to *H. virescens* BBMV.....98

Figure 12: Testing N-linked oligosaccharides on *H. virescens* α-arylphorin and their role in Cry1Ac binding 99

Figure 13: Analysis of dsALP effects on silencing expression of *H. virescens* mALP 134

Figure 14: Testing the effects of dsALP and dsArylphorin on Cry1Ac toxicity in *H. virescens*..135

Figure 15: Analysis of dsALP effects on silencing expression of *H. virescens* mALP 137

Figure 16: Microinjection of dsALP causes reduction in mALP expression in *H. virescens*.....138

Introduction

The gram-positive bacterium *Bacillus thuringiensis* (Bt) produces Cry (from crystal) toxins that are used to provide species-specific and environmentally safe protection against agriculturally important insect pests. While tremendous efforts have gone forth to characterize the Bt mode of action, there are unique epithelial regenerative mechanisms elicited by Cry toxins in target insects that need to be investigated. The intestinal epithelium of insects is a highly dynamic tissue that responds to nutritional, environmental, and physiological stimuli, such as pore formation caused by insertion of Cry toxin oligomers into the intestinal epithelium. Upon this loss of epithelial integrity in the *Heliothis virescens* (tobacco budworm) intestinal epithelium, a healing response mediated by the proliferation and differentiation of multipotent stem cells is activated to replace those mature cells, which have incurred damaged. While this healing mechanism has been recognized, the roles of biochemical mediators in this regenerative healing mechanism are poorly understood. In this research, we developed a feeding protocol that allowed us to probe the developmental contributions of a hexameric growth factor, α-arylphorin, in the *H. virescens* intestinal epithelium. Immunohistochemical and histopathological approaches were used to examine the cell-specific effects and morphological changes associated with α-arylphorin ingestion and how these changes affected a subsequent exposure to Cry1Ac. Ingestion of α-arylphorin induced dose-dependent intestinal stem cell proliferation, enabling the intestinal epithelium to be repaired when insects were exposed to Cry1Ac and reducing larval toxicity. Unexpectedly, this phenomena disappeared with the highest α-arylphorin concentration tested and was replaced by a novel tolerance mechanism involving sequestration of Cry1Ac in the lumen by α-arylphorin, thus reducing the toxin binding to receptors along the brush border membrane. We characterized the glycosylation of α-arylphorin using lectin binding experiments and determined that the Cry1Ac binding specificity we observed was mediated by binding to N-linked N-acetylgalactosamine (GalNAc) residues.

These data support that α-arylphorin participates in the Cry toxin mode of action and may be involved in reduced susceptibility in some insects. Our work contributes to the growing body of evidence suggesting that the host proteins involved in the Cry intoxication process are not confined to proteins in the intestinal epithelium.

Chapter 1

A review on the regulation of midgut stem cell behavior in insects

This chapter to be submitted to Insect Biochemistry and Molecular Biology

Jackson, J. and J.L. Jurat-Fuentes. (2015). A review on the regulation of midgut stem cell behavior in insects

.

My contributions included: (1) data collection and analysis, (2) writing the manuscript and making figures. Juan Luis Jurat-Fuentes assisted with (2) and to a lesser degree (1).

Abstract

The intestinal epithelium of insects is maintained through the proliferation and differentiation of multipotent stem cells. While most of the available information originates from studies performed in *Drosophila melanogaster*, significant efforts have also been devoted to study this regenerative mechanism in lepidopteran larvae. In Lepidoptera, stem cell activity achieves an impressive 200-fold increase in the gut surface area during larval development. The observed growth is a result of both the proliferation and differentiation of stem cells lying on top of the basolateral membrane and wedged between mature columnar and goblet cells. During molting, increasing ecdysteroid titers in circulating hemolymph induce stem cells to rapidly proliferate and differentiate into new columnar and goblet cells. This promotes the continued growth and expansion of the midgut, which will need to accommodate the nutritional demands of a larger insect in the next instar. In this chapter, available information on the factors that regulate proliferation and differentiation of insect gut stem cells will be discussed. Our aim is to distinguish the factors primarily responsible for inducing proliferation (mitogens) from those that are involved in the control of differentiation leading to mature epithelial cells (cell fate). We also discuss the role that stem cells play in mediating the response to acute midgut epithelium injury. We aim to provide a comprehensive analysis of available data on regulation of midgut stem cell behavior during development and following injury in multiple insect models.

1.1 Introduction

The digestive epithelium is one of the tissues with the fastest turnover rates due to continuous stress by abrasion, microbes, and toxic compounds. In all insects where it has been studied, this high regeneration rate is supported by proliferation and differentiation of stem cells (Rost 2006). The midgut of lepidopteran larvae is composed of a pseudo-stratified epithelium, with the apical cell surface facing the midgut lumen and the basal membrane lying adjacent to

the hemocoel (Chapman 1982; Wigglesworth 1939). Tall cuboidal columnar cells, lined with glycocalyx-coated microvilli along the apical surface (Chapman 1982), are the most abundant cell type within the midgut (Chapman 1982; Wigglesworth 1939). The extensive network of rough endoplasmic reticulum and nearby ribosomes specializes them to perform both the synthesis and secretion of digestive enzymes and the absorption of nutrients (Chapman 1982). The basolateral membrane of enterocytes generates tightly apposed infoldings which separate following a meal, increasing direct contact and transport of water and ions to the hemolymph (Lehane and Billingsley 1996). Goblet cells form the second most abundant mature midgut cell type, and are surrounded by four to six columnar cells (Hakim et al. 1988). Goblet cells are characterized by the presence of a deep invagination of the apical membrane, creating a cavity that encloses some of the extracellular luminal space while remaining contiguous with the midgut lumen through a narrow valve-like structure created by apposing microvilli (Chapman 1982; Hakim, Baldwin et al. 1988; Wigglesworth 1939). Microvilli in the basal region of the goblet cavity are rich in mitochondria and vacuolar-type proton ATPase (V-ATPase) enzymes that pump intracellular H^+ to the lumen, as well as K^+/nH^+ antiporters. The combined activity of these transporters establishes a high transepithelial electrical and pH gradient between the lumen and the cytoplasm of mature cells (Chao et al. 1990; Dow and Harvey 1988; Wieczorek et al. 1989). This gradient is then used by K^+/amino acid symporters on the microvilli of columnar cells to absorb amino acids into the cell cytoplasm (Hanozet et al. 1980).

Endocrine cells are generally found adjacent to the basolateral membrane and can take on various shapes, causing them to remain inconspicuous in histological preparations of midgut tissues (Baldwin and Hakim 1991). In contrast to mature columnar and goblet cells, the basolateral membranes of endocrine cells do not exhibit a high degree of infolding, and the cells are categorized as either ‘open’ (extending through the epithelium to the lumen) (Fujita and Kobayashi 1977) or ‘closed’ (having no apical contact with the lumen) (Hecker 1977). Signals

transmitted by innervations of visceral muscle, which cause midgut mechanical tension, and the perception of luminal nutrient content trigger the synthesis and secretion of specific peptides by closed and open endocrine cells, respectively (Fujita et al. 1988; Žitňan et al. 1993).

Larval stem cells (AMPs, adult midgut progenitors), the primary focus of this chapter, lie adjacent to the basolateral membrane wedged individually in between mature cells (Baldwin and Hakim 1991), or in clusters commonly referred to as “nidi” (Illa-Bochaca and Montuenga 2006; Micchelli and Perrimon 2006). In adults, intestinal stem cells (ISCs) are found more interspersed among the differentiated cell types. Proliferation and differentiation of these stem cells mediates expansion or remodeling of the midgut during development and metamorphosis (Baldwin and Hakim 1991; Jiang and Edgar 2009a; Micchelli et al. 2011; Parthasarathy and Palli 2008) and in response to acute midgut damage (Amcheslavsky et al. 2009; Buchon et al. 2009b; Buchon et al. 2009a; Forcada et al. 1999; Jiang et al. 2009b; Martinez-Ramirez et al. 1999; Spies and Spence 1985).

Early studies on the embryonic development of *D. melanogaster* suggested that adult midgut progenitors (AMPs) give rise to adult intestinal stem cells (ISCs) and lie quiescent on top of the basal lamina during larval development (Bodenstein 1994). More recent studies identified expression of the *escargot* gene as a marker for larval AMPs, which is also a marker for adult intestinal stem cells (ISCs). AMP growth depends both on local cues such as the epithelial growth factor EGF (Jiang and Edgar 2009a) and systemic cues such as the hormone ecdysone (Micchelli, Sudmeier et al. 2011). The interaction between those signals likely times the phases of growth of AMPs to changes in instar. Expression and secretion of the EGFR ligand, Vein, by visceral muscle tissue underlying the basal lamina is sufficient to promote proliferation and expansion of AMPs during this early larval development (Jiang and Edgar 2009a). An asymmetric division follows AMP dispersal, whereby one daughter cell retains self-renewal capabilities characteristic of stem cells while the second daughter cell becomes a peripheral

cell, that will extend long processes around the other AMPs to form an AMP cluster or adult imaginal island (Mathur et al. 2010). Following the establishment of adult imaginal islands, AMPs continue to divide symmetrically in response to autocrine mitogenic signals such as the EGFs *Keren* and *Spitz*, that trigger the activation of the EGFR pathway and subsequent phosphorylation of the extracellular signal-regulated kinase (ERK) (Jiang and Edgar 2009a). In ISCs, the EGFR pathway is repressed by *hippo*, and ISC proliferation after tissue damage requires loss of *hippo* and the presence of the *hippo* pathway regulator *Yorkie* (Ren et al. 2010; Staley and Irvine 2010).

Following a series of pioneering studies that demonstrated the existence of hematopoietic stem cells capable of regenerating diverse cell types in the mammalian circulatory system, the mechanisms underlying stem cell lineage differentiation have been under intense investigation, revealing both intrinsic and extrinsic cues (Crooks and Weinberg 2006; Elkind and Sutton 1960; Lockart et al. 1961). A similar discussion, which focuses on ISCs in *D. melanogaster*, must be preceded by acknowledging obvious differences between the ISC environment and, the environment encountered by hemocytes circulating in the hemolymph. Following the establishment of the first midgut, ISCs are constrained on all sides by either the basal lamina or differentiated cells and, subsequently, do not move about freely (Wigglesworth 1939). Consequently, it is possible that they encounter more macromolecules than they are physiologically capable of recognizing. It has been demonstrated that the selectivity of the porous insect basal lamina underlying the intestinal epithelium depends on particle size as well as charge (Brac 1983), and serves to restrict the bidirectional passage of proteins $>$15 nm in diameter (Reddy and Locke 1990). Apart from the restricted movement of stem cells within the epithelial niche and the controlled accessibility of soluble hemolymph factors to the intestinal epithelium, macromolecules reaching the intercellular space must also be recognized by specific receptors to activate intracellular signaling pathways. All these factors support highly

selective extrinsic stem cell lineage determination, by which stem cells respond to specific signaling macromolecules produced by either neighboring cells or permeated through the basal lamina. Therefore, even though stem cells may be responsive to multiple growth factors *in vitro*, the biological significance of this response needs to be tested. For instance, while primary midgut stem cells from *H. virescens* larvae exposed to all-trans retinoic acid or epidermal growth factor (EGF) differentiated to squamous and scale-like cells *in vitro*, these cell types were not observed in the midgut epithelium *in vivo* (Loeb et al. 2003). Conversely, proliferative effects of known mitogens such as arylphorin are only manifested in those cells expressing both an arylphorin receptor and the transcriptional machinery capable of activating mitosis (Shivdasani and Orkin 1996). Therefore, lineage specification of insect stem cells, as it applies to maintaining homeostasis of the midgut epithelium is extrinsically activated and intrinsically executed.

The aim of this review is to summarize what is known about the factors that regulate stem cell activity (proliferation or differentiation) in relevant insect model systems, but also to highlight knowledge gaps that may be filled by cross-referencing experimental evidence that has been generated from multiple model insects. The synthesis of data from molecular, biochemical, and physiological characterizations of stem cell behavior will provide an integrative understanding of stem cell behavior in invertebrate and vertebrate systems, and guide the development of novel strategies to control agriculturally devastating insect pests.

1.2 Factors regulating midgut stem cell proliferation

1.2.1 Mitogens identified in *Drosophila*

Most available information on mitogens controlling midgut stem cell proliferation is derived from studies on the adult *Drosophila* midgut. Proliferation of these cells is mostly regulated by ligands produced in the cells neighboring ISCs, including the circular inner layer of

visceral muscles and the enteroblasts, that arguably constitute the ISC niche, although tracheae have been proposed to also influence gut homeostasis (Li et al. 2013). ISC maintenance and activity are regulated by the Wnt/*Wingless* (*Wg*) pathway, the EGFR and the Janus kinase/signal transducer and activator of transcription (JAK/STAT) pathway (Lin et al. 2008; Xu et al. 2011b). Silencing of *Wg* expression results in quiescence and differentiation. The EGFs are produced by the niche: Vein is produced by the visceral muscle, and Keren and Spitz are produced by ISCs and EBs to promote ISC proliferation (Xu et al. 2011a). Interestingly, the expression of EGFs is under the control of the JAK-STAT pathway, suggesting that JAK-STAT controls niche activity, and that EGFs are the true mitotic signal (Buchon, Broderick et al. 2009b; Buchon et al. 2010; Buchon, Broderick et al. 2009a; Jiang and Edgar 2009a; Zhou et al. 2013). Over proliferation of ISCs is repressed by the *Adenomatous polyposis coli* gene, which is a negative regulator of Wnt signaling pathway (Lee, W. C. et al. 2009). ISCs proliferate mainly through asymmetrical division (90% divisions), but can also divide symmetrically, giving rise to two ISCs, or two differentiated daughters (de Navascues et al. 2012; Goulas et al. 2012; O'Brien et al. 2011). Upon asymmetric ISC division, ISCs express the Notch ligand Delta, which activates Notch signaling in neighboring enteroblasts (Ohlstein and Spradling 2007). Through a negative feedback loop, elevated Notch signaling in enteroblasts suppresses ISC proliferation by repressing transcription of the JAK/STAT cytokine Unpaired (*Upd*) (Liu et al. 2010; Micchelli and Perrimon 2006). The loss of proper Delta or Notch signaling results in tumors that comprise both undifferentiated cells and cells with enteroendocrine properties (express prospero). Alternatively, it has been proposed that ISC proliferation under normal and stressed conditions requires expression of the JAK/STAT ligand Unpaired3 (Upd3) by enteroblasts and enterocytes, but not ISCs (Buchon, Broderick et al. 2009b; Buchon, Broderick et al. 2010; Buchon, Broderick et al. 2009a; Jiang, Patel et al. 2009b; Zhou, Rasmussen et al. 2013). Upd3 is induced in response to damage, and triggers a feedback loop that couples ISC proliferation to challenges

inflicted to the epithelium. Production of Upd3 has also been detected in healthy gut cells at basal levels and has been hypothesized to involve interactions with the gut microbiota (Buchon, Broderick et al. 2009b). Activation of gut stem cell proliferation and differentiation was reported to be associated with the production of reactive oxygen species (ROS) by the epithelium in response to the microbiota (Buchon, Broderick et al. 2009b; Ha et al. 2005b; Ha et al. 2005a; Jones et al. 2013; Lee 2009; Park et al. 2003). Evidence for the effects of factors from commensal bacteria on stem cell proliferation is further provided by stem cell hyperproliferation observed during dysbiosis (Guo et al. 2013).

1.2.2 Ecdysone and 20-Hydroxyecdysone

An extensive amount of research has been done to establish correlations between the cyclical fluctuations in hemolymph ecdysteroid titers and the behavioral and morphological stages of insect development (Riddiford 1994). Two ecdysteroids are critical to insect development and metamorphosis: ecdysone and its derivative 20-hydroxyecdysone (20HE). In larvae, ecdysone synthesis from sterols takes place in the prothoracic gland during a series of oxidation and hydroxylation reactions that rely on trafficking of reaction intermediates between the mitochondria and endoplasmic reticulum (Grieneisen et al. 1993; Kappler et al. 1988). Both ecdysone and the analog 3-dehydroecdysone are products of this biosynthetic pathway and are released into the hemolymph as prohormone. Ecdysone is further converted into the active molting hormone, 20HE, by 20-hydroxy monooxygenase in peripheral tissues (Grieneisen, Warren et al. 1993). Ecdysteroids bind the nuclear receptor EcR and regulate downstream target genes (Riddiford et al. 2000). An example of these effects is the activation of the proliferation and differentiation of stem cells during ecdysis (Baldwin and Hakim 1991).

In vitro studies using primary midgut cell cultures have accelerated our understanding of the mechanisms underlying endocrine control of the midgut during larval development and

metamorphosis. In primary midgut stem cell cultures from lepidopteran larvae, biologically relevant ecdysone or 20HE titers (1 to 10 μM), induced stem cell proliferation after a 72-hour incubation (Smagghe et al. 2005b). In these studies, ecdysteroid agonists such as RH-2485, induced a higher stem cell proliferation than observed with ecdysteroids (Smagghe et al. 2003). In cultured larval midgut cells from the coleopteran *Tribolium castaneum* (red flour beetle), 10 μM of 20HE increased stem cell proliferation, determined by measuring the relative fluorescence intensity (RFI) after pulsing cultures with the thymidine analog BrdU (5-bromo-2′-deoxyuridine). Stem cell proliferation could be reduced by 50% by either the simultaneous addition of 10 μM juvenile hormone III (JH III) or by silencing expression of the ecdysteroid receptor (EcR) gene prior to the preparation of midgut cell cultures (Parthasarathy and Palli 2008).

Surprisingly, the role of 20HE is strikingly different in mature midgut cells, where it has been shown to drive midgut histolysis. In *Drosophila*, ecdysone regulates the phosphatase PTP52F that in turn triggers apoptosis and autophagy (Santhanam, Meng 2014), the latter being key for midgut histolysis (Denton, Kumar, 2009). It has been also demonstrated *in vivo* that supplementing artificial diet with 624 μM 20HE induces fourth instar *Bombyx mori* (silkworm) larvae to molt within three days, resulting in “precocious” fifth instar larvae that are smaller than control larvae fed a standard diet. Histological analysis of the midgut after subsequent feeding of 20HE to precocious fifth instar larvae revealed a single-layered epithelium and intracellular accumulation of lysosomes in mature and stem cells, a phenotype characteristic of cellular degeneration, histolysis, and death (Akai 1976; Tanaka and Yukuhiro 1999). In contrast, no lysosomes were detected in stem cells when precocious larvae were fed a diet containing ecdysone. Furthermore, ecdysone induced stem cell proliferation, resulting in the regeneration of the midgut epithelium twice prior to the beginning of apolysis (Tanaka and Yukuhiro 1999). Ecdysteroid-mediated lysosomal degradation of midgut epithelial cells was also reported in

larvae of the dipteran *Sarcophaga bullata* (flesh fly) injected with 20HE (Radford and Misch 1971), yet direct evidence of increased lysosome numbers in midgut stem cells was not tested. However, similarities in the response to 20HE treatment suggest that similar physiological consequences occur in larvae across diverse taxonomic orders (Tanaka and Yukuhiro 1999). Altogether these results suggest a dual role for 20HE, which promotes the proliferation of stem cells and simultaneously promotes the histolysis of mature larval tissues.

1.2.3 Alpha-arylphorin (α-Arylphorin)

Arylphorins are high molecular weight (400-500 kDa) insect storage proteins that are characterized by a high phenylalanine and tyrosine content (15-20 mol %) and belong to a larger family of insect storage proteins called hexamerins (Tojo et al. 2012). Apart from their main storage function, arylphorins have also been described to play significant roles in development (Shelby and Webb 1994, 1997), humoral immune defense (Hayakawa 1994), and caste determination in social insects (Zhou, Oi, et al. 2006; Zhou, Tarver, et al. 2006). Similar to other hexamerin storage proteins, arylphorins are stored in fat body tissue as six-subunit hetero-oligomers (three alpha and three beta subunits), which are released into circulating hemolymph of intermolt larvae. While traditionally considered as a fat body protein in Lepidoptera, arylphorin has also been shown to be expressed by midgut cells and secreted basally towards the basal lamina in *Calpodes ethlius* (Palli and Locke 1987c). Moreover, hemolymph arylphorin may also be able to permeate the basal lamina to reach the epithelial layer, as mitogenic arylphorin was experimentally determined to be below the discriminating molecular size threshold (Palli and Locke 1987a). Immediately prior to pupation, a shift in the role of insect fat body from protein synthesis to protein storage results in the sequestration of hexameric growth factors, including arylphorin, methionine-rich hexamerins (MtH), riboflavin-binding hexamerins (RbH), and biliverdin-binding proteins (Haunerland 1996; Kramer et al. 1980; Telfer and Kunkel

1991; Tojo, Liu et al. 2012). Most biochemical and functional analyses of hexamerins have been performed on tissues from holometabolous insects (Haunerland and Bowers 1986; Tojo et al. 1980), but members of each hexamerin subgroup have also been identified in hemimetabolous species (De Kort and Koopmanschap 1987; Duhamel and Kunkel 1983; Kunkel and Lawler 1974). These pioneering studies established a critical role for arylphorins as nitrogen reserves during larval ecdysis and metamorphosis, when the insects do not actively feed (Levenbook and Bauer 1984; Telfer et al. 1983). Multiple papain cleavage sites identified within heteroligomeric arylphorin from *B. mori* fat body tissue have been proposed to facilitate papain cleavage of arylphorin during molting and metamorphosis to liberate amino acids for use during these energy demanding processes (Hou et al. 2014).

Besides serving as energy storage, arylphorin has also been described to display mitogenic activity in gut stem cells. Chromatographically pure monomeric α-arylphorin from an extract of excised fat body tissue (FBX) of *Manduca sexta* (tobacco hornworm) stimulated proliferation of freshly prepared *H. virescens*, *Spodoptera littoralis* (African cotton leafworm), and *Leptinotarsa decemlineata* (Colorado potato beetle) midgut stem cells *in vitro* (Blackburn et al. 2004). From these studies it was determined that the maximum mitogenic effects of α-arylphorin on midgut stem cells *in vitro* occurs in the range of 100-125 ng/mL when added to freshly prepared cultures (Blackburn, Loeb et al. 2004; Hakim et al. 2007). An FBX fraction devoid of α-arylphorin had no mitogenic activity, suggesting that either α6 or α3/β3 hexamers function as stem cell mitogens or the presence of additional, less abundant, growth factors in FBX (Hakim, Blackburn et al. 2007). In the same study, a total arylphorin fraction (α/β subunits) collected from *M. sexta* fat body extract (FBX) had the same mitogenic activity as a fraction containing only monomeric α-arylphorin, supporting that the α subunit is responsible for mitogenic effect of FBX.

1.2.4 Insulin-like peptides

Brain neuropeptides regulate insect growth and metamorphosis by stimulating the prothoracic gland to synthesize and release ecdysone (Nagasawa et al. 1984). A 5 kDa brain peptide member of the insulin family identified in *B. mori* (bombyxin) exerts prothoracicotropic activity in the heterologous *Samia cynthia ricini* (Eri silkworm), but not in *B mori*. Thus, injection of bombyxin into brainless *B. mori* pupae elicited no effect on adult development. However, injection of the same peptide into brainless *S. cynthia ricini* pupae was shown to reactivate adult metamorphosis (Ishizaki et al. 1983). Subsequent studies support an insulin-like function for bombyxin. For instance, injection of bombyxin into neck-ligated *B. mori* larvae induced a concomitant reduction in hemolymph trehalose levels and an increase in midgut trehalase activity (Satake et al. 1997). Additionally, bombyxin levels in the hemolymph increase in response to increasing glucose levels, mediated by either feeding or direct injection of glucose (Masumura et al. 2000). Unlike mammalian insulin, however, bombyxin seems to be involved in the mobilization of fat body carbohydrate stores and the uptake of trehalose into target tissues, where it is converted to glucose and used for the production of ATP (Masumura, Satake et al. 2000; Satake, Masumura et al. 1997). Studies on the *in vitro* effects of synthetic bombyxin demonstrated that it also induces proliferation of freshly prepared stem cells from pharate 4th instar *H. virescens* and *Mamestra brassicae* (cabbage moth) midgut tissues (Goto et al. 2005). Compared to controls, addition of 10^{-12} M bombyxin to modified Grace's culture medium in 80% homogenous stem cell cultures induced a 51.1% increase in stem cell number. The mitogenic effects of bombyxin on stem cells decreased three days after the initial treatment but could be restored following a second bombyxin dose, suggesting that it undergoes inactivation and/or degradation. In mixed cell cultures, 10^{-13} M bombyxin induced a 67.2% increase in stem cell number relative to controls (Goto, Loeb et al. 2005). Together, these results suggest that while bombyxin may activate pathways involved in the uptake of carbohydrates, it may also exert

mitogenic effects on midgut stem cells *in vivo*.

1.2.5 Midgut peptides

Reverse-phase high pressure liquid chromatography (RP-HPLC) fractionation of *Periplaneta americana* (American cockroach) midgut extracts isolated fractions containing peptides with gut myotropic activity and inducing proliferation of primary *H. virescens* midgut stem cells or an established fat body cell line *in vitro* (Takeda et al. 2001). Other fractions were shown to contain peptides inducing mature cell death. To date, the identities of the mitogenic component(s) remain unknown.

1.2.6 Calcium (Ca^{2+})

Fluctuations in calcium ion (Ca^{2+}) concentration were described to regulate epidermal cell growth in mammals (Hennings et al. 1980). The higher concentration of calcium in the hemolymph of lepidopteran larvae drives the movement of Ca^{2+} into the gut cells, which is counteracted by an active efflux from the gut cells. Experiments to model transepithelial Ca^{2+} delivery from the gut lumen to the hemolymph in lepidopteran insects demonstrated that transport required an ATP-dependent Ca^{2+} transporter (Sheppard and Loeb 1992; Wood and Harvey 1976). In light of these findings and the reported effect of fluctuations in calcium levels in regulating epithelial cell growth in mammals, a role for Ca^{2+} in regulating insect gut stem cell proliferation was hypothesized. The addition of ethylene glycol-bis (2-aminoethylether)-N,N,N'N'-tetraacetic acid (EGTA), a high-affinity calcium-binding chelator, to modified Grace's culture medium induced a significant increase in the percentage of stem cells after four to seven days relative to controls (Loeb 2005). These results support a role for Ca^{2+} efflux from midgut stem cells in the regulation of stem cell proliferation and further substantiate the role of Ca^{2+} as a secondary messenger involved in transcription factor activation in invertebrate systems

(Berridge 1983).

1.2.7 Platelet-derived growth factor

Cell signaling by members of the platelet-derived growth factor (PDGF) and vascular endothelial growth factor (VEGF) families of receptor tyrosine kinases is conserved throughout the animal kingdom and has roles in many developmental and pathological functions in vertebrate and invertebrate tissues (Andrae et al. 2008). It has been demonstrated in a recent study that autocrine *Pvf/Pvr* signaling participates in homeostasis of the *Drosophila melanogaster* posterior midgut by regulating intestinal stem cell (ISC) proliferation (Bond and Foley 2012). A β-factor peptide of PDGF induced approximately a two-fold increase in stem cell number in partially purified *H. virescens* midgut stem cell cultures after 14-day incubation, suggesting that similar PDGF/PDGFR signaling may regulate homeostatic proliferation of midgut stem cells in Lepidoptera (Loeb, Clark et al. 2003). However, these factors have not been identified to date.

1.2.8 Albumax II

The biologically active components in vertebrate and invertebrate sera are vital to the long-term sustainability of and experimentation with tissue cultures *in vitro* (Barnes and Sato 1980). However, the use of rich culture media complicates the process of ascertaining whether or not the dependent variable being tested is directly responsible for eliciting the cellular response being measured (Ferkovich and Oberlander 1991). Recently, AlbuMAX II, a lipid-rich commercially available media additive used as a serum alternative, was shown to induce asymmetrical proliferation of freshly prepared *H. virescens* midgut stem cells *in vitro* (Castagnola et al. 2011). A previous report, which tested the utility of AlbuMAX II for sustaining human embryonic stem cell (hESC) pluripotency, demonstrated that albumin-associated lipids

were critical to ensuring that continually cultured hESCs would retain the ability to differentiate to ecto-, meso-, and endoderm embryonic germ layers *in vitro* (Garcia-Gonzalo and Izpisua Belmonte 2008). Although additional experiments will be necessary to confirm parallel lipid-mediated signaling events, these reports suggest that albumin-associated lipids may regulate vertebrate and invertebrate stem cell proliferation through homologous receptors.

1.3 Regulation of midgut stem cell proliferation

Most available information on regulation of midgut stem cell proliferation is focused on the adult *Drosophila* midgut tissue. The stem cells in this tissue originate from progenitor cells that during the first two larval instars proliferate symmetrically in response to the Vein ligand and then disperse to form midgut imaginal islands (Jiang and Edgar 2009a). In these imaginal islands Notch signaling induces some progenitor cells to differentiate into peripheral cells during the L3 developmental stage, and these cells extend long processes around residing progenitor cells to maintain the niche environment (Mathur, Bost et al. 2010). The adult gut can adapt its size to nutrient availability. Particularly, in the fed state, gut derived insulin signaling induces accelerated and symmetric midgut stem cell division, resulting in the increase in total gut cells (O'Brien, Soliman et al. 2011).

As in larvae, expression of the *escargot* gene serves as a marker for adult stem and progenitor cells, and a number of signaling pathways have been demonstrated to regulate stem cell proliferation and differentiation. The Wg ligand produced by the intestinal epithelium is essential for ISC proliferation following damage but dispensable for proliferation associated with homeostatic tissue turnover (Cordero et al. 2012). Commonly observed asymmetric stem cell division results in the expression of Delta in ISCs, and the consecutive activation of Notch signaling in enteroblasts. The level of Notch signaling determines the fate of the daughter cells (enteroblasts), high Notch signaling being required to acquire enterocyte fate (Ohlstein and

Spradling 2007). Both the EGFR and JAK/STAT pathways participate in gut homeostasis, and they are also critical for regeneration after cellular stress, infection, or damage. Activation of JAK/STAT signaling is initiated by the binding of Unpaired (Upd, Upd2 and Upd3) cytokines produced by enterocytes and ISCs to downstream effectors (Gilbert et al. 2005; Harrison et al. 1998; Hombria et al. 2005). Overexpression of *Upd* causes a significant increase in ISC mitosis, and is observed under enterocyte stress or damage (Jiang, Patel et al. 2009b). Among the three Drosophila Upds, Upd1 is required cell autonomously in ISCs for stem cell maintenance, Upd2 and Upd3 are produced by the epithelium in response to damage to promote rapid turnover (Osman et al. 2012). Binding of Upds initiates a phosphorylation cascade resulting in phosphorylated STAT92E translocating to the nucleus to induce target gene expression in the ISC niche. The EGF vein is induced in the visceral muscle, while spitz is produced in progenitor cells, both triggering EGFR pathway in ISCs and subsequent proliferation (Biteau and Jasper 2011; Buchon, Broderick et al. 2010; Jiang et al. 2011; Yan et al. 1996). Enteric infection with *Pseudomonas entomophila* induced *Upd* and *STAT92E* expression in all gut cell types, resulting in an increase in the number cells expressing *Delta* and *Notch*. This regenerative response could be suppressed by RNAi-mediated silencing of JAK/STAT pathway (Buchon, Broderick et al. 2009b; Jiang, Patel et al. 2009b; Zhou, Rasmussen et al. 2013), confirming the role of this signaling pathway in a regenerative response to infection.

Upon damage to the epithelium, Wg is required for stem cell proliferation and tissue regeneration (Cordero, Stefanatos et al. 2012). Expression of members of the bone morphogenetic protein (BMP) pathway during injury limit proliferation and return ISCs to quiescence (Guo, Driver et al. 2013). Another pathway participating in response to stress conditions is the Jun N-terminal kinase (JNK) signaling pathway, which comprises a subgroup of protein kinases referred to as stress-activated protein kinases (SAPKs) (Davis 2000; Weston

and Davis 2002). Overstimulation of the JNK pathway results in cell autonomous overproliferation of ISCs (Biteau et al. 2008) and JNK pathway is required in ISCs upon infection (Buchon 2009 Genes dev). In addition, RNAi-mediated silencing of a JNK negative regulator or overexpression of a JNK kinase in enterocytes, also increases the number of mitotic cells (Jiang, Patel et al. 2009b). Age plays a role in the control of ISC homeostasis, as an age-dependent increase in Hedgehog (Hh) signaling was shown to overcome the inhibitory effects of Debra-mediated polyubiquitination leading to JNK-induced ISC proliferation (Dai et al. 2003; Li et al. 2014). In agreement with these findings, cytoprotective JNK signaling in aged *Drosophila* increased the number of ISCs detected in response to oxidative stress (Choi et al. 2008). This dysregulation of differentiation and loss of homeostasis with age is due to aberrant expression of Delta and Notch in proliferating ISCs (Biteau, Hochmuth et al. 2008), and probably a downstream consequence of age-related changes in the microbiota (Buchon Lemaitre 2009 Genes dev and Guo Jasper 2014).

1.4 Factors regulating midgut stem cell differentiation

1.4.1 Midgut Differentiation Factor 1 (MDF-1)

Cell-free conditioned medium from mixed midgut cell cultures prepared from pharate 4th instar *M. sexta* larvae was shown to contain a soluble heat-stable peptide (3-10 kDa) which promoted near homogenous stem cell populations to differentiate to mature columnar and goblet cells *in vitro* (Sadrud-Din et al. 1996). A chromatographically pure biologically active fraction from this medium was sequenced to contain the peptide HVGKTPIVGQPSIPGGPVRLCPGRIRYFKI (M_r, 3,244), and was termed midgut differentiation factor 1 (MDF-1) (Loeb et al. 1999). A BLAST search using MDF-1 as query revealed that it was identical to a 30 amino acid sequence near the carboxy terminus of bovine fetuin, a high molecular weight glycoprotein comprising nearly 45% of the total protein found in fetal calf

serums (Demetriou et al. 1996; Loeb, Jaffe et al. 1999; Pedersen 1944). In vertebrate cell cultures, fetuin acts as a protagonist and antagonist to transforming growth factor beta 1 (TGFβ1). For example, titers of ($<$10pM) that promote osteogenesis in dexamethasone-treated rat bone marrow cultures are inhibited by fetuin, while the inhibitory effects of elevated titers of TGFβ1 ($\geq$10pM) on osteogenesis are attenuated by the addition of fetuin (Binkert et al. 1999; Demetriou, Binkert et al. 1996). A smaller synthetic MDF-1 peptide (HVGKTPIVGQPSIPGGPVRLCPGRIR, Mr, 2,689) induced dose-dependent (10^{-14}-10^{-8} M) differentiation of midgut stem cells prepared from pharate 4th instar *H. virescens* larvae after seven days of culture, while fetuin exhibited no effect (Loeb, Jaffe et al. 1999). Consequently, and since no matches to insect proteins are identified when searching the NCBI database with the MDF-1 peptide as the query, the detected MDF-1 was probably derived from digestion of fetuin in the culture medium by mature midgut cells. However, localization of MDF-1 to the inside and brush border surface of midgut columnar cells *in vitro* was demonstrated using a polyclonal antibody (Goto et al. 2001). Moreover, MDF-1 cross-reactivity was detected in columnar and goblet cells after exposure to a crystal toxin from the bacterium *Bacillus thuringiensis* (Bt) but not in BSA-treated controls (Loeb, Martin, Hakim, et al. 2001). Further evidence for MDF-1 being produced by midgut cells is provided by increased MDF-1 staining of paraffin-embedded *H. virescens* midgut tissue sections between newly molted, mid-instar, and pharate stages of larval development, suggesting that increased MDF-1 synthesis may be involved in regulating stem cell differentiation prior to ecdysis (Goto, Takeda et al. 2001). Unexpectedly, treatment of mixed midgut cell cultures prepared from pharate 4th instar *H. virescens* larvae with antisera against MDF-1 did not inhibit differentiation. In contrast, MDF-1 antisera treatment resulted in increased rates of apoptosis in mature cells and stimulated an increase in the number of differentiating stem cells (Loeb et al. 2004). It is difficult to explain why antisera to MDF-1 would increase apoptosis in mature cells. It is possible that production

of additional factors by apoptotic cells induced the detected increased stem cell differentiation. Further research is needed to determine whether midgut cells synthesize MDF-1 and its putative role as a biologically-relevant insect growth factor.

1.4.2 Midgut Differentiation Factor 2 (MDF-2)

Based on the biological activity of peptides derived from fetuin (such as MDF-1), efforts were devoted to identify additional differentiation factors by digesting bovine fetuin with chymotrypsin. A biologically active product between 3-10 kDa in molecular size stimulated differentiation of midgut stem cell cultures prepared from pharate 4th instar *H. virescens* larvae. Purification of the biologically active product by RP-HPLC followed by Edman degradation amino acid sequencing identified the active peptide as HRAHY (M_r, 682), which was termed Midgut Differentiation Factor 2 (MDF-2) (Loeb, Jaffe et al. 1999). Database searches using BLAST revealed that MDF-2 represented a sequence near the carboxy terminus of bovine fetuin (amino acids 305-309) that did not overlap with MDF-1. Maximum differentiation of midgut stem cells prepared from pharate *H. virescens* larvae was detected when using concentrations between 10^{-15} and 10^{-5} M of MDF-2 (Loeb, Jaffe et al. 1999). As with MDF-1, it is not clear whether MDF-2 results from synthesis by midgut cells or digestion of fetuin in the medium by midgut cell proteases. Incubation of near homogeneous midgut stem cell cultures prepared from pharate 4th instar *H. virescens* larvae in conditioned medium (25% conditioned: 75% standard) at 4°C for two days increased stem cell responsiveness to MDF-2 (Loeb, Clark et al. 2003). This observation may be explained by additional differentiation factors enhancing the stem cell response to MDF-2, or by increased levels of proteases necessary to digest fetuin being present in conditioned medium. Microvillar and cytoplasmic regions of fixed midgut columnar cells and paraffin-embedded midgut tissue sections prepared from late last instar *H. virescens* larvae stained positively for MDF-2, as did round droplets expelled into the lumen,

which may support a cytokine-like role of MDF-2 in larval development (Loeb, Coronel et al. 2004). Similar to antisera against MDF-1, the addition of antisera against MDF-2 to mixed cell cultures prepared from *H. virescens* larvae induced apoptosis in mature cells, which resulted in increased stem cell proliferation and differentiation (Loeb, Coronel et al. 2004).

1.4.3 Midgut Differentiation Factors 3 and 4 (MDF-3 and -4)

Chymotrypsin proteolysis followed by heat denaturing of hemolymph drawn from *L. dispar* pupae generated two biologically active peptide nonamers, named Midgut Differentiation Factor 3 (MDF-3, EEVVKNAIA) and Midgut Differentiation Factor 4 (MDF-4, ITPTSSLAT), which were similar in size to the previously discussed MDFs (3-10 kDa). *In vitro*, MDF-3 and MDF-4 stimulated maximum differentiation of near homogenous midgut stem cell cultures prepared from pharate 4th instar *H. virescens* larvae when applied at 10^{-6} M and 10^{-8} M, respectively (Loeb and Jaffe 2002). Unlike MDF-1 and -2, which were identical to separate regions of bovine fetuin (Loeb, Jaffe et al. 1999), BLAST searches failed to identify homologous sequences containing either MDF-3 or -4.

1.4.4 Ecdysone and 20-Hydroxyecdysone

Primary midgut stem cell cultures prepared from pharate 5th-instar *S. littoralis* larvae differentiated to mature columnar and goblet cells after 72-hours of exposure to the ecdysteroid molting hormones ecdysone (E) or 20-hydroxyecdysone (20HE) (Smagghe, Vanhassel et al. 2005b). Equivalent titers of either ecdysone or 20HE induced 46±9% and 86±8% more stem cells to differentiate, respectively, providing additional direct evidence for ecdysteroids inducing stem cell differentiation. These data suggested that 20HE preferentially induces stem cell differentiation while E displays higher mitogenic activity (Smagghe, Vanhassel et al. 2005b). However, as stated above, stem cell proliferation was observed when treating *T. castaneum*

stem cell culture with 20HE in the absence of juvenile hormone (Parthasarathy and Palli 2008), suggesting that hormonal control may regulate the mitogenic or differentiative effects of ecdysteroids.

1.4.5 Perlecan

In *D. melanogaster,* expression of the *trol* gene in intestinal epithelial cells results in production of a basement membrane-specific heparin sulfate proteoglycan, Perlecan (Pcan), which is deposited to the extracellular matrix (ECM) in order to facilitate cellular attachment (Friedrich et al. 2000; Spring et al. 1994). Immunohistochemical staining of posterior midgut tissue from *Drosophila trol*$^{-/-}$ mutants detected delaminated ISCs as well as reduced ISC proliferation and *Delta* (*Dl*) expression (You et al. 2014). Armadillo (Arm) and DE-cadherin (E-CAD) encircled detached ISCs instead of localizing to apical and lateral membrane regions, respectively (Maeda et al. 2008; Ohlstein and Spradling 2006), suggesting that Perlecan participated directly in establishing apical-basal cell polarity. Moreover, ectopic expression of the β-integrin gene *myospheriod* (*mys*) activated proliferation in detached ISCs (You, Zhang et al. 2014). Taken together, these data suggest that ISCs intrinsically regulate niche structure through Perlecan synthesis and deposition, and in return, are regulated by their basal lamina through integrin signaling.

1.4.6 Integrin β1-like protein

Staining of cultured midgut cells from pharate 3rd-instar *H. virescens* larvae with antisera against integrin β1-like protein suggested a role for integrin adhesion in communication between mature and stem midgut cells (Loeb and Hakim 1999). Small columnar cells as well as stem cell daughters resulting from asymmetrical division stained faintly, suggesting that integrin adhesion is reduced in midgut cell types undergoing differentiation. Furthermore, intense

staining of stem cells clusters supported the importance of adhesion amongst undifferentiated cells residing in midgut imaginal cell islands (Loeb and Hakim 1999; Loeb, Martin, Narang, et al. 2001; Mathur, Bost et al. 2010). Subsequent *in vitro* studies have showed that low cross-reactivity with antisera against integrin in midgut cell cultures prepared from pharate 4th-instar *H. virescens* larvae corresponded with an approximate 10-fold increase in the number of differentiating cells (Loeb 2006). These results support an *in vivo* mechanism whereby integrin adhesion supports the undifferentiated state of stem cells, and that differentiation reduces integrin expression promoting differentiation and allowing the differentiating cells to ascend apically into permanent positions within the midgut epithelium. The requirement of integrin signaling in ISCs is supported by a recent report demonstrating ectopic expression of a β-integrin gene (*mys*) could partially rescue ISC proliferation in *trol*$^{-/-}$ mutants, indicating that β-integrin signaling is necessary but not sufficient to fully restore ISC proliferation (You, Zhang et al. 2014). These data corroborate the previously described role of intercellular or cell-matrix integrin-mediated adhesion in promoting gut stem cell proliferation (Lin et al. 2013; Okumura et al. 2014). In addition, another report demonstrated that RNAi-mediated silencing of three different integrin genes results in symmetrical ISC proliferation in the *D. melanogaster* midgut (Goulas, Conder et al. 2012), suggesting that integrins are also required for the apical-basal polarization of ISCs, and serve as a cue for the orientation of ISC division.

1.5 Regulation of midgut stem cell differentiation

The balance between proliferation and differentiation in midgut stem cells is controlled by highly conserved pathways. Intestinal stem cells in the adult *Drosophila* midgut express the Notch ligand Delta (Dl). After asymmetrical division of ISCs, the Notch pathway controls the fate of one of the daughter cells (enteroblast), which will undergo differentiation to either an enterocyte (characterized by being *Pdm1* positive) or enteroendocrine cell (characterized by

being *prospero* positive) (Koch et al. 2013). Repression of the Notch target genes by the ligand Hairless In ISCs prevents differentiation and contributes to ISC maintenance (Bardin et al. 2010). Moreover, under normal conditions Notch signaling inhibits production of Unpaired, blocking activation of the JAK-STAT pathway and limiting ISC proliferation in basal conditions (Liu, Singh et al. 2010). Chronic JNK activation under stressful conditions results in the dysregulation of Delta/Notch signaling and promotes overproliferation of ISCs (Biteau, Hochmuth et al. 2008). In the enteroblast, high levels of Notch signaling promote differentiation to enterocyte, while low Notch levels lead to the enteroendocrine fate (Perdigoto et al. 2011). Differentiated cells can produce factors that affect cell fate of new enteroblasts to respond to tissue needs. For instance, enteroendocrine cells secrete the ligand Slit that is recognized by Robo2 receptors in ISCs. Robo2 activation leads to the inhibition of prospero in ISCs, and as a consequence the lack of commitment of ISC lineage to generate enteroendocrine cells (Biteau and Jasper 2014).

Molecular signals disseminated by differentiated cells function to maintain resident stem cells residing in niches of various tissues in an undifferentiated state (Bausek 2013). Signaling pathways also control the fate of differentiated cells in these niches. In the stem cell niche during the L3 instar, peripheral cells are maintained through signaling factors in the transforming growth factor-β (TGFβ) superfamily of proteins. The ligand Decapentaplegic (Dpp) is produced by the peripheral cells and binds to thick veins (tkv) (Penton et al. 1994), activating expression of Dpp target genes. Silencing of *Dpp* by RNAi in *Drosophila* larvae resulted in disappearance of peripheral cell processes, which maintain the stem cell niche, and an outward migration of progenitor cells, which remain in an enteroblast-like stage, from the midgut imaginal islands (Mathur, Bost et al. 2010).

1.6 Midgut response to pathogens

The ingestion of foods rich in microbes inevitably risks exposure of the alimentary canal to non-commensal and pathogenic microorganisms that can inflict physical damage on the epithelial barrier. Gut stem cells are vital to the regenerative response during pathogenic attack, since upon enterocyte damage they repair the epithelial layer by generating new enterocytes. This process is imperative to withstand infection and has to be tightly regulated to avoid hyperplasia but, at the same time, ensures timely regeneration to prevent collapse of the epithelial barrier. Immunohistochemical staining of midguts from unchallenged *D. melanogaster* Relish mutants (Rel^{E20}) with anti-phosphohistone H3 (anti-PH3) antibody, a marker for mitosis, detected a significant increase in mitotic cells relative to wild-type controls, supporting a role for IMD-mediated antimicrobial peptide synthesis in the regulation of basal level epithelial turnover induced by endogenous microbiota (Buchon, Broderick et al. 2009b; Buchon, Broderick et al. 2009a). Later studies have demonstrated that Ras/MAPK signaling activates expression of Pirk, a negative regulator, which limits the strength of IMD signaling in the absence of infection (Ragab et al. 2011). In agreement with this study, antibiotic treatment reduced midgut expression of diptericin in *D. melanogaster* wild-type and *big bang* ($bbg^{B211/B211}$) mutant strains with reduced septate junction cohesion. However, a significant increase in the number of PH3-positive cells was detected in the midguts of $bbg^{B211/B211}$ mutants relative to wild-type controls, indicating that expression of big bang is necessary limit epithelial turnover caused by endogenous bacteria that invade the paracellular space (Bonnay et al. 2013).

Oral ingestion of highly virulent *Pseudomonas aeruginosa*, *P. entomophila,* or *Erwinia carotovora carotovora* by *D. melanogaster* and *P. aeruginosa* by *Bemisia tabaci* (whitefly) activated the JNK and apoptotic pathways in mature enterocytes (Apidianakis et al. 2009; Buchon, Broderick et al. 2009b; Jiang, Patel et al. 2009b). In the case of *D. melanogaster*, mature cell apoptosis was associated with a sequential increase in mitotic stem cells detected in

the posterior midgut (Apidianakis, Pitsouli et al. 2009; Buchon, Broderick et al. 2009a; Jiang, Patel et al. 2009b), an observation that is consistent with reports describing JAK/STAT-mediated stem cell proliferation and differentiation following infection (Jiang, Patel et al. 2009b). A lack or marginal effects of pathogens on the gut epithelium has been suggested (Limmer et al. 2011), although relatively low bacterial loads were tested compared to alternative reports supporting significant effects on the gut epithelium (Apidianakis, Pitsouli et al. 2009; Buchon, Broderick et al. 2009b; Buchon, Broderick et al. 2010; Chatterjee and Ip 2009; Cronin et al. 2009). Analysis of differentially expressed genes in *B. tabaci* following bacterial challenge with *P. aeruginosa* using transcriptome profiling revealed up-regulation of innate immune response signaling pathways, including JAK/STAT, Egfr, and Wingless, which was associated with increased occurrence of Gene Ontology terms related to cellular proliferation and epithelium development (Zhang et al. 2014). While functional characterization of these pathways in regenerating the *B. tabaci* gut has not been reported, the available data strongly suggests a similar paradigm for gut regeneration among diverse insect orders.

IHC staining of paraffin embedded midgut tissue sections from *Plutella xylostella* (diamondback moth) following natural infection with entomopathogenic *Pseudomonas taiwanensis* detected increased JNK-2 and cleaved-caspase-3 relative to uninfected controls. However, stem cell proliferation was only detected in sections prepared from midguts of *P. xylostella* larvae fed a *P. taiwanensis* strain lacking expression of the TccC toxin, suggesting that extensive damage may inhibit or hinder detection of gut regenerative responses (Chen et al. 2014). In agreement, translational blockage of Upd3 repressed ISC proliferation and differentiation in *D. melanogaster* orally infected with high doses of *P. entomophila* relative to those infected with *Erwinia carotovora carotovora 15*, supporting translational arrest as a mechanism used by entomopathogens to dysregulate signaling of host immune and repair pathways (Chakrabarti et al. 2012). In contrast, extensive epithelial damage after treatment of

H. virescens larvae with Cry1Ac toxin was neutralized by the gut regenerative response (Forcada, Alcacer et al. 1999; Martinez-Ramirez, Gould et al. 1999). This response to Cry toxins was also observed in primary *H. virescens* midgut cell cultures *in vitro* (Loeb, Martin, Hakim et al. 2001). Moreover, midgut regeneration was documented to occur more rapidly, allowing for survival, in Cry1Ac-resistant larvae, supporting the relevance of this response to survival upon pathogenic challenge. In agreement, numerous reports have identified the gut regenerative response as a target for entomopathogens. Interestingly, ISC proliferation in *D. melanogaster* was suppressed during infection with the human pathogen *vibrio cholerae* (Wang et al. 2013). In the case of intracellular microsporidia (Dussaubat et al. 2012) or virus infection (Shelby and Webb 1994), this inhibition is due to negative regulation of key genes in the regenerative pathway (Kim 2005; Shelby and Webb 1997). In contrast, in the case of extracellular pathogens the lack of effective midgut regeneration is probably related to irreparable epithelial damage.

While the factors controlling the regenerative response after pathogenic attack in Lepidoptera are mostly unknown, there is evidence for the participation of arylphorin in the gut healing process. For instance, increased arylphorin gene expression was detected after bacterial ingestion in *Trichoplusia ni* (cabbage looper) (Freitak et al. 2007). In contrast, down-regulation of arylphorin was detected in *Lymantria dispar* (gypsy moth) larvae at 24 h. post-infection with Bt (Sparks et al. 2013). Constitutive increased arylphorin expression was detected in *Spodoptera exigua* (beet armyworm) resistant to *Bacillus thuringiensis* (Bt), although no increased gut proliferation was detected in resistant compared to susceptible larvae (Hernandez-Martinez et al. 2010). Another factor that has been involved in midgut response to pathogens is MDF-1, which was more frequently observed at the base of mature columnar cells after treatment with Bt compared to untreated cells (Loeb, Martin, Hakim et al. 2001).

1.7 Conclusions

Biological stimuli that activate ISC proliferation and differentiation in the insect midgut epithelium have been the primary focus of this review. A vast majority of the research has capitalized on the amenable genetics of *D. melanogaster* to exploit the role of ISCs in maintaining homeostasis, age-induced intestinal dysplasia, and the regenerative healing response of the intestine to chemical and pathogen-induced damage. These findings have emphasized the fact that gut epithelial cells respond to adverse environmental conditions by activating a complex network of intracellular signaling pathways and synthesizing proteins that mediate intercellular cross-talk with undifferentiated progenitor cells as well as tissues forming the ISC niche.

The coordinated retention of a population of undifferentiated progenitor (larval) and ISCs (adult) enables the intestinal epithelium to be repaired upon exposure to external and endogenous stimuli that disrupt homeostasis and compromise epithelial function and integrity. The production of JAK/STAT Unpaired ligands in the absence of challenge as well as in response to enterocyte stress and physical damage has been shown to induce ISC proliferation, demonstrating individual roles for these cytokine mitogens (Amcheslavsky et al. 2011; Buchon, Broderick et al. 2009a; Osman, Buchon et al. 2012; Zhou, Rasmussen et al. 2013). Likewise, there is extensive data describing the proliferative effects of JNK signaling on ISCs. Interestingly, the upstream physiological cues that drive elevated Hh signaling and consequently JNK expression and the development of intestinal dysplasia in aged *Drosophila* include ROS generated during oxidative bursts and age-related changes in the composition of gut microbiota (Buchon, Broderick et al. 2009b; Buchon, Broderick et al. 2009a). Given that Hh (Li, Guo et al. 2014) and Dpp (Li, Zhang et al. 2013) can regulate ISC proliferation after being transported from neighboring tissues, it is reasonable to postulate that both cell autonomous and non autonomous stimuli can serve as critical determinants of age-related intestinal malfunction and

homeostatic loss.

The role of IMD signaling in the regulation of ISC proliferation and differentiation has only recently begun to take shape. Ras/MAPK signaling represses immune signaling and the synthesis of antimicrobial peptides. Subsequently, epithelial damage caused by resident microbiota induces elevated levels of ISC proliferation. It is plausible that pathogens can be detected and cleared prior to exerting any physical damage to the midgut epithelium by the production of AMPs, and these circumstances would not require ISC proliferation. Interestingly, none of the pathogens used in *D. melanogaster* models of infection traverse the peritrophic matrix or epithelium, yet they're the strongest elicitors of epithelial immune and repair signaling.

Studies in Lepidoptera have revealed several unique aspects of intestinal stem cell regulation. While α-arylphorin and bombyxin synthesis primarily occurs in fat body and brain tissue, respectively, the mechanisms by which both mitogens gain entry into midgut stem cells for processing remain unclear. Moreover, midgut expression has only been reported in the case of α-arylphorin. Research in our group (Castagnola, A., unpublished data) has shown that α-arylphorin is secreted by *H. virescens* primary midgut cell cultures following exposure to Cry1Ac toxin from *B. thuringiensis*. However, the role of α-arylphorin in susceptibility to Cry1Ac and its mechanistic role in epithelial healing during the regenerative response have not been studied.

Soluble MDFs have only been identified during studies utilizing lepidopteran species (Goto, Takeda et al. 2001; Loeb and Jaffe 2002; Loeb, Jaffe et al. 1999). However, the possibility that MDF-like peptides are synthesized in the intestinal epithelia of other insect species cannot be ruled out. How the regulation of MDF synthesis in lepidopteran insects conforms to accepted paradigms describing the stem cell lineage determination in the intestinal epithelium is still unclear. While it is not definitive that MDFs are synthesized by enterocytes, the efficiency of ISC-mediated epithelial regeneration might be enhanced significantly by the simultaneous synthesis and secretion of α-arylphorin and MDFs following enterocyte damage.

The identification of lineage-specific intestinal cell markers in *Drosophila* has greatly expanded our ability to characterize the specific roles of molecules and signaling pathways mediating the physiological and morphological changes associated with stem cell mediated intestinal homeostasis in invertebrate as well as vertebrate systems. Moving forward, the development and application of reverse genetic tools that can be used to characterize gene functionality in diverse insect models will be necessary to elucidate species-specific regulatory mechanisms governing intestinal stem cell behavior.

Appendix

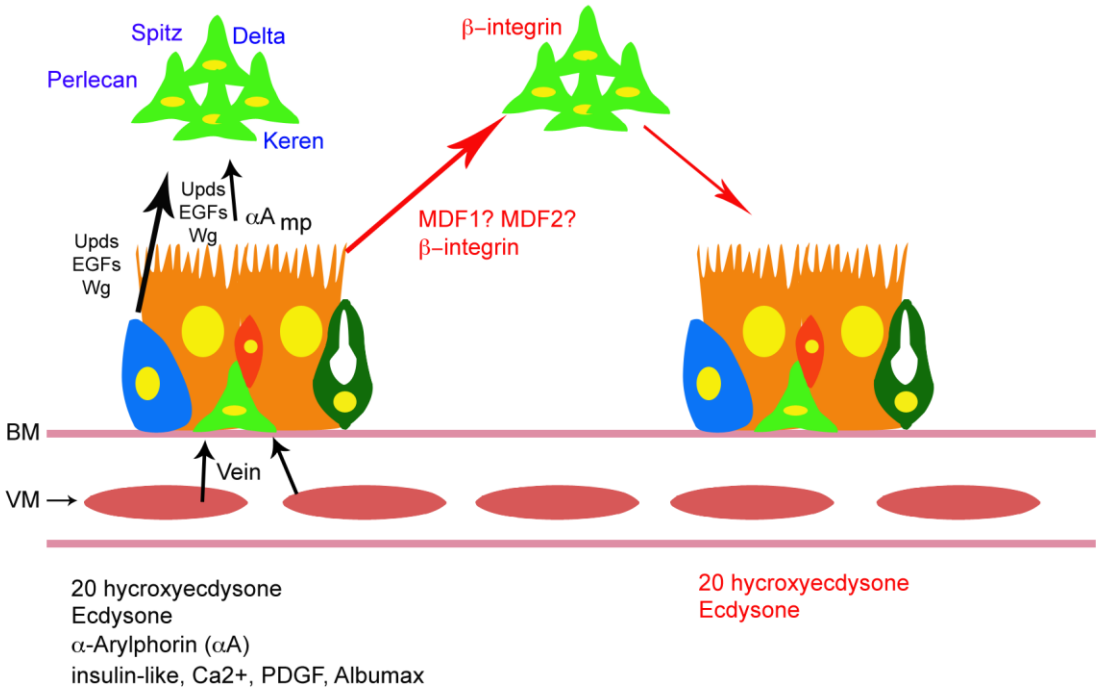


Figure 1: Integrative model for stem cell proliferation and differentiation in the insect midgut epithelium. Black arrows indicate cell or tissue of origin of factors inducing proliferation. Red arrows indicate cells producing differentiation factors. Blue writing indicates autonomous synthesis; intestinal stem cells (green triangles); columnar cells (orange cuboidal); goblet cells (dark green ovals); enteroblasts (blue ovals); enteroendocrine cells (small red ovals); BM, basement membrane; VM, visceral muscle; PDGF, platelet-derived growth factor; Ca^{2+}, calcium.

Chapter 2

Mitogenic α-arylphorin in circulating hemolymph activates intestinal stem cell proliferation

This chapter to be submitted to Insect Biochemistry and Molecular Biology

Jackson, J., Miller, D.L., and J.L. Jurat-Fuentes. (2015). Mitogenic α-arylphorin in circulating hemolymph activates intestinal stem cell proliferation.

My contributions included: (1) devising experiments, (2) performing experiments, (3) data collection and analysis, (4) writing the manuscript and making figures. Debra Miller assisted with (3) and (4). Juan Luis Jurat-Fuentes assisted with (1) and (4).

Abstract

Homeostasis in the intestinal epithelium of lepidopteran insects is maintained by multipotent intestinal stem cells (ISCs). Diverse physiological and environmental stimuli activate intracellular signaling pathways that regulate asymmetrical ISC proliferation to maintain epithelial homeostasis. However, the specific molecular signals controlling activation of ISC proliferation in lepidopteran insects remain poorly understood. In this work, we tested the *in vitro* and *in vivo* response of *Heliothis virescens* (tobacco budworm) larval midgut ISCs to α-arylphorin, a hexameric growth factor synthesized by fat body tissue and released into circulating hemolymph during larval development. Incubation of *H. virescens* primary midgut cell cultures with increasing α-arylphorin titers resulted in dose-dependent ISC proliferation relative to untreated controls. Oral ingestion of purified α-arylphorin stimulated dose-dependent ISC proliferation manifested by a significantly higher number of mitotic cells in histological midgut tissue sections. To further test the role of α-arylphorin-mediated ISC proliferation during development of *H. virescens* larvae, we attempted RNA interference (RNAi) to transiently silence α-arylphorin gene expression in intestinal tissues, but variations in arylphorin gene expression prevented successful confirmation of gene knockdown. However, larvae with silenced α-arylphorin showed no detectable decrease in weight gain compared to controls. These data confirm that α-arylphorin is a mitogenic component that induces ISC proliferation *in vivo* in *H. virescens* larvae. Moreover, our data highlights the complexity and biological significance of hemolymph growth factor fluctuations during larval development.

2.1 Introduction

Endocrine signaling triggers the activation of molting during insect development. In lepidopteran larvae, this process is characterized by a concomitant 200-fold expansion of the intestinal epithelium surface area (Baldwin and Hakim 1991; Riddiford 1994). The genetic

tractability of *Drosophila melanogaster* (fruit fly) has allowed the characterization of the intestinal regenerative biology in this insect, with similarities expected to occur in alternative insect groups. In *Drosophila*, multipotent intestinal stem cells (ISCs) residing in niches between mature cells and adjacent to the basal lamina undergo asymmetrical proliferation, which generates one stem-like cell and an intermediate daughter cell (enteroblast) (Ohlstein and Spradling 2007). Enteroblast differentiation to the enterocyte or enteroendocrine lineage is subsequently determined by the strength of intrinsic Notch signaling (Micchelli and Perrimon 2006; Ohlstein and Spradling 2006). Although ISCs are the only proliferative cell type in the insect gut, mature (differentiated) cells can undergo endoreplication whereby DNA synthesis is uncoupled from mitosis, resulting in polyploid nuclei (Micchelli and Perrimon 2006; Ohlstein and Spradling 2006, 2007; Smith and Orr-Weaver 1991). This endoreplicative process enables differentiated cells to increase in size and maximize mRNA and protein synthesis (Lee, H. O. et al. 2009; Lemaitre and Miguel-Aliaga 2013). While asymmetrical ISC proliferation and differentiation has also been observed in several lepidopteran and coleopteran species, the molecules involved in controlling this process in Lepidoptera are mostly unknown.

Previous research identified an extract from fat body of *Heliothis virescens* (tobacco budworm) and *Manduca sexta* (tobacco hornworm) larvae as containing growth factors capable of inducing regeneration in primary midgut cell cultures from these insects (Loeb and Hakim 1996). The hexameric storage protein alpha-arylphorin (α-arylphorin) was proposed as one of the mitogens from fat body with a potential role in lepidopteran midgut growth and regeneration (Blackburn, Loeb et al. 2004). This protein is synthesized primarily by perivisceral fat body tissue and released into the circulating hemolymph of intermolt larvae (Kramer, Mundall et al. 1980), although it has also been detected as secreted by midgut cells towards the basal lamina (Palli and Locke 1987c). *In vitro* bioassays demonstrated that monomeric α-arylphorin induced dose-dependent proliferation of primary ISC cultures from *Heliothis virescens* (Blackburn, Loeb

et al. 2004), *Leptinotarsa decemlineata* (Colorado potato beetle) and *Spodoptera littoralis* (African cotton leafworm) larvae (Hakim, Blackburn et al. 2007). Moreover, these analyses also supported that maximal ISC proliferation occurred in response to α-arylphorin titers between 100-125 μM, above which the mitogenic effect significantly and rapidly decreased. This observation is in agreement with reduced α-arylphorin levels observed after the initiation of apolysis but prior to the completion of ecdysis into the fat body tissue, which allows α-arylphorin to serve as an amino acid reserve for non-feeding pharate larvae (Haunerland 1996; Telfer, Keim et al. 1983). Consequently, we hypothesized a dual role of arylphorin as storage protein and growth factor depending on concentration. A prediction from this hypothesis is that expansion of the midgut epithelium prior to completion of ecdysis necessitates a sufficient reduction of α-arylphorin titers in the hemolymph to levels that no longer inhibit stem cell proliferation. This tight dependency on α-arylphorin concentration would be consistent with the existence of a negative feedback mechanism whereby high α-arylphorin titers in intermolt hemolymph suppress ISC proliferation during the larval feeding period until initiation of the molting process.

In the present study, we tested the *in vitro* effects of α-arylphorin on *H. virescens* primary ISCs and the *in vivo* effects of α-arylphorin supplementation on proliferation of ISCs in the *H. virescens* larval midgut epithelium. Treatment of primary stem cell cultures with purified α-arylphorin demonstrated its mitogenic activity. Using immunohistochemical staining we discriminated and recorded the relative abundance of stem, mitotic, polyploid, and mature cells in midgut tissue sections from control and α-arylphorin-supplemented *H. virescens* larvae. Further, we silenced expression of the α-arylphorin gene in *H. virescens* larvae and determined its effect on ISC proliferation and larval growth by comparing to control larvae.

2.2 Materials and methods

2.2.1 Insects

H. virescens eggs were purchased from Benzon Research Inc. (Carlisle, PA). After hatching, larvae were maintained on artificial diet (BioServ, Frenchtown, NJ) as described elsewhere (Jurat-Fuentes et al. 2011), under a 16L:8D photoperiod at 26°C.

2.2.2 Purification and proteomic analysis of α-arylphorin

Hemolymph was collected from 60 pharate 5th instar *H. virescens* larvae by making a small incision at the base of the first 1st and/or 2nd proleg and collecting droplets of hemolymph into 15 mL conical centrifuge tubes (Falcon™) containing 5 mg of phenylthiourea (to block hemolymph phenoloxidase activity) and maintaining on ice. After collection, hemolymph was frozen at -20°C until used (no longer than 2 months). Frozen hemolymph was thawed on ice and diluted 5-fold in 20 mM Tris pH 7.9 (buffer A). For fractionation, hemolymph was filtered (0.22 μm) and loaded onto a HiTrap Q HP column (GE Healthcare), previously equilibrated with buffer A and connected to an AKTA FPLC system (GE Healthcare). Proteins were eluted with a 0-1 M linear gradient of 20 mM Tris 1 M NaCl pH 7.9 (buffer B) at a flow rate of 1 mL/min, collecting 1 mL fractions. To reduce the presence of smaller proteins co-purifying with α-arylphorin, fractions containing α-arylphorin (based on Western blotting, described below) were combined and filtered using an Amicon Ultra-15 mL centrifugal unit (Millipore) with a MWCO of 50 kDa. After concentration, partially purified α-arylphorin was quantified by the method of Bradford (Bradford 1976) with the Coomassie Plus Protein Assay (Pierce) using BSA as the standard, and then aliquoted and maintained at -80°C.

To assess the purity of the partially purified α-arylphorin preparation, it was analyzed by one-dimensional electrophoresis followed by nano liquid chromatography and tandem mass

spectrometry (1Dgel-LC-MS/MS, MS Bioworks, Ann Arbor, MI). The sample was loaded onto a Bis-Tris SDS-10% PAGE gel (Novex, Invitrogen) and separated approximately 1 cm. Following Coomassie staining and excision of the mobility region, gel segments were washed with 25 mM ammonium bicarbonate and acetonitrile, and then reduced with dithiothreitol (10 mM) at 60°C and alkylated with 50 mM iodoacetamide at room temperature. The sample was then digested with trypsin (Promega) for 4-h at 37°C and digests pooled, concentrated and analyzed with a Waters NanoAcquity HPLC system interfaced to a ThermoFisher Orbitrap Velos Pro. The fifteen most abundant ions were selected for MS/MS and data were queried against a custom database containing a complete *H. virescens* transcriptome (Perera *et al*. submitted) using Mascot (Matrix Science, London, UK). Carbamidomethylation was specified as a fixed modification, whereas methionine oxidation, N-terminal acetylation, N-terminal glutamate to pyroglutamate conversion, and deamidation of asparagine and glutamine were all specified as variable modifications. Search parameters included a peptide mass tolerance of 10 ppm, fragment mass tolerance of 0.6 Da, and 2 maximum missed cleavages. Mascot DAT files were parsed into the Scaffold software (Proteome Software, Inc., Portland, OR) for validation, filtering and to create a non-redundant list per sample. Data were filtered using a minimum protein value of 99.9%, a minimum peptide value of 97.5% (Prophet scores) and required at least five unique peptides per protein for valid identification.

2.2.3 Sequence analysis

To identify open reading frames for in arylphorin contigs in a custom *H. virescens* transcriptome, nucleotide sequences were translated using the ExPASy translate tool (Artimo et al. 2012), and then the amino acid sequences were used to query the NCBInr database using BLAST (Altschul et al. 1990). Multiple sequence alignments with 90 BLAST hits, excluding predicted sequences, were constructed and percent identity scores were calculated from single

pairwise sequence alignments using Clustal Omega version 1.2.1 (Sievers et al. 2011), hosted by the European Molecular Biology Laboratory – European Bioinformatics Institute (EMBL-EBI) and Molecular Evolutionary Genetic Analysis (MEGA) software version 6.06 (Tamura et al. 2013). Data obtained from alignments were used to generate a phylogenetic tree in MEGA using the Neighbor-Joining (NJ) algorithm and bootstrap analysis of 1,000 replicates was estimated by the Jones-Taylor-Thornton model of amino acid substitution (Jones et al. 1992).

2.2.4 Electrophoresis and Western blotting

To identify FPLC fractions containing α-arylphorin, 5 μL aliquots of fractions corresponding to major absorbance peaks on the FPLC chromatogram were resolved by SDS-10% PAGE followed by staining with ProtoBlue Safe (National Diagnostics, Atlanta, GA) or electrotransferred overnight at 4°C to PVDF Immobilon-P filters (Millipore) using 20 mV constant voltage. Filters were blocked by incubating in blocking buffer (PBS pH 7.4, 0.1% Tween-20, 3% BSA) for one hour at room temperature, and then probed with rabbit antisera (1:10,000 dilution in blocking buffer) against a 14 amino acid peptide (CQRSNNYNIHSEKNY) of *H. virescens* α-arylphorin (p76) (GenScript, Piscataway, NJ). After washing filters 6 times (10 min per wash) in washing buffer (PBS pH 7.4, 0.1% Tween-20, 0.1% BSA), they were probed with a 1:20,000 dilution of anti-rabbit antisera conjugated to horseradish peroxidase (HRP) in washing buffer for one hour. Filters were then washed as previously and developed using the SuperSignal™ West Pico chemiluminescence substrate (Pierce) followed by exposure to photographic film.

2.2.5 Preparation of primary midgut cell cultures

Primary *H. virescens* midgut cell cultures were prepared in a biological safety cabinet as previously (Castagnola, Eda et al. 2011), with minor differences. After anesthetization, surface sterilization, dissection, and removal of contaminating particles and tissues from fourth instar *H.*

virescens midguts, five to six whole midguts were incubated in incubation media, a 3:1 ratio of Grace's Insect Medium containing lactoalbumin hydrosylate and yeastolate (Invitrogen, CA) supplemented with 1x antibiotic/antimycotic, 0.1% gentamicin and sterile Ringer's. Midguts were incubated for 90 minutes without cutting into smaller sections to permit migration of loosely associated ISCs into the incubation media. Media containing mostly ISCs was passed through a 70-μm filter, large tissue fragments caught in the sievate were discarded, and the filtrate was centrifuged for 5 min. at 600 x g. Density gradient centrifugation with a suspension containing primary ISCs was performed as described elsewhere (Loeb and Jaffe 2002). The stem cell-enriched filtrate was suspended in 1 mL of working Grace's media overlaid on 3 mL of Ficoll-Paque (GE LifeSciences, NJ) in a 15 mL conical tube and centrifuged (600 x *g* for 15 minutes at 4°C). Stem cells were collected from the top 1 mL and the remaining 2 mL volume was discarded. Residual Ficoll-Paque was eliminated from midgut stem cell samples by washing twice with incubation medium (600 x *g* for 5 minutes at 4°C). Final stem cells pellets were suspended in 0.3 mL of working Grace's and counted using a hemacytometer (Bright-Line, Horsham, PA). Using this procedure, we obtained approximately 2.5 x 10^5 stem cells from 30 larvae.

2.2.6 *In vitro* cell proliferation assays

Primary midgut stem cell cultures (minimum 80% stem cells) were diluted to 2 x 10^5 cells/mL in working Grace's, and 10 μL were seeded per well of a 24-well plate containing working Grace's supplemented with 20 mM Tris pH 7.9 (control), or containing 0.5 or 1.0 mg/mL of partially purified α-arylphorin. Cultures were kept in a sterile incubator at 26°C, and after 8 hours they were collected into sterile microcentrifuge tubes. Cell proliferation was determined using an Accuri C6 flow cytometer (BD Biosciences). The forward scatter channel (FSC) threshold was set to 60,200 to exclude debris, and total events in 400 μL were counted.

Statistical significance of differences among treatments was tested using a Student's t-test (p<0.05) in the SigmaPlot v 12.0 software (Systat Software Inc., IL).

2.2.7 Arylphorin feeding bioassays

Artificial diet was dispensed into wells of 128-well bioassay trays (both from Bio-Serv, Flemington, NJ) and left to dry in a laminar flow cabinet. A five-concentration dilution series of α-arylphorin (0.195, 0.781, 3.125, 12.5, or 50.0 μg/mL) was prepared in 20 mM Tris, pH 7.9 and distributed (75 μL) to the dry diet surface of each well and gently swirled to ensure even coating. Upon drying, a single neonate larva was placed in each well and the wells were covered with pressure-sensitive polyethylene seals (BioServ, Pittman, N.J.). Larvae were allowed to feed on diet containing α-arylphorin for five days under standard rearing conditions. Bioassays were conducted with 16 neonate larvae per α-arylphorin treatment and replicated three times.

2.2.8 EdU incorporation and preparation of histological midgut sections

Synthesis of DNA in polyploid mature and proliferative stem cells was detected by incorporation of the thymidine analog 5-ethynyl-2'-deoxyuridine (EdU), following manufacturer's recommendations (Click-IT® Plus EdU Imaging Kit, Molecular Probes). Each larvae received a 10 μL intrahemocoelic injection of 0.5 mM EdU in PBS using a 26s gauge syringe (Hamilton, Reno, NV), and was returned to diet. At approximately 5 hours post-microinjection, a small incision was made at the base of one proleg of each larva to facilitate the hemocoelic infusion of fixative. Larvae (4-6 per treatment) were then placed in Tissue-Loc biopsy cassettes (Thermo Scientific) that were submerged in freshly prepared ice-cold Carnoy's solution (60% EtOH, 30% chloroform, 10% glacial acetic acid) and stored at 4°C overnight. Biopsy cassettes were then transferred to freshly prepared 70% EtOH. Larval tissues were processed using a Tissue-Tek VIP processor (Sakura, Torrance, CA) and embedded in paraplast medium (Sigma-Aldrich, St.

Louis, MO). Block sections were obtained by cutting 5 μm slices using a Micron HM355s microtome (Thermo Scientific). For hematoxylin and eosin (H&E) staining and immunostaining, tissues were mounted on Fisherbrand Superfrost and Superfrost Plus Slides (Fisher Scientific, Waltman, MA), respectively, according to recommended guidelines (Slaoui and Fiette 2011).

Slides prepared for immunostaining were deparaffinized by two 10 minute washes in xylene followed by a rehydration series of ethanol washes (absolute, 95%, 70%) for 5 minutes each, and finally washed twice for 5 minutes in ddH_20. Tissues were permeabilized by treatment with 10 mM citrate buffer pH 6.0 at 95-99°C for 20 minutes and rinsed in two 1-minute washes of PBS pH 7.4. Blocking was performed in PBS containing 0.1% Tween-20 and 3% BSA for 1 h. After blocking, detection of DNA synthesis (EdU incorporation) was performed according to the Click-iT manufacturer's instructions and tissues were mounted in medium containing DAPI (4',6-diamidino-2-phenylindole) for nuclear detection. Stained tissue sections were visualized using an EVOS® FL Auto Imaging System (Life Technologies). Stem (DAPI) and mitotic stem (EdU) cells were discriminated from mature cells on the basis of having small nuclei and being adjacent to the basal lamina, whereas mature (DAPI) and endoreplicating (EdU) cells were identified by large nuclei in the middle or apical regions of the intestinal epithelium. The relative percentage of each cell type per treatment was calculated by counting a total of 75 cells in each of three biological replicates.

2.2.9 Preparation of *H. virescens* midgut cDNA

Total RNA was extracted from frozen *H. virescens* midguts using TRI® Reagent (MRC, Cincinnati, OH) according to the manufacturer's protocol. The quantity and purity (260/280 nm ratio) of total RNA was measured with a NanoDrop 2000 Spectrophotometer. First strand cDNA synthesis was performed from 2 μg of total RNA with the High Capacity cDNA Reverse Transcription Kit (Applied Biosystems), according to the manufacturer instructions, and cDNA

was quantified with a NanoDrop 2000 Spectrophotometer (Thermo Scientific).

2.2.10 Cloning of *H. virescens* arylphorin

Contigs encoding *H. virescens* arylphorins were identified from a custom *H. virescens* transcriptome. A gene-specific forward primer, (HvAryl1, Table 1) designed based on the 5' sequences of arylphorin contigs 2428 and 2879 and olido-$dT_{(18)}$ were used to amplify an arylphorin coding sequence from 1 μg of *H. virescens* midgut cDNA using Platinum® Blue PCR SuperMix (Invitrogen™). Electrophoresis of PCR products was performed on 1% UltraPure™ agarose (Invitrogen™) using Tris-Acetate-EDTA (TAE) buffer. A 2,200 bp amplicon was excised and gel purified using the PureLink™ Quick Gel Extraction & PCR Purification COMBO kit (Invitrogen™). Restriction enzyme cleavage sites were identified using Serial Cloner version 2.6.1 (available at: http://serialbasics.free.fr/Serial_Cloner.html) and purified PCR products were enzymatically digested with FastDigest HindIII restriction enzyme (Fermentas, Pittsburgh, PA). Following the restriction digest, products were gel purified as before and ligated into pJET1.2/blunt (Thermo Scientific) according to the manufacturer's protocol. Alternatively, gel purified PCR products were ligated directly into the pPrime Cloning Vector (5 Primer, Gaithersburg, MD) according to the manufacturer's protocol. Ligation products from both procedures were used to transform *TransMax*™ chemically competent FB5α *Escherichia coli* (Fisher Scientific) according to the manufacturer's protocol. Positive transformants were selected at 37°C in LB medium supplemented with 100 μg/mL ampicillin, and plasmid DNA was extracted using the Qiaprep Spin Miniprep Kit (Qiagen, Valencia, CA).

2.2.11 dsRNA preparation and RNA interference (RNAi)

A 405 bp internal region of the p76 α-arylphorin transcript (GenBank accession number AY172683.1) was amplified from *H. virescens* midgut cDNA with the primers HvAryl-F and

HvAryl-R (Table 2) using Platinum® Blue PCR SuperMix (Invitrogen™). After 1% agarose gel electrophoresis, the PCR product was excised and purified with the QIAquick Gel Extraction Kit (Qiagen, Valencia, CA) according to the manufacturer's instructions. This fragment was used as template in PCR reactions (see Table 2 for primers) to introduce T7 RNA polymerase promoter sequences to the 5' ends. A 441 bp region of cycle 3 green fluorescent protein (GFP) was amplified from pIZT/V5-His (Invitrogen™) with the primers T7GFP-F and T7GFP-R (Table 2) and modified with T7 RNA polymerase promoter sequences as above. Double-stranded RNAs (dsGFP and dsHvarylphorin) were prepared using the PCR constructs as template with the TranscriptAid T7 High Yield Transcription kit (Thermo Scientific, Kalamazoo, MI), according the manufacturer's instructions. Following transcription, 2 μL of DNase I (1U/μL, Thermo Scientific) was added directly to each reaction and the tubes were incubated at 37°C for an additional 15 minutes. After DNase I deactivation with 2 μL of 0.5 M EDTA pH 8.0 (Thermo Scientific) and incubation at 65°C for 10 minutes, dsRNA duplexes were precipitated with 7.5 M lithium chloride (Ambion) and solubilized in 0.1% DEPC-treated deionized water. An aliquot of each dsRNA preparation was diluted 300-fold and measured with a NanoDrop 2000 spectrophotometer (Thermo Scientific), to determine 260/280 absorbance ratios and concentration. An aliquot of each construct was subjected to RNase A degradation in Saline-Sodium Citrate (SSC) buffer to confirm structural integrity of the dsRNA duplexes as previously described (Pryor and Boelen 1987). Purified dsRNAs were stored at -70°C until they were used in insect bioassays.

For RNAi, 100 μL of artificial diet was dispensed into the wells of polystyrene flat bottom 96-well plates (Fisher Scientific) using a multichannel pipet. After diet solidification, 10 μL of a 2.5 μg/μL dilution of dsGFP, or dsHvarylphorin was applied on the surface and allowed to dry in a laminar flow cabinet. Upon drying, a single neonate larva was placed in each well, and the

wells were covered with polyurethane gas permeable Breath-Easy® Membranes (MIDSCI, St. Louis, MO).

2.2.12 Real-time quantitative PCR (RTqPCR)

Total RNA was prepared from individual larvae from control (dsGFP) and experimental (dsHvarylphorin) treatment groups using TRIzol® Reagent (Ambion), according to manufacturer's instructions. Purified total RNAs were incubated at 37°C for 15 minutes in 1X DNase buffer (10 mM Tris-HCL pH 7.5, 2.5 mM $MgCl_2$, 0.1 mM $CaCl_2$) containing one unit of DNase I (Thermo Scientific) to remove contaminating genomic DNA. After inactivation of DNase I with 31 mM 0.5 M EDTA pH 8.0 (Thermo Scientific) and incubating at 65°C for 10 minutes, total RNAs were precipitated with 7.5 M lithium chloride (Ambion) and then solubilized in 0.1 % DEPC-treated deionized water. After quantification using a NanoDrop spectrophotometer, total RNA from individual larvae (12.5 ng) was used for first strand cDNA synthesis with the High Capacity cDNA Reverse Transcription Kit (Applied Biosystems), according to manufacturer's instructions. The resulting cDNAs were quantified with a NanoDrop spectrophotometer.

Relative quantities of target and reference gene transcripts in individual templates were measured in a 7900HT Fast Real-Time PCR System (Applied Biosystems) in standard mode using SDS 2.3 and SDS RQ manager software to collect threshold cycle (C_t) values for individual templates using the Power SYBR® Green PCR Master Mix. All primers used in RT-qPCR are listed in Table 2. Primers targeting α-arylphorin in a *H. virescens* transcriptome (Perera et al. submitted) were designed using Primer3 software (Untergasser et al. 2012). An *H. virescens* α-tubulin transcript identified in the transcriptome and exhibiting a high degree of similarity to *Xestia cnigrum* α-tubulin (accession number EU100015), was used as a reference gene in the relative quantification calculations. Based on data from microarray studies, this

gene has been deemed appropriate to use as an internal control (O.P. Perera, unpublished data). The target gene fold expression level in each template was calculated with triplicate threshold cycle (C_t) values normalized to a reference gene (α-tubulin) according to the method of Pfaffl (Pfaffl 2001).

2.3 Results

2.3.1 Purification of α-arylphorin from hemolymph of *H. virescens* larvae

Hemolymph from *H. virescens* larvae was used as starting material for purification of α-arylphorin using anion exchange chromatography. To identify fractions from anion exchange purification containing the expected 76 kDa band corresponding to α-arylphorin, we used silver staining and Western blotting with antisera against the p76 α-arylphorin large subunit of *H. virescens*. Two minor fused peaks ("shoulders") eluted prior to the major absorbance peak, and the fractions eluting into each of those regions were pooled to generate samples F3, F4 and F5. Electrophoretic analysis of the pooled fractions detected 8 discrete bands spanning approximately from 30-76 kDa in silver stained gels (Fig 2C). Fraction F3 contained the fewest number of detected bands apart from the expected 76 kDa band of the p76 arylphorin (Fig. 2C, lane 1), and was selected for further analysis. Probing blots of sample F3 proteins with antisera against the p76 subunit identified the 76 kDa band in the sample as arylphorin (Fig. 2D). A single band was detected when sample F3 proteins were probed with antisera against the p76 (Fig. 2A). No bands were detected with pre-immune antisera (Fig. 2B)

Proteins contained in fraction pool F3 sample were identified by 1Dgel-LC-MS/MS using a custom *H. virescens* transcriptome (Perera et al. submitted) for searches, and quantified using spectral counting. Arylphorins (transcriptome contigs 2428, 2879, 3325, and 2013 in transcriptome) accounted for 89.7% of the total spectral counts detected (Table 1). A protein blast of the four detected transcriptome arylphorin contigs showed that they were 83-91%

identical to *Helicoverpa armigera* arylphorin (accession number AEO51737.1). Much lower levels (<6%) of prophenoloxidase subunits 1 and 2 (transcriptome contigs 775 and 1927), and a trypsin inhibitor (transcriptome contig 6169) were also detected in the sample. Negligible levels (1.2%) of a 27 kDa precursor protein of unknown function from *H. virescens* (accession number ABL74241.1, transcriptome contig 14849) were also detected. The relative abundance of the detected proteins supported that fraction pool F3 represented a purified sample of α-arylphorin, which was also the only protein in the sample with reported mitogenic activity (Blackburn, Loeb et al. 2004).

2.3.2 Analysis of purity of purified α-arylphorin

In a percent identity matrix (not shown) generated from a Clustal Omega multiple sequence alignment of the *H. virescens* arylphorins detected in sample F3 (Fig. 3), contigs 2879 and 3325 were 98% identical, whereas contigs 2428 and 2013 were 95 % identical. A cross-comparison of amino acid sequences in both pairs indicated that the pairs were >85% identical, suggesting that the purified sample comprised α-arylphorin proteins representing allelic variants from possibly two highly identical α-arylphorin genes. We have cloned a full-length α-arylphorin transcript (Fig. 7). Cloned sequences are being confirmed by sequencing at the Molecular Biology Resource Facility at the University of Tennessee-Knoxville.

A BLAST query of the NCBInr database using the four *H. virescens* arylphorin contigs identified 90 sequences from 37 insect species from the orders Lepidoptera, Coleoptera, Diptera, and Hymenoptera. Phylogenetic analysis of sequences identified as hexameric, arylphorin, storage, serum, diapause-associated, and encapsulation-inducing proteins showed that amino acid sequence identity was higher within insect orders (Fig. 4). In the phylogenetic tree, all four *H. virescens* arylphorin contigs clustered into a group that also included the p76 subunit of *H. virescens* (accession number AAO20844.1) and the full-length arylphorin from *H.*

armigera (accession number AEO51737.1). Within this cluster, contigs 2428 and 2013 exhibited the highest similarity with the p76 subunit of *H. virescens* and were closely related to the full-length arylphorin from *H. armigera*. Conversely, contigs 2879 and 3325 branched off separately, indicating they were least similar to the aforementioned four arylphorin sequences.

2.3.3 α-Arylphorin bioactivity on *H. virescens* primary intestinal stem cell cultures

The mitogenic properties of the partially purified arylphorin from hemolymph were tested on freshly prepared primary midgut stem cell cultures from *H. virescens* larvae. Cultures were exposed to different concentrations of α-arylphorin for 12 hours, and the number of cells determined by flow cytometry. Microscopic inspection of cultures treated with 0.5 mg/mL α-arylphorin showed little evidence of proliferation relative to initial conditions or buffer-treated controls (compare Figs. 5A, 5B and 5C). In contrast, treatment with 1.0 mg/mL of α-arylphorin resulted in significant proliferation of stem cell cultures (Fig. 5D). These qualitative analyses were confirmed quantitatively by flow cytometry (Fig. 5E).

2.3.4 α-Arylphorin induces dose-dependent ISC proliferation *in vivo*

The *in vivo* effects of α-arylphorin ingestion on gut morphology and ISC proliferation and differentiation were tested by feeding newly emerged *H. virescens* neonates with different concentrations of purified α-arylphorin for five days. Compared to controls, hematoxylin and eosin (H&E) staining of midgut tissues from larvae fed 0.781 μg/mL of α-arylphorin showed elaborate folding of the gut epithelial membrane. In contrast, gut tissues obtained from larvae fed 12.5 and 50 μg/mL of purified α-arylphorin did not exhibit much folding and appeared similar in morphology to controls (compare Figs 6A-6D).

Staining of proliferating cells with EdU detected an apparent increase in the number of

small EdU-positive ISCs near the basal lamina of larvae fed 0.781 μg/mL purified α-arylphorin relative to controls or treatments with 12.5 μg/mL or 50 μg/mL of purified α-arylphorin (compare Figs. 6A'-6D'). Quantification of the number of stem, mitotic, mature, and endoreplicating mature cells in tissue sections stained with EdU confirmed that 0.781 μg/mL α-arylphorin induced a 2-fold increase in ISC proliferation relative to controls (p=0.003, Student's t-test), but had no effect on the number of endoreplicating mature cells (p=0.059 Holm-Sidak). High α-arylphorin titers induced a significant decrease in the percentage of endoreplicating mature cells (p=0.01, Holm-Sidak) and a significant increase in the number of non-endoreplicating mature cells (p=0.032, Holm-Sidak) relative to controls. Moreover, feeding 0.781 μg/mL α-arylphorin resulted in a significant increase in the total number of cells per midgut surface area relative to controls or the 12.5 μg/mL and 50 μg/mL treatments (p= 0.011, Holm-Sidak) (Fig. 6F).

2.3.5 Identification of α-arylphorin expressed in the *H. virescens* midgut

The full-length coding sequence of α-arylphorin was obtained by reverse transcription PCR of cDNA prepared from pooled midgut tissue obtained from 4th instar *H. virescens* larvae, using a custom *H. virescens* transcriptome as a reference for the design of gene specific primers (Fig. 7). Based on the similarity of their 5' nucleotide sequences, a gene-specific primer was designed to target contigs 2428 and 2879..

2.3.6 Developmental effects of α-arylphorin silencing on *H. virescens* larvae

The role of α-arylphorin in *H. virescens* larval development was tested using gene silencing by RNAi. Newly emerged neonates were placed on diet that was surface-contaminated with 25 μg of dsArylphorin or dsGFP (control). After 5 days, larvae treated with dsGFP weighed 4.53 ± 0.80 mg, whereas dsArylphorin-treated larvae weighed 4.35 ± 0.77 mg,

indicating that silencing of α-arylphorin had no significant effect on weight accumulation up to that point. No significant weight differences were observed when the larvae were transferred to regular diet for an additional three days.

When testing for effective RNAi response, α-Arylphorin expression was detected in less than one-half of the control (dsGFP) and treated (dsArylphorin) midgut tissues of individual *H. virescens* larvae during the RT-qPCR analysis of gene expression. Conversely, tubulin (calibrator) was detected in all samples, suggesting that α-arylphorin expression is too low and variable to draw any definitive conclusions about the effects of RNAi-mediated gene silencing in individual larvae at the developmental stage used in the bioassays.

2.4 Discussion

The intestinal epithelium of lepidopteran insects is a highly dynamic tissue involved in nutrient acquisition and metabolism as well as in the innate defensive response to invasive bacterial and viral entomopathogens (Hakim et al. 2010). During larval development, exponential midgut growth is mediated by intestinal stem cells that undergo rapid proliferation, most notably in response to ecdysteroid-induced fat body synthesis and release of growth factors into circulating hemolymph (Baldwin and Hakim 1991; Smagghe 2009). Previous studies on midgut growth factors contained in fat body extracts identified α-arylphorin as a mitogen capable of inducing proliferation of freshly prepared primary ISC cultures *in vitro* (Blackburn, Loeb et al. 2004; Hakim, Blackburn et al. 2007) or promoting the growth of several lepidopteran and coleopteran species (Hakim, Blackburn et al. 2007). However, no direct correlations between α-arylphorin and ISC proliferation *in vivo* have been reported thus far. In the absence of experiments elucidating these effects, it cannot be concluded with absolute certainty that the *in vivo* effects of α-arylphorin parallel what has been reported following *in vitro* testing. In this study, we purified α-arylphorin and developed insect bioassays to test the effects

of diverse concentrations of this protein on *H. virescens* ISC proliferation *in vivo*. The data obtained strongly support α-arylphorin titers as critical to determining the mitogenic or storage function of this protein.

The high levels of α-arylphorin (60-80% of the total soluble protein) during the penultimate instar of lepidopteran larvae (Levenbook 1985) makes hemolymph a viable source of α-arylphorin for extraction and experimentation. Using spectral counting (Liu et al. 2004) we established the relative purity of our α-arylphorin sample. Additional proteins detected in this sample, such as prophenoloxidases (I and II) and chymotrypsin inhibitors, are common hemolymph proteins involved in the hemocyte innate immune response (Shelby and Popham 2008) and the insect humoral response (Eguchi et al. 1993; Jiang and Kanost 1997; Vilcinskas and Wedde 1997), respectively. Trace levels of an uncharacterized 27 kDa protein with homology (88% identity) to an uncharacterized protein (accession number EF600055) from the gut lumen of *H. armigera* larvae (Pauchet et al. 2008) were also detected. While the function of this uncharacterized protein needs to be established, we speculate based on the trace levels detected (<2%) that it does not participate in the mitogenic activity detected for the purified arylphorin samples. Taking into consideration the relative abundances and predicted function of detected proteins in the purified sample, we concluded that it contained 98.8% of potentially mitogenic arylphorin.

Most of the described hexamerin and arylphorin protein sequences are of lepidopteran origin, yet the vast majority remains uncharacterized. Diverse hexamerin proteins seem to have similar localization (and potentially function) across insect orders. Within the cluster of coleopteran protein arylphorin sequences in our phylogenetic tree, the 86 kDa encapsulation-inducing hexamerin (accession number BAA81665) from *Tenebrio. molitor* was highly expressed in the fat body and detected in the hemolymph during the late larval stages, similar to previously characterized *T. molitor* encapsulation-related proteins (Cho, Choi, et al. 1999; Cho,

Lee, et al. 1999). Analysis of *Aedes aegypti* hexamerin-2α (accession number AAB46714) indicated that was the predominant hemolymph protein during larval development in both males and female larvae, but was not preferentially expressed by females during pupation. This suggests that dipteran hexamerins may have evolved sex-specific roles (Gordadze et al. 1999). Interestingly, two juvenile hormone-suppressible hexamerins (accession numbers BAF45385 and BAF45386) from *Plutella xylostella* larvae, that fell within the same clade as *A. aegypti* hexamerins, also exhibited sex-specific expression profiles during late larval development (Ashfaq et al. 2007). Expression of *Choristoneura fumiferana* hexamerin (accession number AAC35428) peaked prior to metamorphosis and diapause (Palli et al. 1998), whereas *Plutella. interpuctella* hexamerin (accession number AAK71136) was observed during larval development most notably prior to pupation (Zhu et al. 2002), supporting an amino acid storage role for hexamerins in both species. Arylphorins clustered with the purified α-arylphorins in this work were the *H. virescens* large subunit arylphorin p76 subunit (accession number AAO20844), *Helicoverpa armigera* arylphorin (accession number AEO51737), *Spodoptera litura* arylphorin subunit (accession number CAB55605), and two arylphorins from *Cerura vinula* (accession numbers AFP55240 and AFP55241). Analysis of expression profiles of these sequences was limited to the *H. virescens* large subunit, which indicates that these proteins are synthesized by the fat body, accumulate during larval development, and are stored in the fatbody prior to metamorphosis (Leclerc and Miller 1990).

To test mitogenic activity in the purified α-arylphorin we performed assays with primary midgut stem cell cultures, as reported elsewhere (Blackburn, Loeb et al. 2004). Based on previous reports suggesting that 100-125 ng/mL titers of α-arylphorin activate maximal proliferation of *M. sexta*, *H. virescens* and *Mamestra brassicae* (cabbage moth) primary ISC cultures after three days of incubation (Blackburn, Loeb et al. 2004; Hakim, Blackburn et al. 2007), we expected treatment of *H. virescens* primary midgut cell cultures with α-arylphorin to

induce ISC proliferation. As expected, treatment with 1.0 mg/mL α-arylphorin induced significant ISC proliferation relative to controls, although lower arylphorin levels did not result in significant proliferation. This observation may be explained by the tight dependency of stem cell proliferation on arylphorin titers. Previous reports on the mitogenic effects of α-arylphorin *in vitro* (Blackburn, Loeb et al. 2004; Hakim, Blackburn et al. 2007) indicated that titers above 100-125 ng/mL resulted in reduced proliferation. While the α-arylphorin titers used to treat our cultures exceeded those used in previous reports, one possible explanation for the lack of proliferation at the low concentration tested may be that this concentration may have been sufficient to prevent ISC proliferation but not high enough to be a detriment to the health of the culture. In contrast, the proliferative response to 1 mg/mL α-arylphorin may have resulted from mature cell death and the sequential activation of ISC proliferation. In support of this hypothesis, it has been shown previously that the activation of apoptotic signaling in enterocytes results in ISC proliferation (Apidianakis, Pitsouli et al. 2009; Jiang, Patel et al. 2009b; Loeb, Martin, Hakim et al. 2001). These results suggest that a negative feedback mechanism may regulate the ISC response to α-arylphorin titers *in vitro*. This hypothesis, while currently not well understood mechanistically, would explain the hypothesized dual function of arylphorin as mitogen (at low titers) and as a storage protein when present at high concentrations. In support of this hypothesis, high intermolt hemolymph α-arylphorin titers do not stimulate ISC proliferation (Kramer, Mundall et al. 1980; Telfer, Keim et al. 1983). Future work will be necessary to elucidate the molecular mechanism of activation of ISC proliferation and its negative regulation by increasing α-arylphorin titers.

The weight gain detected after ingestion of α-arylphorin in 4th instar *M. sexta*, 6th instar *S. littoralis*, 2nd instar *L. decemlineata*, and 6th instar *T. ni* (Hakim, Blackburn et al. 2007), supports that ISC proliferation results in expansion of the midgut epithelium. Interestingly, no effects were detected in the hemipteran *Bemisia tabaci* (silverleaf whitefly) (Hakim, Blackburn et al.

2007). Potential explanations for this specificity include sequence divergence, and physiological differences in gut architecture, including stylet canals, restrictive filter chambers (Rosell et al. 2003) and perimicrovillar membranes (Mehrabadi and Bandani 2011), that may have interrupted arylphorin action. Immunohistochemical observations of midguts from *H. virescens* larvae fed α-arylphorin detected no significant difference compared to control treatments in the number of ISCs that were not actively proliferating. This observation is in accordance with previous reports showing that asymmetrical ISC proliferation maintains a relatively constant percentage of ISCs in the intestinal epithelium (Loeb and Hakim 1996; Micchelli and Perrimon 2006; Ohlstein and Spradling 2006). In larvae treated with α-arylphorin, we detected dose-dependent ISC proliferation. Relative to larvae fed the control diet, ingestion of low α-arylphorin titers induced a significant increase in the number of small EdU positive stem cells, which are the only intestinal cells that undergo mitosis during molting (Baldwin and Hakim 1991; Sadruddin et al. 1994) or during the regenerative response to injury (Jiang, Patel et al. 2009b; Loeb, Martin, Hakim et al. 2001). Increasing the α-arylphorin titer did not result in a concomitant increase in ISC proliferation relative to controls, which is supported by previous reports showing that ISC proliferation is suppressed by hemolymph α-arylphorin titers in lepidopteran intermolt larvae (Telfer, Keim et al. 1983).

As with ISC proliferation, the number of endoreplicating mature cells in the midgut epithelium of lepidopteran larvae increases immediately prior to molting (Hakim et al. 2001). However, treatment with low α-arylphorin titers did not result in a significant difference in endoreplicating mature cells, suggesting that additional factors such as ecdysteroids may play a role in the endogenous activation of mature cell endoreplication. Conversely, endoreplicating cells were significantly reduced in the guts of larvae fed high titers of α-arylphorin relative to controls, suggesting that the suppressive effects that high α-arylphorin titers exhibit on ISC proliferation may be extended to simultaneously suppressing endoreplication of mature cells.

In contrast to treatment with low α-arylphorin titers, high α-arylphorin concentrations resulted in a significant increase of the relative percentage of mature cells in the midgut. Initially, we predicted that the relative abundance of each intestinal cell type would be comparable in the high arylphorin and control treatments, given the proposed inhibition of proliferation by high α-arylphorin titers. One possible explanation for the differences observed between controls and high α-arylphorin titers is that ISC proliferation and subsequent differentiation to mature cells could occur at a faster rate in the presence of high compared to low α-arylphorin titers. However, quantification and comparison of total cell numbers detected in gut epithelial sections confirmed that treatment with a low α-arylphorin titer was the only treatment inducing a significant increase in cell density in the intestinal epithelium. Consequently, and because there was no significant difference in total cell density between high α-arylphorin titer and control treatment, the observed increase in enterocytes may suggest increased differentiation (but not proliferation) of stem cells after treatment with high α-arylphorin titers. In fact, and while the percentage of stem cells remained constant among treatments, lower (although not significantly) numbers of mitotic cells were observed in larvae treated with high compared to low α-arylphorin titers or control treatments.

Treatment of larvae with dsRNA targeting α-arylphorin did not affect larval weight gain. In previous reports in other lepidopteran larvae, α-arylphorin mediated stimulation of ISC mitosis contributed to expansion of the intestinal epithelium and subsequently larval weight gain (Hakim, Blackburn et al. 2007). It is possible that RNAi was not induced at all or insufficiently resulting in no detectable reduction in gene expression. Furthermore, additional proteins may function redundantly as α-arylphorin to stimulate larval growth. For instance, a growth-blocking peptide (GBP) from *Psudaletia separata* (Oriental armyworm) displayed growth-inducing effects similar to arylphorin at low titers (Hayakawa and Ohnishi 1998). Considering that the

physiological titer of α-arylphorin increases while that of GBP decreases during larval development, it is interesting that they exhibit maximal mitogenic activity within the same concentration range (Ohnishi et al. 1995). To date, no direct correlations between GBP and ISC mitosis *in vitro* or intestinal epithelium expansion have been established, but functional characterizations will facilitate assigning a role of GBP in tissue-specific development in lepidopteran larvae.

Collectively, the results presented here directly link α-arylphorin to ISC proliferation *in vivo* and strongly support that the observed changes in hemolymph α-arylphorin titers are important to regulate the effect of α-arylphorin on ISC proliferation (Telfer, Keim et al. 1983; Telfer and Kunkel 1991). Similarly to the *in vitro* effects of α-arylphorin on primary midgut cell cultures from diverse insects, we observed a maximum effective concentration *in vivo* above which ISC proliferation was not observed. Future work will be necessary to identify the negative feedback mechanism responsible for the ISC response to elevated α-arylphorin titers *in vitro* and *in vivo* in repressing proliferation.

Appendix

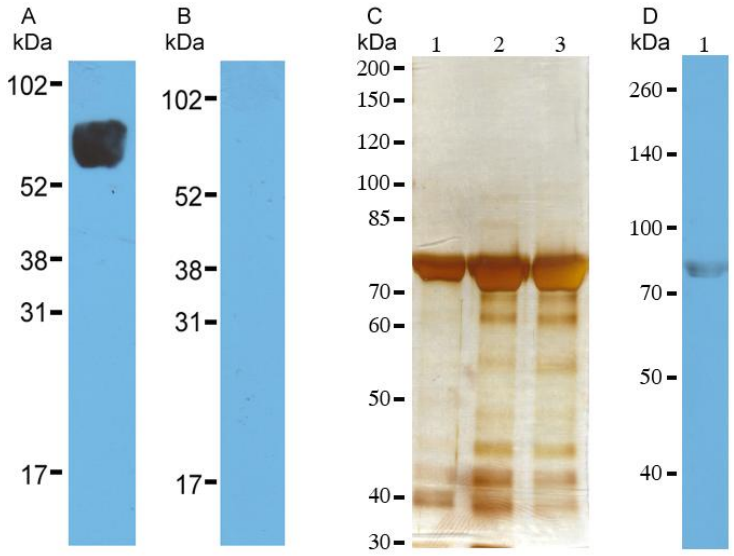


Figure 2: Silver staining and Western blotting detection of proteins in pooled fractions from anion exchange chromatography of *H. virescens* hemolymph proteins. (A) Silver stain detection of total proteins in a 10% SDS-PAGE gel containing hemolymph proteins from fraction pool F3 (lane 1), F4 (lane 2) and F5 (lane 3). (B) Detection of α-arylphorin in fraction pool F3 by Western blotting using specific antisera to the p76 arylphorin subunit.

Table 1: Proteins identified in partially purified α-arylphorin (fraction pool F3).

Contig Number	Database match (accession number)	Organism	Description	Predicted Molecular weight (kDa)	E-value	Predicted location	Spectral counts	Relative abundance (%)
2013	AEO51737.1	*Helicoverpa armigera*	Arylphorin	80	0	Fat body/ hemolymph	360	29.654
2879	AEO51737.1	*Helicoverpa armigera*	Arylphorin	81	0	Fat body/ hemolymph	314	25.865
2428	AEO51737.1	*Helicoverpa armigera*	Arylphorin	78	0	Fat body/ hemolymph	212	17.463
3325	AEO51737.1	*Helicoverpa armigera*	Arylphorin	76	0	Fat body/ hemolymph	203	16.722
6169	AAK52495.1	*Bombyx mori*	Chymotrypsin inhibitor CI-8A	43	4E-153	hemolymph	44	3.624
775	ABH10016.2	*Heliothis virescens*	Prophenoloxidase-1	78	0	Fat body/ hemocytes	38	3.130
1927	ABM65701.1	*Heliothis virescens*	Prophenoloxidase-2	79	0	Fat body/ hemocytes	29	2.389
14849	ABU98620.1	*Helicoverpa armigera*	Uncharacterized protein	25	1E-138	Multiple	14	1.153



Figure 3: Protein sequence alignment of arylphorins from *Heliothis virescens* larvae. The presence of a single fully-conserved residue (*), conservation between groups of strongly similar properties (:), and conservation between groups of weakly similar properties (.) is denoted below each residue

Figure 4: A phylogenetic tree generated by MEGA alignment of hexamerin amino acid sequences. The bootstrap values expressed as percentages of 1000 replications are shown at branch points, and GenBank accession numbers are displayed within the tree. Insect species abbreviations for Lepidoptera (black circles), Coleoptera (green triangles), Diptera (maroon squares), and Hymenoptera (red diamonds): Aa, *Aedes aegypti* (mosquito); Ad, *Anopheles darling* (mosquito); Ag, *Anopheles gambiae* (mosquito); Am, *Apis mellifera* (western honey bee); Ang, *Anoplophora glabripennis* (Asian long-horned beetle); Ap, *Antheraea pernyi* (Chinese tussah moth); Apg, *Apriona germari* (mulberry longhorn beetle); As, *Anopheles sinensis* (mosquito); Bm, *Bombyx mori* (silkworm); Caf, *Camponotus floridanus* (carpenter ant); Cb, *Cerapachys biroi* (clonal raider ant); Cc, *Corcyra cephalonica* (rice moth); Cf, *Choristoneura fumiferana* (spruce budworm); Cq, *Culex quinquefasciatus* (southern house mosquito); Cs, *Chilo suppressalis* (striped rice stem borer); Cv, *Cerura vinula* (puss moth); Dep, *Dendroctonus ponderosae* (mountain pine beetle); Dp, *Danaus plexippus* (monarch butterfly); Gm, *Galleria melonella* (greater wax moth); Ha, *Helicoverpa armigera* (cotton bollworm); Hc, *Hyalophora cecropia* (cecropia moth); Hs, *Harpegnathos saltator* (Indian jumping ant); Hv, *Heliothis virescens* (tobacco budworm); Hz, *Helicoverpa zea* (corn earworm); Lg, *Leguminivora glycinivorella* (soybean pod borer); Ms, *Manduca sexta* (tobacco hornworm); Nv, *Nasonia vitripennis* (jewel wasp); Of, *Ostrinia furnacalis* (Asian corn borer); Omf, *Omphisa fuscidentalis* (bamboo borer); Pax, *Papilio xuthus* (Asian swallowtail); Pi, *Plodia interpunctella* (Indian mealmoth); Pr, *Pieris rapae* (imported cabbageworm); Px, *Plutella xylostella* (diamondback moth); Sl, *Spodoptera litura* (Oriental leafworm); Sr, *Samia ricini* (Eri silkmoth); Tc, *Tribolium castaneum* (red flour beetle); Tm, *Tenebrio molitor* (mealworm). Protein functional abbreviations: diap, diapause associated; ei, encapsulation inducing; pa, plasminogen activator; rec, receptor; sp, serum protein; stp, storage protein; stpc, storage protein complex; unk, unknown.

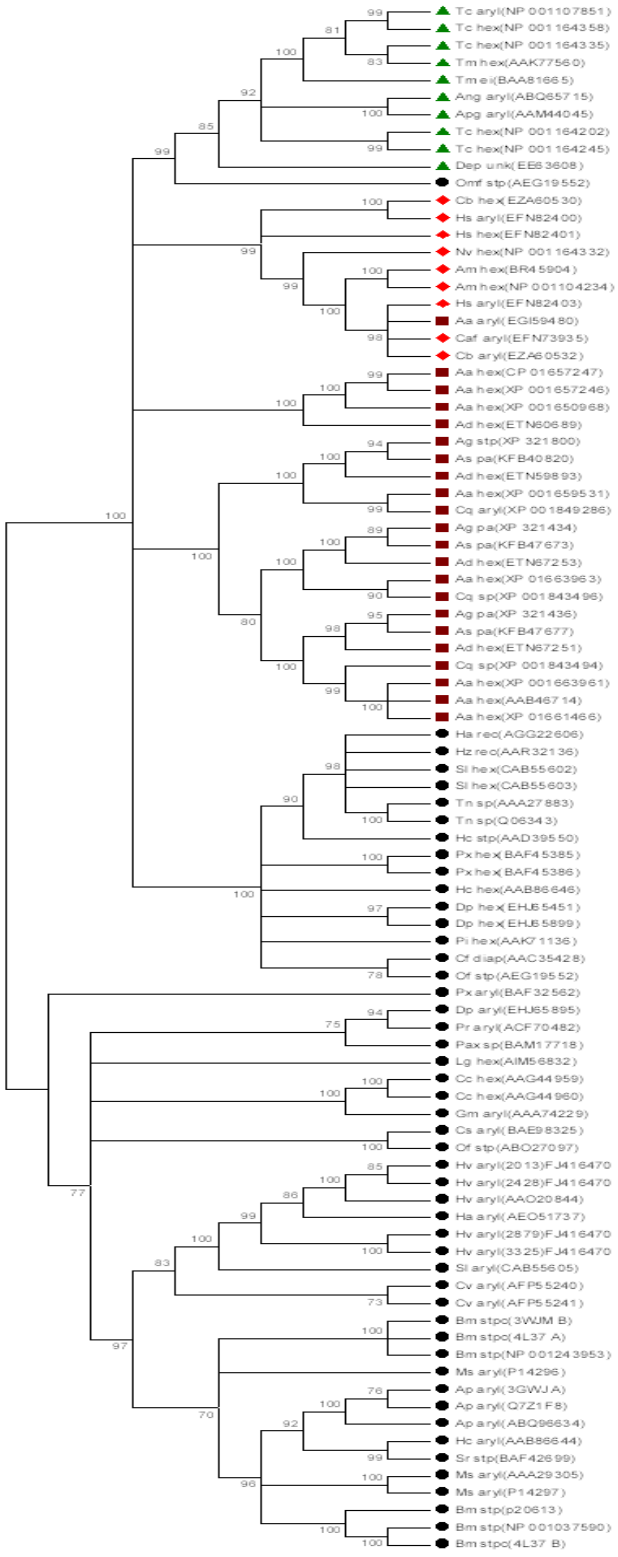


Figure 4 continued

Figure 5: Bioactivity of purified α-arylphorin on primary midgut stem cell cultures from *H. virescens* larvae. Microscopic examination of primary stem cell cultures before (A), or after treatment with control buffer (B), 0.5 mg/mL (C), or 1.0 mg/mL α-arylphorin (D) for 12 h. (E) Quantification of the number of cells in 0.4 mL of primary midgut stem cell cultures treated with control buffer (Control), 0.5 mg/mL (0.5), or 1.0 mg/mL (1.0) of α-arylphorin for 12 h. Bars denote standard error of the mean calculated from triplicate biological measurements; statistically significant differences are denoted by different letters for each column (P=0.029, Mann-Whitney rank sum test).

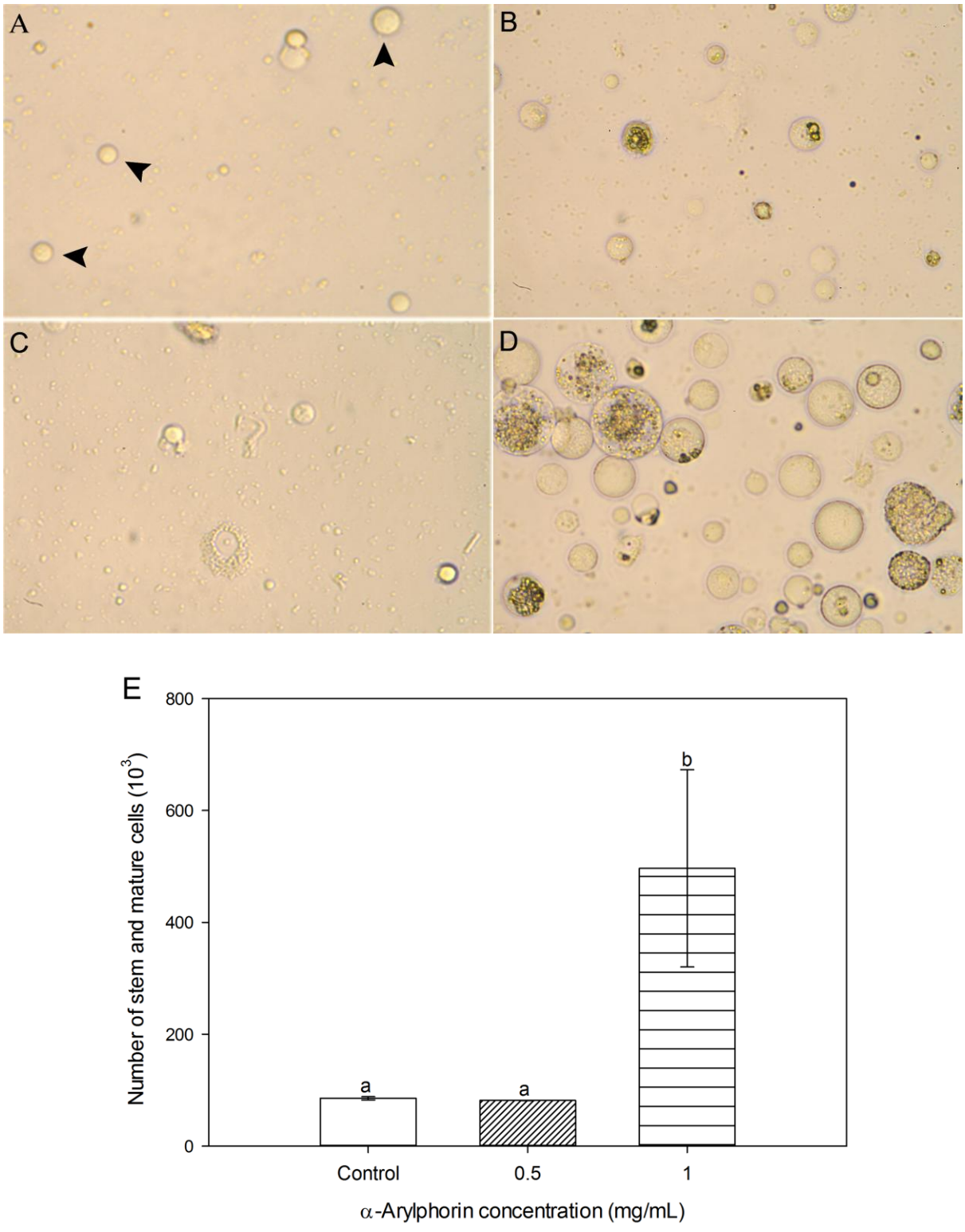
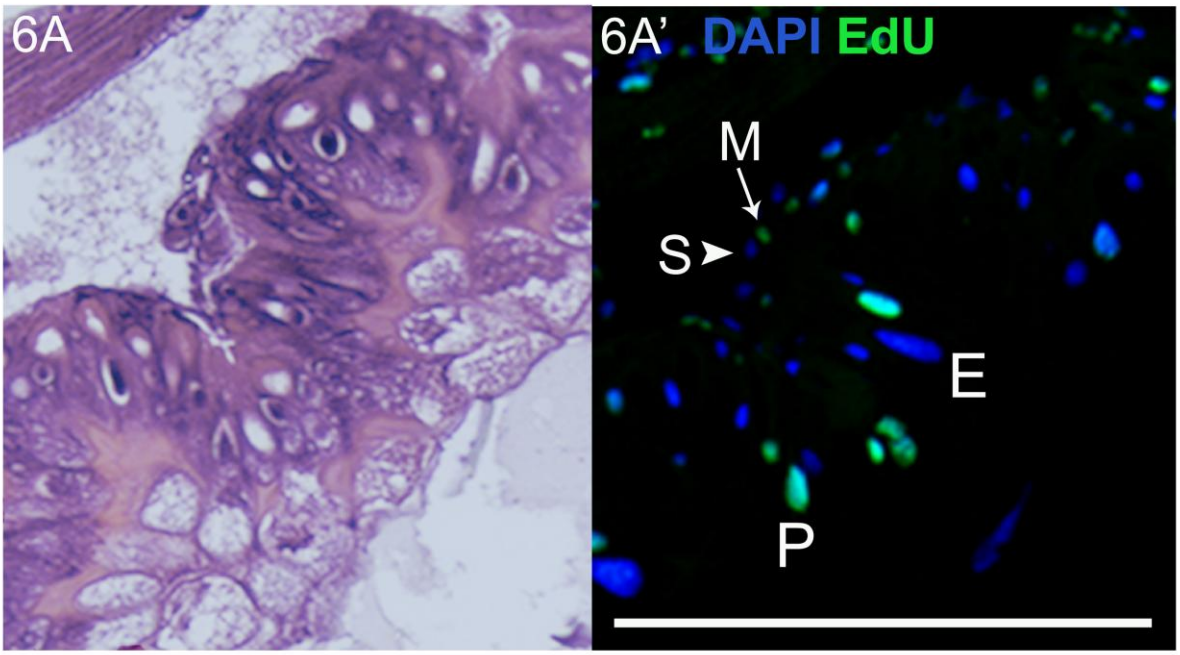


Figure 5 continued

Figure 6: Purified α-arylphorin induces dose-dependent ISC proliferation *in vivo* in *H. virescens* larvae. Immunohistological examination of midgut epithelial tissues in control (A-A'), or after treatment with 0.781 μg/mL (B-B'), 12.5 μg/mL (C-C'), or 50 μg/mL of purified α-arylphorin (D-D') for 5 days. (E) Percentage of stem (white columns), mitotic stem (green columns), mature (red columns), and polyploid mature (blue columns) cells per 75 total cells in control or larvae treated with 0.781 μg/mL, 12.5 μg/mL, or 50 μg/mL of purified α-arylphorin for 5 days. (F) Quantification of the total number of cells per 100 $\mu g/cm^2$ of midgut epithelial tissue in control (open bar), or after treatment with 0.781 μg/mL (diagonal lines), 12.5 μg/mL (horizontal lines), or 50 μg/mL of purified α-arylphorin (square) for 5 days. In E and F, bars denote standard error of the mean for each treatment calculated by counting cell types (stem, mitotic, mature, endoreplicating) and total cells in three individual midguts sections respectively; statistically significant differences within treatment groups are denoted by different letters for each column.



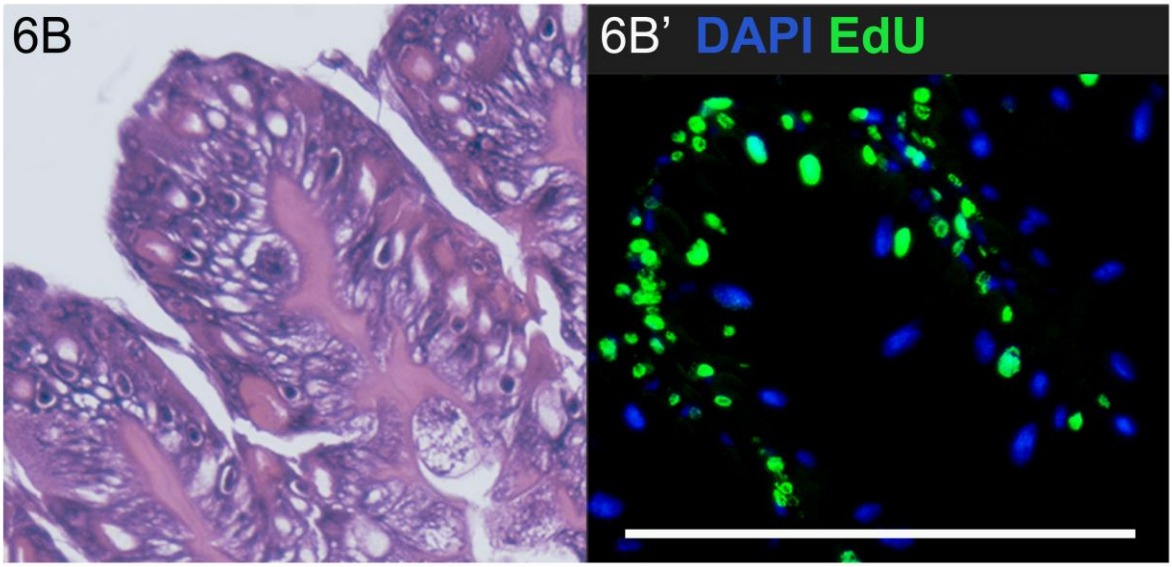
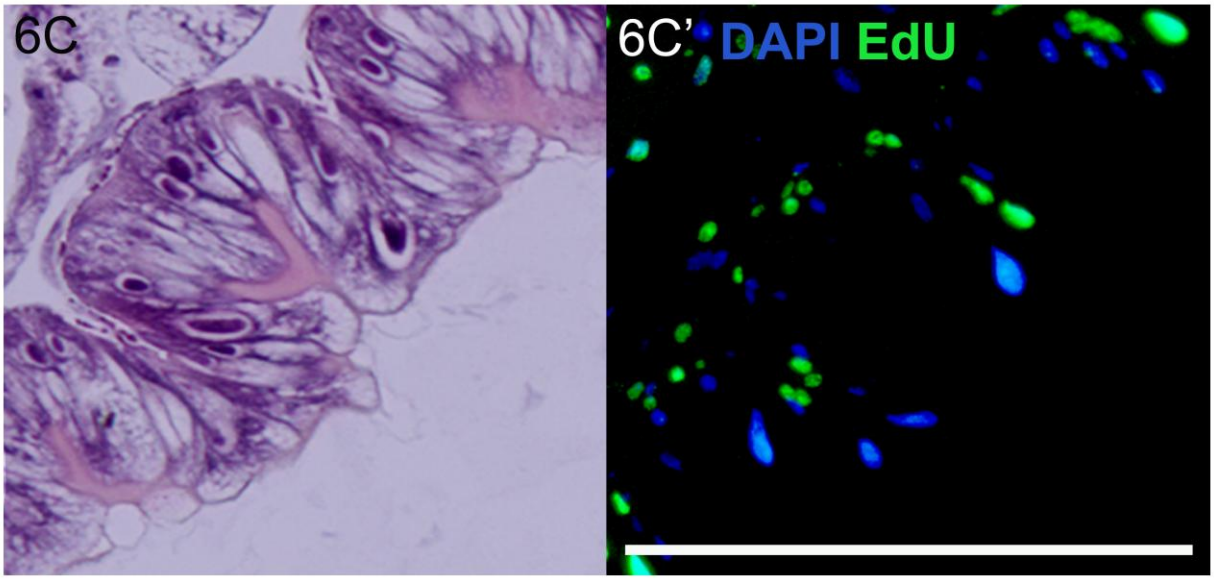


Figure 6 continued



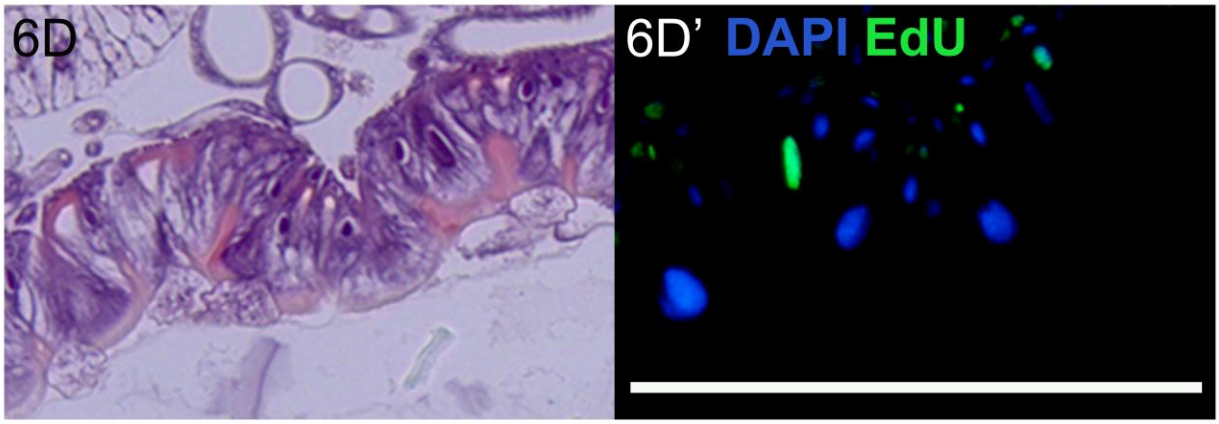


Figure 6 continued

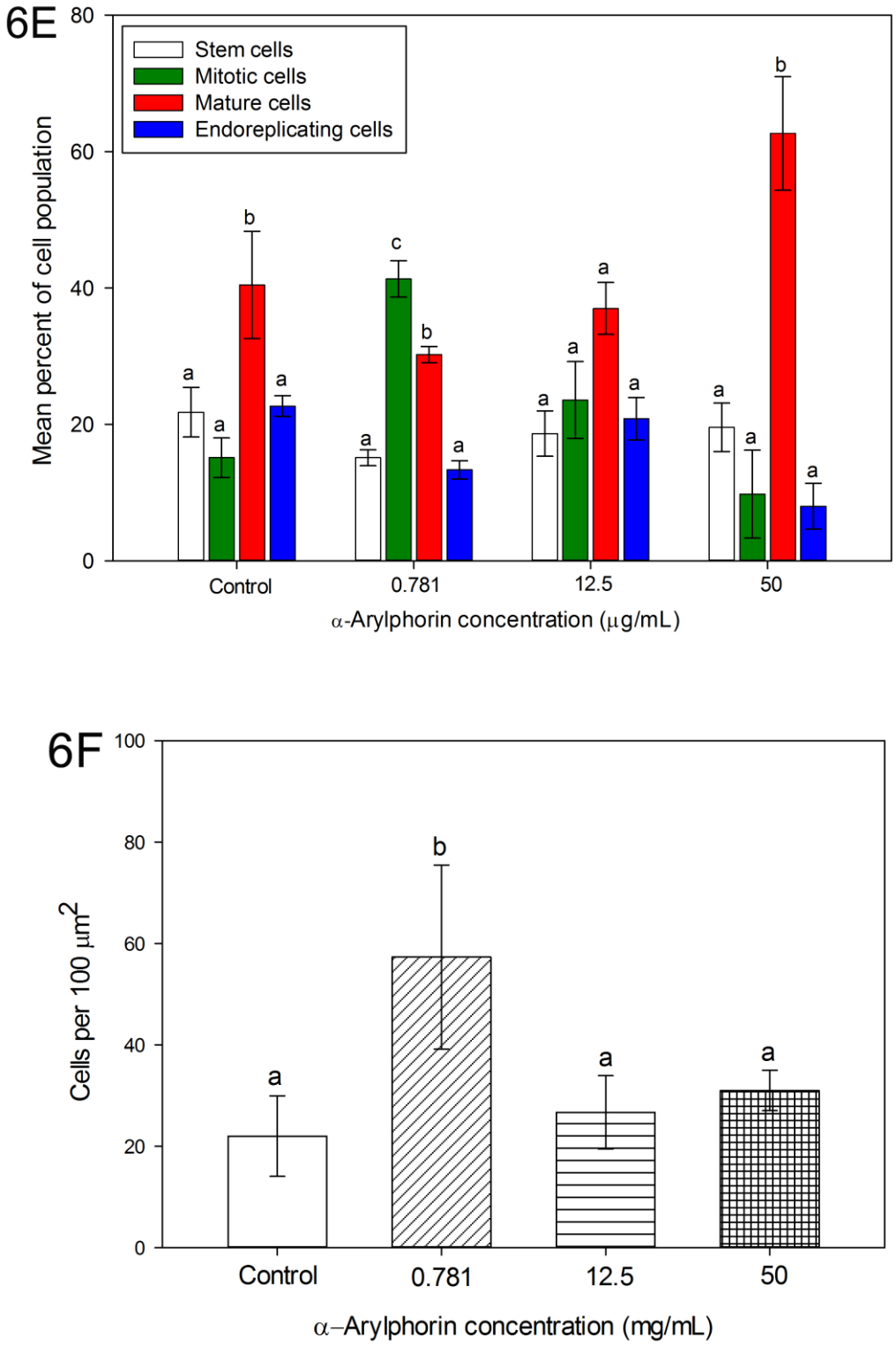


Figure 6 continued

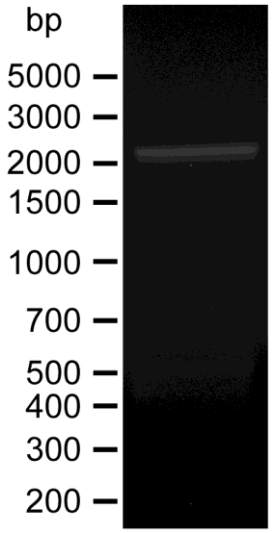


Figure 7: Amplification of full-length α-arylphorin cDNA from *H. virescens* midgut tissue. A gene specific forward primer was designed to amplify full-length α-arylphorin. PCR products were separated by 1.0% agarose gel electrophoresis.

Table 2: Primers used for cloning α-arylphorin, *in vitro* synthesis of dsArylphorin, and RT-qPCR.

Name	5' --- 3' Sequence	Direction
HvAryl1	CTGCGGTTCTGGCAACGATGAAG	Forward
OligodT	Oligo-dT(18)	Reverse
T7GFP1	TAATACGACTCACTATAGGGGGTGAAGGTGATGCTACATA	Forward
T7GFP2	TAATACGACTCACTATAGGGCATCTTCAATGTTGTGACGA	Reverse
T7Aryl1	TAATACGACTCACTATAGGGGGCAACTACTGGCACATGAA	Forward
T7Aryl2	TAATACGACTCACTATAGGGTTGACGAACAACGAATCCAG	Reverse
HvAryl3	GAGCACTCGGAACAACTTGA	Forward
HvAryl4	TTTCAGTATAACCGGCGATG	Reverse
HvTub1	CGGAGTCCAGATCGGTAACG	Forward
HvTub2	GGCTGGATTCCATGCTCAAG	Reverse

Chapter 3

Dose dependent mitogenic effect of α-arylphorin during midgut healing in response to Cry1Ac intoxication of *Heliothis virescens* larvae

This chapter to be submitted to Insect Biochemistry and Molecular Biology

Jackson, J., Miller, D.L., and J.L. Jurat-Fuentes. (2015). Dose-dependent mitogenic effect of arylphorin during midgut healing in response to Cry1Ac intoxication of *Heliothis virescens* larvae.

My contributions included: (1) devising experiments, (2) performing experiments, (3) data collection and analysis, (4) writing the manuscript and making figures. Debra Miller assisted with (3) and (4). Juan Luis Jurat-Fuentes assisted with (1), (3) and (4).

Abstract

Following damage to the insect intestinal epithelium, dying cells and visceral muscle in the surrounding niche synthesize proteins that stimulate intestinal stem cell (ISC) proliferation and differentiation to replace dying cells that are being sloughed off into the gut lumen. This regenerative mechanism has been extensively studied in several insects, yet the molecular signals mediating the intercellular communication in this response remain poorly understood, especially in non-model insects. Our previous work with *Heliothis virescens* primary midgut cell cultures (Castagnola, A., unpublished data) suggests that gut epithelial damage by Cry1Ac toxin from the gram-positive bacterium *Bacillus thuringiensis* induces a regenerative healing response mediated by α-arylphorin and involving asymmetrical intestinal stem cell (ISC) proliferation and differentiation. In this work, we tested the *in vivo* role of α-arylphorin titers during the *H. virescens* epithelial response to Cry1Ac intoxication. Oral ingestion of purified α-arylphorin significantly reduced larval mortality upon Cry1Ac toxin exposure relative to controls, but this response was dependent on the relative arylphorin dose. To understand the diverse processes occurring when midgut cells were exposed to low or high arylphorin doses, we compared histological sections and tested the possibility of binding between α-arylphorin and Cry1Ac in solution as a potential mechanism sequestering toxin and reducing larval mortality. To test the importance of α-arylphorin in gut healing after Cry1Ac intoxication, we silenced its expression by RNA interference (RNAi) and tested the effect on larval toxicity upon exposure to Cry1Ac. Our data support that mitogenic effects of α-arylphorin and its interactions with Cry1Ac toxin may alleviate intoxication, depending on the existent arylphorin titers

3.1 Introduction

Most available information describing the response of the intestinal epithelium to injury or the loss of integrity in lepidopteran larvae has been derived from histopathological studies on

the damage caused by entomopathogens such as the gram-positive bacterium *Bacillus thuringiensis* (Bt) (Forcada, Alcacer et al. 1999; Martinez-Ramirez, Gould et al. 1999; Spies and Spence 1985), the gram-negative *Photorhabdus luminescens* (Blackburn et al. 1998), or *Autographa californica* M nucleopolyhedrovirus (AcMNPV) (Hoover, K. et al. 2000; Kirkpatrick et al. 1998). *In vitro* studies using primary midgut cell cultures have complemented these analyses by revealing cell intrinsic responses to cell-free conditioned media (Sadrud-Din, Loeb et al. 1996), hormones (Goto, Loeb et al. 2005; Smagghe et al. 2005a), secondary messengers (Loeb, Clark et al. 2003), growth factors (Blackburn, Loeb et al. 2004; Hakim, Blackburn et al. 2007; Takeda, Sakai et al. 2001), and crystal (Cry) toxins from Bt (Loeb et al. 2000; Loeb, Martin, Hakim et al. 2001). Despite these extensive descriptions of the regenerative gut mechanisms in lepidopteran larvae, little is known about the molecular mechanisms involved and their regulation by growth factors.

Reports on the molecular signaling events involved in intestinal epithelial healing response to loss of integrity *in vivo* in model insects such as *Drosophila melanogaster* have focused primarily on immunohistochemical detection of intestinal stem cell (ISC) proliferation in response to acute injury or gene silencing experiments (Cordero and Sansom 2012; Cordero, Stefanatos et al. 2012; Jiang, Patel et al. 2009b). This information (reviewed in Chapter 1 of this Thesis) has greatly advanced our understanding of intestinal healing in Diptera. However, there is a current knowledge gap on potential similarities in alternative insect groups, including Lepidoptera. Moreover, these models do not sufficiently describe the molecular signaling events underlying enhanced epithelial regenerative capabilities, as reported for some lepidopteran strains, which enable them to diminish the extent of physical injury to the intestinal epithelium. Most importantly, the biochemical mediators of these tolerant phenotypes remain poorly understood.

In the case of midgut damage by Bt toxins, one instance of tolerance to a commercial Bt

formulation was associated to immune induction in a laboratory colony of *Ephestia kuehniella* (flour moth) (Rahman et al. 2004). To address the possibility that the observed immune induction was mediated through the expression and release of a pro-coagulant into the midgut lumen, a *Helicoverpa armigera* (cotton bollworm) strain exhibiting the same patterns of heritable resistance was found to up-regulate expression of a 85 kDa hexamerin upon exposure to sublethal doses of Cry1Ac (Ma et al. 2005). More recently, it was shown that membrane glycolipids and lipophorin, a diacylglycerol transport complex in hemolymph, form insoluble aggregates with Cry1Ac, suggesting a potential role for lipophorin in toxin sequestration (Blacklock and Ryan 1994; Ma et al. 2012). Similarly, resistance to Xentari (Bt formulation) in larvae from a strain of *Spodoptera exigua* (beet armyworm) was shown to involve constitutive increased expression of arylphorin (Hernandez-Martinez, Navarro-Cerrillo et al. 2010). Recent work in our group (Castagnola et al, in preparation) supported that treatment of *Heliothis virescens* (tobacco budworm) primary mature midgut cell cultures with Cry1Ac induced increased arylphorin expression, suggesting a role for arylphorin in the immune response of the midgut epithelium to Cry toxin-induced damage. While these data support that members of the hexamerin family of proteins are involved in elevated tolerance to Cry toxins, mechanistic details are lacking.

The goal of the present work was to test the effects of α-arylphorin ingestion on the intestinal epithelium during the *H. virescens* response to Cry1Ac intoxication *in vivo*. Using bioassays and immunohistochemical staining, we observed the damaging effects of Cry1Ac on *H. virescens* midgut tissue sections and monitored the effect of arylphorin ingestion on survival and regeneration. We also used competitive binding assays to examine the potential role of α-arylphorin in disrupting toxin-receptor interactions. Finally, we silenced α-arylphorin expression using RNA interference (RNAi) and determine its contribution in susceptibility to Cry1Ac toxin. Our data support a role for α-arylphorin in strengthening the intestinal epithelium prior to Cry

intoxication and reveal a previously unknown protective role against Cry1Ac in the midgut lumen.

3.2 Materials and methods

3.2.1 Insects

H. virescens eggs were purchased from Benzon Research Inc. (Carlisle, PA). After hatching, larvae were maintained on artificial diet (BioServ, Frenchtown, NJ) under standard rearing conditions of a 16-h light 8-h dark photoperiod at 26°C

3.2.2 Purification and proteomic analysis of α-arylphorin

Hemolymph was collected from 60 pharate 5th instar *H. virescens* larvae by making a small incision at the base of the first 1st and/or 2nd proleg and collecting droplets of hemolymph into 15 mL conical centrifuge tubes (Falcon™) containing 5 mg of phenylthiourea (to block hemolymph phenoloxidase activity) and maintaining on ice. After collection, hemolymph was frozen at -20°C until used (no longer than 2 months). Frozen hemolymph was thawed on ice and diluted 5-fold in 20 mM Tris, pH 7.9 (buffer A). For fractionation, hemolymph was filtered (0.22 μm) and loaded onto a HiTrap Q HP column (GE Healthcare), previously equilibrated with buffer A connected to an AKTA FPLC system (GE Healthcare). Proteins were eluted with a 0-1M linear gradient of 20 mM Tris 1M NaCl pH 7.9 (buffer B) at a flow rate of 1 mL/min, collecting 1 mL fractions. To reduce the presence of smaller proteins co-purifying with α-arylphorin, fractions containing α-arylphorin (based on Western blotting, described below) were combined and filtered using an Amicon Ultra-15 mL centrifugal unit (Millipore) with a MWCO of 50 kDa. After concentration, partially purified α-arylphorin was quantified by the method of Bradford (Bradford 1976) with the Coomassie Plus Protein Assay (Pierce) using BSA as the standard, and then aliquoted and maintained at -80°C. Analysis by one dimensional electrophoresis

followed by nano liquid chromatography and tandem mass spectrometry analysis (1Dgel-LC-MS/MS, MS Bioworks, Ann Arbor, MI) revealed that in the final partially purified sample arylphorin accounted for approximately 90% of the total protein (see Chapter 2).

3.2.3 α-Arylphorin feeding bioassays

Artificial diet was dispensed into wells of 128-well bioassay trays (BioServ, Pitman, NJ) and left to dry in a laminar flow cabinet. Once the diet was dry, a five-concentration dilution series of α-arylphorin (0.195, 0.781, 3.125, 12.5, or 50.0 μg/mL) was prepared in 20 mM Tris, pH 7.9 and distributed (75 μL) to the surface of each well and gently swirled to ensure even coating of the diet surface. Upon drying, a single neonate larva was placed in each well and the wells were covered with pressure-sensitive polyethylene seals (BioServ, Pittman, N.J.). and larvae were allowed to feed on diet containing α-arylphorin for five days under standard rearing conditions. After these five days, larvae were transferred to freshly prepared artificial diet that had been overlaid with 75 μL of activated Cry1Ac toxin (13.3 μg/mL or 0.5 μg/cm^2). The numbers of dead and surviving larvae were monitored daily during a period of seven days under standard rearing conditions. Bioassays were conducted with 16 neonate larvae per α-arylphorin treatment and replicated twice.

3.2.4 Preparation of histological midgut sections

DNA synthesis in polyploid mature and proliferative stem cells was detected by incorporation of the thymidine analog 5-ethynyl-2'-deoxyuridine (EdU), following manufacturer's recommendations (Click-IT® Plus EdU Imaging Kit, Molecular Probes). Each larvae received a 10 μL intrahemocoelic injection of 0.5 mM EdU in PBS using a 26s gauge syringe (Hamilton, Reno, NV), and was returned back to diet. At approximately 5 hours post-microinjection, a small incision was made at the base of one proleg of each larva to facilitate the hemocoelic

infusion of fixative. Larvae (4-6 per treatment) were then placed in Tissue-Loc biopsy cassettes (Thermo Scientific) that were submerged in freshly prepared ice-cold Carnoy's solution (60% EtOH, 30% chloroform, 10% glacial acetic acid) and stored at 4°C overnight. Biopsy cassettes were then transferred to freshly prepared 70% EtOH. Larval tissues were processed using a Tissue-Tek VIP processor (Sakura, Torrance, CA) and embedded in paraplast medium (Sigma-Aldrich, St. Louis, MO). Block sections were obtained by cutting 5 μm slices using a Micron HM355s microtome (Thermo Scientific). For hematoxylin and eosin (H&E) staining and immunostaining tissues were mounted on Fisherbrand Superfrost and Superfrost Plus Slides (Fisher Scientific, Waltman, MA), respectively, according to recommended guidelines (Slaoui and Fiette 2011).

Slides prepared for immunostaining were deparaffinized by two 10 minute washes in xylene followed by a rehydration series of ethanol washes (absolute, 95%, 70%) for 5 minutes each, and finally washed twice for 5 minutes in ddH_20. Tissues were permeabilized by treatment with 10 mM citrate buffer pH 6.0 at 95-99°C for 20 minutes and rinsed in two 1-minute washes of PBS pH 7.4. Blocking was performed in PBS containing 0.1% Tween-20 and 3% BSA for 1 h. After blocking, detection of DNA synthesis (EdU incorporation) was performed according to the Click-iT manufacturer's instructions and tissues were mounted in medium containing DAPI (4',6-diamidino-2-phenylindole) for nuclear detection. Stained tissue sections were visualized using an EVOS® FL Auto Imaging System (Life Technologies). Stem (DAPI) and proliferating stem (EdU) cells were discriminated from mature cells on the basis of having small nuclei and being adjacent to the basal lamina, whereas mature (DAPI) and endoreplicating (EdU) cells were identified by large nuclei in the middle or lumen-exposed regions of the intestinal epithelium.

3.2.5 Bacterial toxin purification and labeling of Cry1Ac and arylphorin

Bacillus thuringiensis var. *kurstaki* strain HD73 producing Cry1Ac toxin was obtained from the *Bacillus* Genetic Stock Center (BGSC, Columbus, OH). Bacterial inoculation, toxin purification, activation and verification were performed as previously described (Perera et al. 2009). Purified activated toxin was quantified by the method of Bradford (Bradford 1976), using the Coomassie Plus Protein Assay (Pierce) with BSA as the standard. Radiolabeling of activated Cry1Ac and α-arylphorin (1 μg each) with 0.5 mCi of ^{125}I-Na was performed as described elsewhere (Jurat-Fuentes and Adang 2004). Labeled proteins were kept at 4°C and used within 10 days. Activated Cry1Ac was biotinylated (1:30 molar ratio) with the EZ-Link sulfo-NHS-LC-Biotin (Pierce) according to the manufacturer instructions and quantified using the method of Bradford (Bradford 1976) or with a Qubit fluorometer (Life Technologies, Grand Island, NY).

3.2.6 Electrophoresis, ligand, and lectin blotting of BBMV and α-arylphorin

For Western blots, purified α-arylphorin (2 μg) was resolved by SDS-10% PAGE followed by staining with ProtoBlue Safe (National Diagnostics, Atlanta, GA) or electrotransfered overnight at 4°C to PVDF Immobilon-P filters (Millipore) using 20 mV constant voltage. Filters were blocked by incubating in blocking buffer (PBS pH 7.4, 0.1% Tween-20, 3% BSA) for one hour at room temperature, and then probed with rabbit antisera (1:10,000 dilution in blocking buffer) against a 14 amino acid peptide (CQRSNNYNIHSEKNY) of *H. virescens* α-arylphorin (p76) (GenScript, Piscataway, NJ). After washing filters 6 times (10 min per wash) in washing buffer (PBS pH 7.4, 0.1% Tween-20, 0.1% BSA), they were probed with a 1:20,000 dilution of anti-rabbit antisera conjugated to horseradish peroxidase (HRP) in washing buffer for one hour. Filters were then washed as previously and developed using the SuperSignal™ West Pico chemiluminescence substrate (Pierce) followed by exposure to photographic film.

Ligand dot blotting experiments were done by pipetting 100 μL of α-arylphorin (100 μg/mL in 20 mM tris pH 7.9) onto a MeOH-activated PVDF filter (Millipore) contained in a 96-well Bio-Dot® microfiltration apparatus (Bio-Rad, Hercules, CA), using a multichannel pipette. Proteins were bound to the membrane through the application of vacuum. Before removing the membrane from the microfiltration apparatus, all wells were washed twice with 200 μL of blocking buffer (PBS pH 7.4, 0.1% Tween-20, 3% BSA). After removal, the membrane was divided into sections and incubated with biotinylated activated Cry1Ac toxin (0.5 μg/mL) alone or in the presence of increasing amounts of unlabeled homologous competitor for 1 hr. Following incubation, filters were washed 6 times (10 min per wash) in wash buffer (PBS pH 7.4, 0.1% Tween-20, 0.1% BSA) to remove excess unbound toxin, then probed with a 1:20,000 dilution streptavidin conjugated to horseradish peroxidase (HRP) in wash buffer for one hour. After incubation, filters were washed as previously described and developed as described above for Westerns.

For Cry1Ac ligand blots, blocked filters were incubated with 0.5 μg/mL biotinylated Cry1Ac for 1 hour in blocking buffer and washed as described for Western blots. Bound Cry1Ac was detected by incubating filters with a streptavidin-HRP conjugate for 1 hr., and then washing and visualizing by enhanced chemiluminescence as described for Western blots.

For lectin blots of α-arylphorin was electrophoresed and transferred as for Western blots, and then blocked PVDF filters were incubated with lectins from *Conavalia ensiformis* (ConA, at 1 μg/mL) or *Glycine max* (soybean agglutinin, SBA, at 1 μg/mL) for 1 hour in blocking buffer (PBS pH 7.4, 0.1% Tween-20, 3% BSA). Both ConA and SBA were conjugated to HRP (Sigma) and were detected using enhanced chemiluminescence as described for Westerns. *H. virescens* BBMV (15 μg) were used as a positive control for lectin binding.

3.2.7 Preparation of brush border membrane vesicles (BBMV)

Individual larvae or dissected midguts were used for BBMV preparation by the $MgCl_2$ precipitation method (Wolfersberger et al. 1987). Individually frozen larvae were homogenized in 500 μL SET buffer (250 mM sucrose, 5 mM EGTA, 17 mM Tris-HCL pH 7.5) with Complete protease inhibitors (Pierce) for 30 seconds with a Brinkmann Polytron PT-2100 homogenizer (Kinematica Inc., Bohemia, NY). An equivalent volume of ice-cold 24 mM $MgCl_2$ 250 mM sucrose was added to the homogenate, followed by incubation on ice for 15 minutes. Homogenates were centrifuged at 4,600 rpm for 15 minutes at 4°C to pellet debris. Supernatants were collected and centrifuged at maximum speed in a microcentrifuge for 20 minutes at 4°C. BBMV pellets were re-suspended in 30-40 μL phosphate buffered saline (PBS) pH 7.5 with protease inhibitors and quantified by the method of Bradford using BSA as a reference (Bradford 1976).

3.2.8 Cry1Ac binding competition assays

Competition experiments were done by incubating 1.3 nM ^{125}I-Cry1Ac with 20 μg *H. virescens* BBMV for 1 h at room temperature in the presence of increasing amounts of unlabeled activated toxin or α-arylphorin in a final volume of 0.1 mL of binding buffer (PBS, pH 7.4, 0.1 % BSA). After incubation, BBMV and bound proteins were pelleted by centrifugation at maximum speed for 10 min in a microcentrifuge and washed in 0.5 mL ice-cold binding buffer. Following a second centrifugation and wash, the radioactivity in each pellet was measured in a Wizard^2 gamma counter (Perkin Elmer). The radioactivity of BBMV pellets incubated with toxin in the absence of competitor represented the 100% binding in all reactions and was used as a reference to calculate the percent of toxin remaining bound in the presence of increasing competitor concentrations.

Binding of biotinylated Cry1Ac toxin to BBMV proteins (25 μg) of *H. virescens* larvae was

analyzed as previously described (Jurat-Fuentes et al. 2002). Reactions contained BBMV, binding buffer (PBS, 0.1 % BSA), 7.69 nM biotinylated Cry1Ac, and in competition assays increasing concentrations of unlabeled α-arylphorin or 300-fold excess unlabeled Cry1Ac or Cry3Aa for 1 hour at room temperature. Following incubation, BBMV were centrifuged at maximum speed in a microfuge for 10 minutes at 4°C. After centrifugation, pellets were washed twice in 0.5 mL of binding buffer and the final BBMV pellets were solubilized and resolved by SDS-10%% PAGE. Bound biotinylated Cry1Ac was electrotransferred overnight in transfer buffer (192 mM glycine, 25 mM Tris, 0.1% SDS, 20% methanol) at 4°C to PVDF Immobilon-P filters (Millipore) using 20 mV constant voltage. Filters were blocked by incubating in blocking buffer (PBS pH 7.4, 0.1% Tween-20, 3% BSA) for one hour at room temperature, and then probed with streptavidin-peroxidase conjugate (1:20,000 dilution in blocking buffer) for 1 h. After washing filters 6 times (10 min per wash) in washing buffer (PBS pH 7.4, 0.1% Tween-20, 0.1% BSA), biotinylated toxins were visualized using the SuperSignal™ West Pico chemiluminescent substrate (Pierce) followed by exposure to photographic film.

3.2.9 Digestion of α-arylphorin with peptide-N-glycosidase F

N-linked oligosaccharides on α-arylphorin were released by digestion of blotted α-arylphorin with peptide-N-glycosidase F (PNG-F). α-Arylphorin (2 μg) was resolved by SDS-10% PAGE and transferred to PVDF Immobilon-P filters (Millipore) as described above for Western blots. Filters were then incubated in 10 mL of NaCl/Pi buffer (pH 7.4) containing 0.1% SDS, 0.5% Triton-X-100 and 1.08 mU of PNG-F (Boehringer-Mannheim) for 20 hours with gentle shaking at 37°C. Following treatment, filters were blocked and processed as described for biotinylated-Cry1Ac and ConA blots above.

3.2.10 Preparation of double stranded RNA (dsRNA)

A 405 bp internal region of α-arylphorin (accession number: AY172683) was amplified from *H. virescens* midgut cDNA with the primers T7Aryl1 and T7Aryl2 (Table 3) using Platinum® Blue PCR SuperMix (Invitrogen™). After 1% agarose gel electrophoresis of the PCR product, the band was excised and purified with the QIAquick Gel Extraction Kit (Qiagen, Valencia, CA) according to the manufacturer's instructions. The cDNA template for *in vitro* transcription of α-arylphorin was generated from the purified PCR product using gene-specific primers (Table 2) flanked on the 5' ends by the T7 RNA polymerase promoter sequence. A 441 bp region of cycle 3 green fluorescent protein (GFP) was amplified from pIZT/V5-His (Invitrogen™) with the primers T7GFPF and T7GFPR and used as a negative control template. Double stranded RNA (dsRNA) was prepared with the TranscriptAid T7 High Yield Transcription Kit (Thermo Scientific, Kalamazoo, MI) according to the manufacturer's instructions. Following transcription, 2 μL of DNase I (Thermo Scientific) was added directly to each reaction and the tubes were incubated at 37°C for an additional 15 minutes. DNase I was deactivated by adding 2 μL of 0.5 M EDTA pH 8.0 (Thermo Scientific) and incubating at 65°C for 10 minutes. dsRNA duplexes were precipitated with 7.5 M lithium chloride precipitation solution (Ambion) according to the manufacturer instructions and solubilized in 0.1% DEPC-treated deionized water. An aliquot of each dsRNA preparation was diluted 300-fold and measured with a NanoDrop 2000 spectrophotometer (Thermo Scientific) to determine 260/280 absorbance ratios and concentration. To confirm the structural integrity of the dsRNA duplexes, we subjected an aliquot of each construct to RNase A degradation in Saline-Sodium Citrate buffer (SSC) as previously described (Pryor and Boelen 1987). Purified dsRNAs were stored at -70°C until they were used in insect bioassays.

3.2.11 Silencing of α-arylphorin expression by RNA interference (RNAi)

For RNAi silencing bioassays, 100 μL of artificial diet was dispensed into the wells of polystyrene flat bottom 96-well plates (Fisher Scientific) using a multichannel pipet. After diet solidification, 10 μL of a 2.5 μg/μL dilution of dsGFP, or dsHvarylphorin was applied on the surface using a pipet and allowed to dry in a laminar flow cabinet. Upon drying, a single neonate larva was placed in each well, and the wells were covered with polyurethane gas permeable Breath-Easy® Membranes (MIDSCI, St. Louis, MO). Larvae were then allowed to feed on diet containing dsRNA for five days under standard rearing conditions. After five days, larvae were flash frozen in liquid nitrogen (LN_2) or transferred to freshly prepared artificial diet that had been overlaid with 75 μL of activated Cry1Ac toxin (45 $\mu g/cm^2$) or control diet overlaid with buffer. The number of dead and surviving larvae was monitored for seven days.

3.2.12 Real Time Quantitative PCR (RT-qPCR)

Total RNA was prepared from individual larvae from control (dsGFP) and experimental (dsHvarylphorin) treatment groups using TRIzol® Reagent (Ambion), according to the manufacturer instructions. Total RNAs were incubated at 37°C for 15 minutes in 1X DNase buffer (10 mM Tris-HCL pH 7.5, 2.5 mM $MgCl_2$, 0.1 mM $CaCl_2$) containing one unit of DNase I (Thermo Scientific) to remove contaminating genomic DNA. After inactivation of DNase I with 31 mM 0.5 M EDTA pH 8.0 (Thermo Scientific) and incubating at 65°C for 10 minutes, total RNAs were precipitated with 7.5 M lithium chloride (Ambion) and then solubilized in 0.1 % DEPC-treated deionized water. Upon quantification in a NanoDrop spectrophotometer, total RNA from individual larvae (50 ng) was used for first strand cDNA synthesis with the High Capacity cDNA Reverse Transcription Kit (Applied Biosystems), according to the manufacturer instructions. The resulting cDNAs were quantified with a NanoDrop spectrophotometer.

Relative quantities of target and reference gene transcripts in individual templates were

measured in a 7900HT Fast Real-Time PCR System (Applied Biosystems) in standard mode using SDS 2.3 and SDS RQ manager software to collect threshold cycle (C_t) values for individual templates using the Power SYBR® Green PCR Master Mix. All primers used in RT-qPCR are listed in Table 3. Primers targeting α-arylphorin in a *H. virescens* transcriptome (Perera et al. submitted) were designed using Primer3 software (Untergasser, Cutcutache et al. 2012). A *H. virescens* α-tubulin transcript from the transcriptome, exhibiting a high degree of similarity to *Xestia cnigrum* α-tubulin (accession number EU100015), was used as a reference gene in the relative quantification calculations. The target gene fold expression level in each template was calculated with triplicate threshold cycle (C_t) values normalized to a reference gene (α-tubulin) according to the method of Pfaffl (Pfaffl 2001).

3.3 Results

3.3.1 Ingesting α-Arylphorin reduces mortality of *H. virescens* larvae exposed to Cry1Ac toxin

The *in vivo* effects of α-arylphorin-induced ISC proliferation on the midgut response to Cry1Ac exposure were tested by feeding newly emerged *H. virescens* neonates with different concentrations of purified arylphorin for five days, and then transferring all larvae to freshly prepared diet overlaid with a low-lethal dose of activated Cry1Ac toxin causing 34.5 ± 5.2% mortality (Fig. 1). Feeding on low concentrations of arylphorin (0.049 or 0.195 μg/mL) reduced larval mortality, although not significantly (16.8 ± 0.07 - 23.8 ± 0.08%). In contrast, mortality in larvae fed 0.781 μg/mL α-arylphorin was significantly reduced (14.7 ± 3.0%, $P = 0.018$) relative to control treatment. Increasing the amount of α-arylphorin fed to larvae to 12.5 μg/mL resulted in similar mortality compared to controls (31.2 ± 9.2%, $P = 0.648$). Further increase in the dose of α-arylphorin fed to the larvae to 50.0 μg/mL resulted in significantly reduced mortality (14.9 ± 4.7%) relative to controls ($P = 0.013$) (Fig 8). Based on these observations, we named the

three observed changes to Cry1Ac-susceptibility in response to increasing arylphorin dosages as phases I to III (Fig. 8)

3.3.2 Histopathology of Cry1Ac intoxication in *H. virescens* larvae fed purified α-arylphorin

After individual larvae were treated for 5 days with different titers of α-arylphorin, they were transferred to freshly prepared diet surface contaminated with 0.5 μg/cm^2 Cry1Ac toxin. Histopathological changes in the larval midguts were determined by H&E staining of tissue sections (Fig. 9). In larvae treated with buffer (control, no α-arylphorin) that were exposed to Cry1Ac for 30 minutes, we observed swelling of mature columnar cells and minimal cell sloughing. Individual ISCs were sparsely scattered along the basal lamina (Fig. 9A). Significant sloughing of dead cells and expulsion of cytoplasmic contents from ruptured mature cells into the midgut lumen could be observed after 60 minutes, indicative of cell death (Fig. 9A'). After 120 minutes, ISC nests were observed along the basal lamina, suggesting activation of the regenerative healing mechanism. Most of the mature cells had become detached from the basal lamina at this time (Fig 9A'').

In larvae treated with 0.781 μg/mL α-arylphorin, numerous ISC nests were observed along the basal lamina after 30 minutes of Cry1Ac exposure. The extent of mature cell sloughing was increased relative to controls and mature cells narrowed to allow newly differentiated mature cells to intercalate into apical positions of the epithelium, replacing sloughed cells (Fig 9B). Enlarged goblet cell cavities were detected after 60 minutes concomitant with a notable decrease in ISC nests along the basal lamina and sloughing of mature cells, suggesting that ISC differentiation and apical ascension into the epithelium had occurred to replace sloughing cells observed after 30 minutes (compare Figs. 9B and 9B'). No swelling or sloughing of mature cells was observed after 120 minutes, suggesting the epithelial healing mechanism had completed (Fig. 9B'').

When the dose of α-arylphorin was increased to 12.5 μg/mL, more extensive swelling and sloughing of mature cells into the midgut lumen was observed after 30 minutes of exposure to Cry1Ac, relative to all treatments at the same time point (compare Fig. 9C). By 60 minutes, integrity of the epithelial membrane was disordered and predominated by sloughing mature cells (Fig. 9C'). After 120 minutes extensive mature cell lysis and sloughing resulted in complete disorganization of the epithelium (Fig. 9C'').

At the highest α-arylphorin dose tested (50 μg/mL), mature cell swelling similar to the 0.781 μg/mL α-arylphorin treatment group was observed after 30 minutes of Cry1Ac exposure (compare Figs. 9C and 9D). In contrast, to the small clusters of ISCs scattered along the basal lamina of midguts from the 0.781 μg/mL α-arylphorin treatment, ISCs were detected individually along the basal lamina in midgut sections prepared from larvae treated with 50 μg/mL α-arylphorin (Fig. 9D). After 60 minutes, mature cell sloughing was observed (Fig. 9D'), but it was undetected by 120 min (compare Figs. 9D' and 9D'').

3.3.3 Cry1Ac binds specifically to α-arylphorin purified from *H. virescens* hemolymph

In ligand dot blots, binding of biotinylated Cry1Ac to immobilized α-arylphorin was significantly reduced in the presence of increasing amounts of unlabeled Cry1Ac as homologous competitor, indicative of specific binding (Fig 10A). To test if this Cry1Ac-α-arylphorin interaction could affect toxin binding to midgut receptors, we tested binding of radiolabeled Cry1Ac to brush border membrane vesicles (BBMV) from *H. virescens* in the presence of unlabeled α-arylphorin. In these competition assays, Cry1Ac binding to BBMV was not reduced by an excess of unlabeled α-arylphorin (Fig 10B). One possibility to explain the conflicting results between dot blots and in solution competition assays was that α-arylphorin could have been interacting with BBMV proteins with higher affinity than with Cry1Ac. To test

this hypothesis, we radiolabeled α-arylphorin and performed a competition assay with BBMV and unlabeled α-arylphorin as homologous competitor. The lack of specific binding detected for labeled α-arylphorin supports that this protein does not recognize receptors in the *H. virescens* BBMV (Fig. 10C).

To further test the possibility of α-arylphorin sequestering Cry1Ac toxin from binding to BBMV receptors, we performed in-solution binding assays with *H. virescens* BBMV and biotinylated Cry1Ac toxin as ligand. In these assays (Fig. 11), we used equivalent Cry1Ac:α-arylphorin ratios as used for the highest α-arylphorin treatments in our feeding bioassay (lane 2 and 3 are equivalent to the 12.5 and 50.0 μg/mL treatments). In a third reaction, we used 30-fold unlabeled α-arylphorin as competitor. For all three reactions, we observed reduced binding of biotinylated Cry1Ac to BBMV as the concentration of unlabeled α-arylphorin was increased (Fig. 11).

3.3.4 Cry1Ac recognizes an N-linked glycan moiety in *H. virescens* α-arylphorin

Since Cry1Ac binding is highly dependent on protein glycosylation, we tested if Cry1Ac binding to α-arylphorin involved oligosaccharides present on *H. virescens* α-arylphorin. Lectin blots with ConA from *Conavalia ensifomis* (Fig.12A), which recognizes N-terminal α-mannose and α-glucose (Debray et al. 1981) confirmed that α-arylphorin contains N-linked oligosaccharides. Since Cry1Ac displays specificity for N-acetylgalactosamine (GalNAc) (Jurat-Fuentes and Adang 2004) we performed lectin blots with the GalNAc-specific lectin SBA from *Glycine max* (Fig. 12A). Only a weak signal, compared to the proteins recognized by SBA among BBMV proteins, was detected for α-arylphorin. Recognition of the α-arylphorin by both lectins is further supported by detection of a band of the same molecular size in blots probed with antisera to arylphorin (Fig. 12A).

To test whether N-linked oligosaccharides mediated binding of Cry1Ac to α-arylphorin, we performed digestion of blotted α-arylphorin with PNG-F glycosidase specific to N-linked oligosaccharides. Digestion with PNG-F eliminated ConA and Cry1Ac binding to α-arylphorin (Figure 12B), confirming that N-linked oligosaccharides on this protein are critical for interaction with Cry1Ac .

3.4 Discussion

While it has traditionally been recognized as a fat body storage protein used to support tissue remodeling during larval ecdysis and construction of adult tissues during metamorphosis (Levenbook and Bauer 1984; Telfer, Keim et al. 1983), accumulating evidence suggest that α-arylphorin (Castagnola, A., unpublished data), hexamerins (Ma, Roberts et al. 2005), and hemolymph transport proteins (Ma, Rahman et al. 2012) are involved in the response of the midgut epithelium to Cry intoxication. Considering its mitotic activity on midgut cells (Blackburn, Loeb et al. 2004; Hakim, Blackburn et al. 2007), α-arylphorin may explain Cry1Ac toxin tolerant phenotypes observed in *H. virescens* associated to enhanced midgut healing (Forcada, Alcacer et al. 1999; Martinez-Ramirez, Gould et al. 1999). Data in this study suggest that the multifunctional extrahemocoelic roles of α-arylphorin in the lepidopteran midgut are regulated by its concentration and may contribute to an enhanced midgut regenerative mechanism potentially contributing to tolerance against Bt Cry toxins.

As describe earlier, ingestion of α-arylphorin purified from *H. virescens* hemolymph and topically applied to artificial diet stimulated dose-dependent ISC proliferation (Chapter 2). This observation explains the mechanism by which ingesting α-arylphorin purified from *Manduca sexta* (tobacco hornworm) fat body tissue stimulated a significant increase in larval weights of lepidopteran insects (Hakim, Blackburn et al. 2007). Extending the application of α-arylphorin

mediated ISC proliferation *in vivo*, we found that ingestion of relatively low arylphorin titers also resulted in significant reductions in susceptibility of *H. virescens* larvae to Cry1Ac toxin (phase I). Examination of histological midgut sections supported that this reduced susceptibility is associated to increased stem cell proliferation when compared to larvae not fed arylphorin. Similar observations of and enhanced regeneration mechanism were reported following Cry toxin exposure in Cry1Ac-resistant strains of *H. virescens* (Forcada, Alcacer et al. 1999; Martinez-Ramirez, Gould et al. 1999), and during sublethal Cry1Ac intoxication of *Corcyra cephalonica* (rice moth) (Chiang et al. 1986) and *Galleria mellonella* (greater wax moth) (Nishiitsutsujiuwo and Endo 1981). Similarly, resistance to *Autographa californica* M nucleopolyhedrovirus in *H. virescens* was also associated to increased rates of midgut cell renewal (Hoover, Kelli et al. 2000). Our data compare with these reports, suggesting that low titers of α-arylphorin induce an energic mitogenic response in gut stem cells that may be sufficient to enable rapid repair of the midgut epithelium following Cry toxin damage. In contrast, excessive titers of purified insect growth factors, including α-arylphorin and bombyxin, have been shown previously to inhibit ISC proliferation of primary lepidopteran cell cultures *in vitro* (Blackburn, Loeb et al. 2004; Goto, Loeb et al. 2005; Hakim, Blackburn et al. 2007). Our data clearly support that a parallel suppression of ISC proliferation *in vivo* due to ingestion of intermediate arylphorin doses limits the regenerative response to Cry1Ac toxicity (phase II), resulting in the onset of rapid and significant structural alterations associated with Cry toxin-induced midgut pathology (Endo and Nishiitsutsuji-Uwo 1980). This unaffected Cry1Ac susceptibility observed when feeding larvae intermediate concentrations of arylphorin was expected based on previous reports with midgut stem cell cultures demonstrating reduced mitogenic activity with increasing arylphorin dosage (Blackburn, Loeb et al. 2004; Hakim, Blackburn et al. 2007).

Unexpectedly, we observed a reduction in Cry1Ac susceptibility when feeding the

highest relative arylphorin concentrations tested (phase III). One possibility to explain phase III was that high levels of α-arylphorin in the midgut may have been preventing Cry1Ac binding to the midgut epithelium. In support of this hypothesis, it was reported that Cry1Ac resistance in *H. armigera* strain was mediated by an immune response including the synthesis and release of an 85 kDa hexamerin that bound Cry1Ac (Ma, Roberts et al. 2005). Our data mirrors this observation in that Cry1Ac binds specifically to α-arylphorin under native conditions and α-arylphorin reduces binding of biotinylated Cry1Ac to BBMV when used as a heterologous unlabeled competitor. Unexpectedly, we did not observe the same reduction when α-arylphorin was used to compete binding of ^{125}I-Cry1Ac to BBMV. This observation may suggest that toxin radio-iodination potentially disrupts toxin binding to α-arylphorin. In support of this hypothesis, Cry toxin radio-iodination has been reported to reduce specific binding to BBMV (Hernández-Rodríguez et al. 2012). In contrast, we did detect specific Cry1Ac binding to BBMV, and only Cry1Ac recognition of α-arylphorin was affected. Additional research will be needed to test the potential effect or iodination on Cry1Ac binding to α-arylphorin.

Previous research has demonstrated that Cry1Ac binds specifically to GalNAc residues on 120- and 170-kDa aminopeptidase-N (APN) (Knight et al. 1994) and 68-kDa alkaline phosphatase (HvALP) (Jurat-Fuentes and Adang 2004) in *H. virescens* BBMV. Similarly, our investigations into the carbohydrate moieties present on α-arylphorin strongly suggest that N-linked oligosaccharides containing terminal GalNAc also mediate Cry1Ac recognition of α-arylphorin. Based on the available observations, we propose that GalNAc-mediated toxin sequestration, which prevents high-affinity binding to receptors on the midgut epithelium, is responsible for phase III.

In this study, we have demonstrated that titers of the *H. virescens* growth factor α-arylphorin are critical to midgut healing and tolerance to Cry1Ac intoxication. Tolerance to

Cry1Ac toxin observed for relatively low and high doses of α-arylphorin results from two physiologically distinct mechanisms. First, we demonstrated that low dose α-arylphorin induced proliferation of intestinal stem cells found on the basal lamina of the midgut enabled a rapid recovery of the midgut epithelium during exposure to Cry1Ac. On the other hand, we present evidence supporting that specific binding of Cry1Ac to α-arylphorin is mediated through GalNAc on N-linked oligosaccharides and we hypothesize it reduces larval toxicity by preventing the Cry1Ac from binding to midgut receptors. The observation that α-arylphorin is a multifunctional growth factor that is expressed in the midgut and involved in two different mechanisms of insect tolerance to Cry1Ac, suggests that insect arylphorins and hexamerin proteins may play much larger roles in Cry toxin resistant phenotypes and the *B. thuringiensis* mode of action. This is especially important to consider for insect strains where reduced toxin binding was not detected using in vitro analysis as a mechanism of resistance. Considering the variability of oligosaccharide moieties present on insect arylphorins and that an overwhelming majority of arylphorins and hexamerins remain to be functionally characterized, future works should investigate potential interactions between Cry toxins and insect arylphorins. Doing so will shed light on alternative mechanisms of insect tolerance and perhaps provide a broader landscape for how the insect midgut epithelium responds to Cry toxins.

Appendix

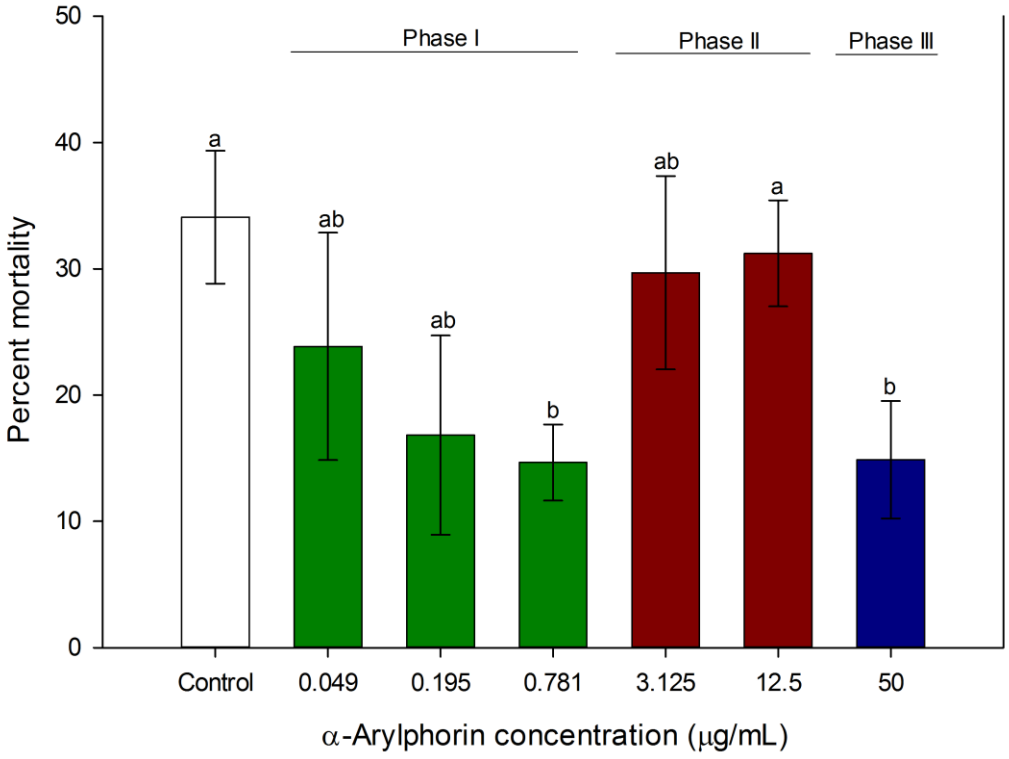


Figure 8: Ingestion of purified α-arylphorin induces dose-dependent effects on susceptibility of *H. virescens* larvae to Cry1Ac toxin. Mortality of *H. virescens* larvae exposed to 0.5 μg/cm^2 Cry1Ac for seven days after feeding on control diet (no α-arylphorin, white column), low α-arylphorin titers (0.049 – 0.781 μg/mL, green columns), medium α-arylphorin titers (3.125 – 12.5 μg/mL, red columns) or a high α-arylphorin titer (50.0 μg/mL, blue column) for five days immediately after neonate emergence. Bars denote standard error of the mean for each treatment of 16 larvae and calculated from three bioassay replicates; statistically significant differences between treatment groups are denoted by different letters for each column ($P< 0.05$, One-way ANOVA).

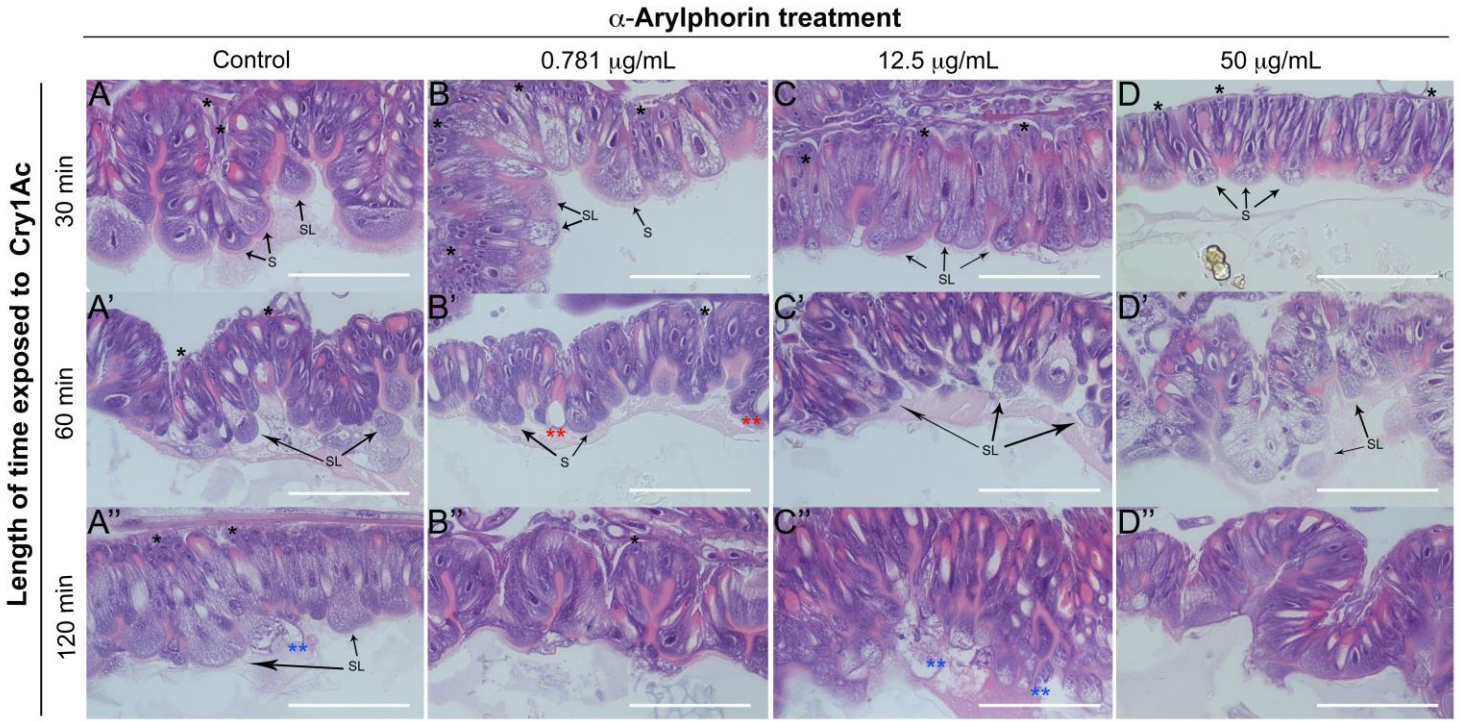
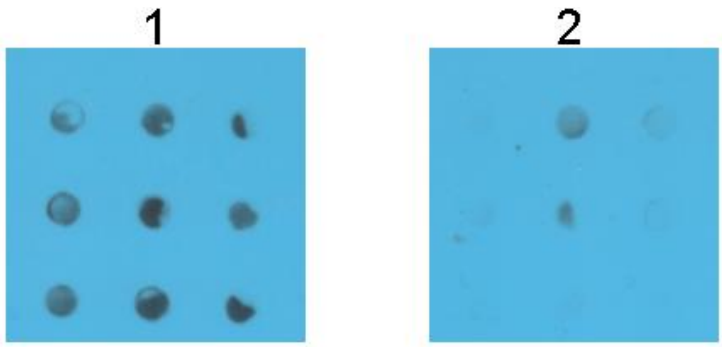
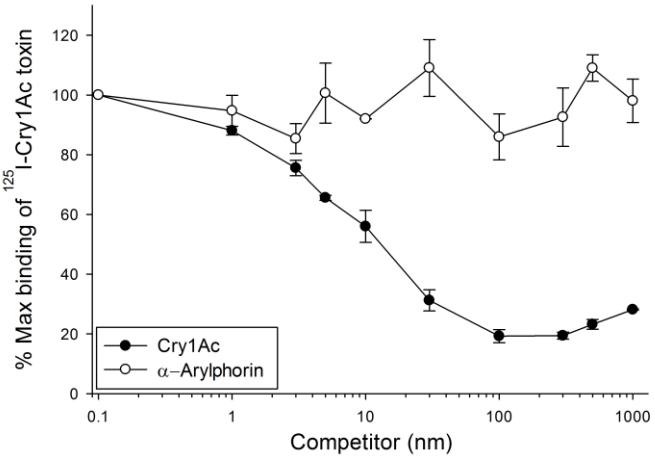


Figure 9: Morphological response of *H. virescens* midgut epithelium to Cry1Ac exposure following ingestion of α-arylphorin. Hematoxylin and eosin stained midgut epithelial tissues from larvae exposed to 0.5 μg/cm^2 Cry1Ac for 30 min. (A-D), 60 min. (A'-D'), or 120 min. (A''-D'') in control (A-A''), or after treatment with 0.781 μg/mL (B-B''), 12.5 μg/mL (C-C''), or 50 μg/mL of purified α-arylphorin (D-D'') for 5 days. Individual or groups of intestinal stem cells are indicated by single black asterisks (*), enlarged goblet cells are indicated by double red asterisks (**), and lysed mature cells are indicated by double blue asterisks (**). S, swelling cells; SL, sloughed cells. Reference bar =100 μM.

Figure 10: Binding of Cry1Ac and α-arylphorin to *H. virescens* BBMV. (A) Binding of biotinylated Cry1Ac to α-arylphorin (10 µg) in dot blots. Filters were probed with (Panel 1) 0.5 µg/mL biotinylated Cry1Ac or (Panel 2) 0.5 µg/mL biotinylated Cry1Ac plus a 300-fold excess unlabeled Cry1Ac. (B) Competition of ^{125}I-Cry1Ac binding to *H. virescens* BBMV by unlabeled Cry1Ac or α-arylphorin, (C) Competition of ^{125}I-α-arylphorin binding to *H. virescens* BBMV by unlabeled Cry1Ac or α-arylphorin. In both (B) and (C) BBMV proteins (20 µg) were incubated in PBS, 0.1%BSA, pH 7.4 buffer with either 0.38 nM of ^{125}I-Cry1Ac or 0.32 nM ^{125}I-α-arylphorin alone or in the presence of increasing concentrations of unlabeled competitors.





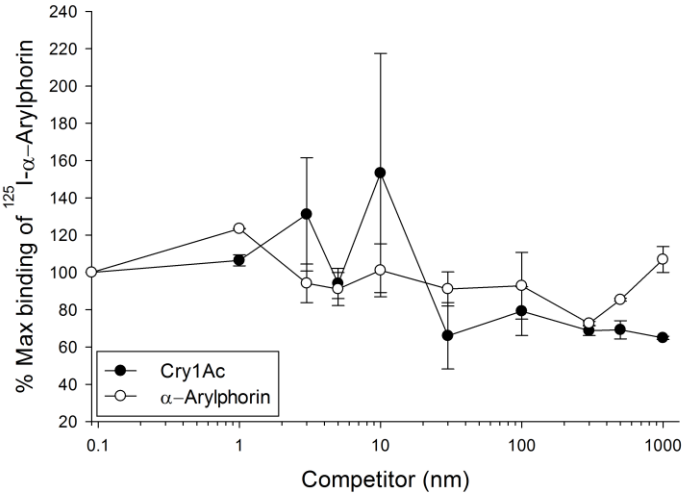


Figure 10 continued

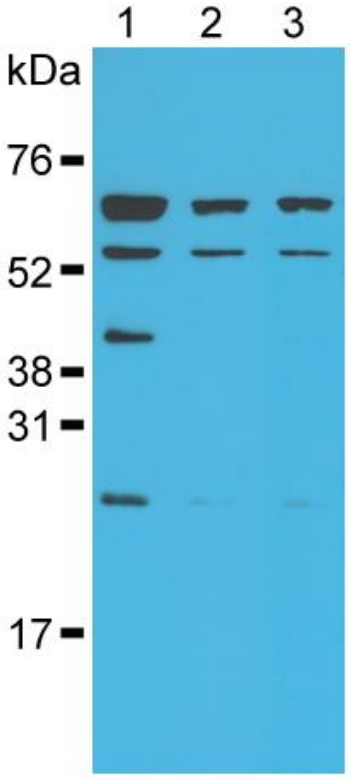


Figure 11: α-Arylphorin reduces Cry1Ac binding to *H. virescens* BBMV. Binding of biotinylated Cry1Ac to *H. virescens* BBMV (25 µg). BBMV were incubated with (Lane 1) 0.9 – fold, (Lane 2) 3.75-fold, and (Lane 3) 30-fold unlabeled α-arylphorin.

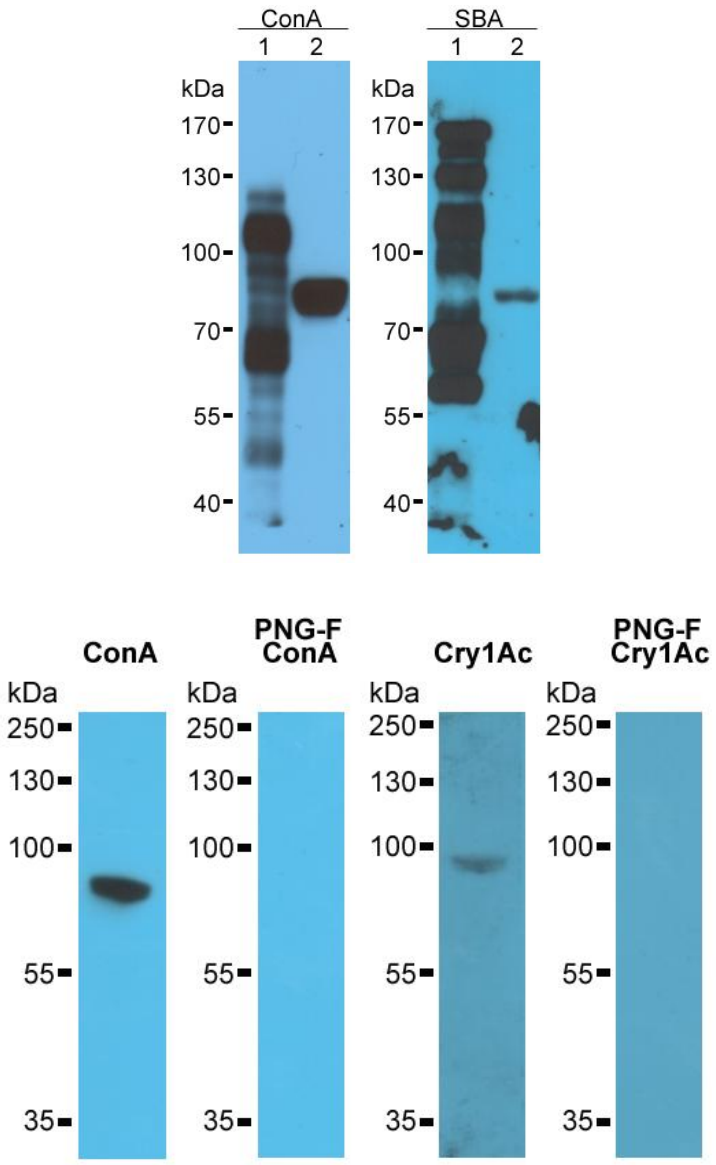


Figure 12: Testing N-linked oligosaccharides on *H. virescens* α-arylphorin and their role in Cry1Ac binding. BBMV proteins and α-arylphorin from *H. virescens* larvae were resolved by electrophoresis and transferred to PVDF Immobilon-P filters. After blocking, filters were incubated with the lectins or biotinylated Cry1Ac as indicated in the figure. In panel (A) bound lectins to BBMV (Lane 1) or α-arylphorin (Lane 2) were visualized by enhanced chemiluminescence. For ligand and lectin blots in panel (B), binding of ConA or Cry1Ac to α-arylphorin was detected by incubating filters with 1 μg/mL ConA or 0.5 μg/mL biotinylated Cry1Ac for 1 hour. The role of N-linked oligosaccharides in ConA (PNG-F/ConA) or biotinylated Cry1Ac binding (PNG-F/Cry1Ac) was tested by digesting α-arylphorin with PNG-F glycosidase. Following digestion, filters were washed, blocked and probed for lectin and toxin binding as described in Materials and Methods.

Table 3: Primers used for *in vitro* synthesis of dsArylphorin and RT-qPCR.

Name	5' --- 3' Sequence	Direction
T7GFP1	TAATACGACTCACTATAGGGGGTGAAGGTGATGCTACATA	Forward
T7GFP2	TAATACGACTCACTATAGGGCATCTTCAATGTTGTGACGA	Reverse
T7Aryl1	TAATACGACTCACTATAGGGGGCAACTACTGGCACATGAA	Forward
T7Aryl2	TAATACGACTCACTATAGGGTTGACGAACAACGAATCCAG	Reverse
HvAryl1	GAGCACTCGGAACAACTTGA	Forward
HvAryl2	TTTCAGTATAACCGGCGATG	Reverse
HvTub1	CGGAGTCCAGATCGGTAACG	Forward
HvTub2	GGCTGGATTCCATGCTCAAG	Reverse

Conclusions and outlook

This dissertation provides an in-depth investigation into one of the factors contributing to epithelial homeostasis in the midgut of *Heliothis virescens*, a common and agriculturally important lepidopteran pest. It is preceded by reports suggesting strong correlations between *in vitro* analyses of α-arylphorin functionality (Blackburn, Loeb et al. 2004) and *in vivo* physiological changes (Hakim, Blackburn et al. 2007), but this work represents a unique attempt to characterize the mechanism through which α-arylphorin directly mediates epithelial homeostasis by taking a multifaceted approach consisting of proteomics, molecular biology, and insect physiological applications. The primary focus of our project was to examine the midgut epithelial response to α-arylphorin, a hexameric growth factor, during growth and development as well as during the midgut response to loss of epithelial integrity caused by ingestion of crystal proteins produced by the gram-positive bacterium *Bacillus thuringiensis*.

The current understanding of proliferation and differentiation of intestinal stem cells (ISCs) in the midgut epithelium of lepidopteran insect pests has been developed primarily through the use of *in vitro* analyses of the response of primary ISC cultures to various biomolecules (Blackburn, Loeb et al. 2004; Hakim, Baldwin et al. 2001; Loeb, Clark et al. 2003; Loeb and Hakim 1996; Loeb, Martin, Narang et al. 2001; Sadrud-Din, Loeb et al. 1996; Sadruddin, Hakim et al. 1994; Smagghe, Vanhassel et al. 2005a; Smagghe, Elsen et al. 2003) and more recently in combination with differential fluorescent flow cytometry to provide cell-specific quantitative data following treatment (Castagnola, Eda et al. 2011). We capitalized on the known mitogenic properties of α-arylphorin *in vitro* to identify a range of titers of α-arylphorin purified from *H. virescens* hemolymph that elicited significantly different levels of ISC proliferation *in vivo* (Chapter 1). This research represents the first report of mitogenic activity observed in α-arylphorin purified from hemolymph, rather than fat body tissue, highlighting it as a viable alternative to fat body for protein purification that requires less mechanical tissue

disruption. We directly establish α-arylphorin as a causative agent of ISC proliferation and provide insight into the biological significance of fluctuating α-arylphorin titers observed in the hemolymph of intermolt lepidopteran insects. A phylogenetic analysis of α-arylphorin contigs in our custom *H. virescens* transcriptome along with those retrieved from BLAST queries of the NCBInr database indicated that several lepidopteran, coleopteran, and dipteran insect pests express α-arylphorin-like homologs that may function similarly as those of lepidopteran insects.

Intriguing questions surrounding the accessibility and passage of α-arylphorin across the basal lamina to the ISC niche emerged from this research. While the restrictive capacity of the insect basal lamina to biomolecules has been studied (Reddy and Locke 1990), and the inhibitory effects of excessively high α-arylphorin concentrations on ISC proliferation observed (Blackburn, Loeb et al. 2004; Hakim, Blackburn et al. 2007), information on molecules expressed during molting that mediate transport across the basal lamina is limited. The identification and characterization of these proteins would glean light on certain phenomena such as the absence of extensive ISC proliferation in midguts of newly molted larvae, when hemolymph α-arylphorin titers are much lower and potentially mitogenic.

Enhanced midgut regenerative properties in resistant *H. virescens* strains have been reported following exposure to Cry toxins from *B. thuringiensis* (Forcada, Alcacer et al. 1999; Martinez-Ramirez, Gould et al. 1999) and α-arylphorin subsequently identified in the secretomes acquired from Cry1Ac-challenged *H. virescens* primary mature cells (Castagnola 2011). However, thorough characterizations of mediators of the midgut healing response remain limited. Using functional bioassays, we characterized dual roles for α-arylphorin during the *H. virescens* midgut response to Cry toxin challenge, including the low titer induction of ISC proliferation that significantly decreased larval mortality and high titers that specifically reduced Cry1Ac binding to brush border membrane (BBMV) receptors. Furthermore, we investigated

the structural properties of α-arylphorin using lectin and ligand binding experiments to identify N-terminal oligosaccharides as key mediators of specific recognition by Cry1Ac.

It has been established that Cry1Ac binds specifically to N-terminal GalNAc residues on GPI-anchored *H. virescens* midgut alkaline phosphatase (HvmALP) (Jurat-Fuentes and Adang 2004). Structural characterizations of arylphorin purified from *M. sexta* (Ryan et al. 1985), *C. vinula* (Kayser et al. 2009), and *A. pernyi* (Kim et al. 2003) hemolymph have all identified the presence of N-terminal N-acetylglucosamine (GlcNAc). Based on my results and those included in previous reports (Budatha et al. 2011; Ma, Roberts et al. 2005), N-terminal GalNAc residues may play a crucial role in the interactions between Cry toxins and members of the hexamerin family of storage proteins. To continue building upon the work described in chapter 3, it will be necessary to conclude whether N-terminal GalNAc residues are present on *H. virescens* α-arylphorin and if they mediate specific interactions with Cry1Ac. The variability in α-arylphorin glycosylation patterns among lepidopteran species might be indicative of specialized roles in stem cell proliferation, tissue remodeling, and the immune response.

List of references

Akai, H. (1976). Ultrastructure of the guts. *Ultrastructural Morphology of Insects, Univ of Tokyo Press, Tokyo*, 237-285.
Altschul, S. F., Gish, W., Miller, W., Myers, E. W., & Lipman, D. J. (1990). Basic local alignment search tool. *J. Mol. Biol., 215*(3), 403-410.
Amcheslavsky, A., Ito, N., Jiang, J., & Ip, Y. T. (2011). Tuberous sclerosis complex and Myc coordinate the growth and division of Drosophila intestinal stem cells. *J. Cell Biol., 193*(4), 695-710. doi: 10.1083/jcb.201103018
Amcheslavsky, A., Jiang, J., & Ip, Y. T. (2009). Tissue damage-induced intestinal stem cell division in Drosophila. *Cell Stem Cell, 4*(1), 49-61. doi: 10.1016/j.stem.2008.10.016
Andrae, J., Gallini, R., & Betsholtz, C. (2008). Role of platelet-derived growth factors in physiology and medicine. *Genes Dev., 22*(10), 1276-1312. doi: 10.1101/gad.1653708
Apidianakis, Y., Pitsouli, C., Perrimon, N., & Rahme, L. (2009). Synergy between bacterial infection and genetic predisposition in intestinal dysplasia. *Proc. Natl. Acad. Sci. U. S. A., 106*(49), 20883-20888. doi: 10.1073/pnas.0911797106
Arimatsu, Y., Kotani, E., Sugimura, Y., & Furusawa, T. (2007). Molecular characterization of a cDNA encoding extracellular dsRNase and its expression in the silkworm, *Bombyx mori*. *Insect Biochem. Mol. Biol., 37*(2), 176-183. doi: 10.1016/j.ibmb.2006.11.004
Artimo, P., Jonnalagedda, M., Arnold, K., Baratin, D., Csardi, G., de Castro, E., . . . Stockinger, H. (2012). ExPASy: SIB bioinformatics resource portal. *Nucleic Acids Res., 40*(W1), W597-W603. doi: 10.1093/nar/gks400
Ashfaq, M., Sonoda, S., & Tsumuki, H. (2007). Expression of two methionine-rich storage protein genes of *Plutella xylostella* (L.) in response to development, juvenile hormone-analog and pyrethroid. *Comp Biochem Physiol B Biochem Mol Biol, 148*(1), 84-92. doi: 10.1016/j.cbpb.2007.04.017
Baldwin, K. M., & Hakim, R. S. (1991). Growth and differentiation of the larval midgut epithelium during molting in the moth, *Manduca sexta*. *Tissue Cell, 23*(3), 411-422.
Bardin, A. J., Perdigoto, C. N., Southall, T. D., Brand, A. H., & Schweisguth, F. (2010). Transcriptional control of stem cell maintenance in the *Drosophila* intestine. *Development, 137*(5), 705-714. doi: 10.1242/dev.039404
Barnes, D., & Sato, G. (1980). Serum-free cell culture: a unifying approach. *Cell, 22*(3), 649-655.
Baum, J. A., Bogaert, T., Clinton, W., Heck, G. R., Feldmann, P., Ilagan, O., . . . Roberts, J. (2007). Control of coleopteran insect pests through RNA interference. *Nat. Biotechnol., 25*(11), 1322-1326. doi: 10.1038/nbt1359
Bausek, N. (2013). JAK-STAT signaling in stem cells and their niches in *Drosophila*. *JAKSTAT, 2*(3), e25686. doi: 10.4161/jkst.25686
Berridge, M. (1983). Calcium as a second messenger. *Endocrinology of Insects, 1*, 615-624.
Bettencourt, R., Terenius, O., & Faye, I. (2002). Hemolin gene silencing by ds-RNA injected into *Cecropia* pupae is lethal to next generation embryos. *Insect Mol. Biol., 11*(3), 267-271.
Binkert, C., Demetriou, M., Sukhu, B., Szweras, M., Tenenbaum, H. C., & Dennis, J. W. (1999). Regulation of osteogenesis by fetuin. *J. Biol. Chem., 274*(40), 28514-28520.
Biteau, B., Hochmuth, C. E., & Jasper, H. (2008). JNK activity in somatic stem cells causes loss of tissue homeostasis in the aging *Drosophila* gut. *Cell Stem Cell, 3*(4), 442-455. doi: 10.1016/j.stem.2008.07.024
Biteau, B., & Jasper, H. (2011). EGF signaling regulates the proliferation of intestinal stem cells in Drosophila. *Development, 138*(6), 1045-1055. doi: 10.1242/dev.056671
Biteau, B., & Jasper, H. (2014). Slit/Robo signaling regulates cell fate decisions in the intestinal stem cell lineage of *Drosophila*. *Cell Rep, 7*(6), 1867-1875. doi: 10.1016/j.celrep.2014.05.024

Blackburn, M., Golubeva, E., Bowen, D., & Ffrench-Constant, R. H. (1998). A novel insecticidal toxin from photorhabdus luminescens, toxin complex a (Tca), and its histopathological effects on the midgut of manduca sexta. *Appl. Environ. Microbiol., 64*(8), 3036-3041.

Blackburn, M. B., Loeb, M. J., Clark, E., & Jaffe, H. (2004). Stimulation of midgut stem cell proliferation by *Manduca sexta* alpha-arylphorin. *Arch. Insect Biochem. Physiol., 55*(1), 26-32. doi: 10.1002/arch.10119

Blacklock, B. J., & Ryan, R. O. (1994). Hemolymph lipid transport. *Insect Biochem. Mol. Biol., 24*(9), 855-873.

Bodenstein, D. (1994). The postembryonic development of *Drosophila*. In Demerec, M. (Ed.), *Biology of Drosophila* (pp. 275-367). Cold Spring Harbor, NY: Cold Spring Harbor Laboratory Press.

Bond, D., & Foley, E. (2012). Autocrine platelet-derived growth factor-vascular endothelial growth factor receptor-related (Pvr) pathway activity controls intestinal stem cell proliferation in the adult *Drosophila* midgut. *J. Biol. Chem., 287*(33), 27359-27370. doi: 10.1074/jbc.M112.378018

Bonnay, F., Cohen-Berros, E., Hoffmann, M., Kim, S. Y., Boulianne, G. L., Hoffmann, J. A., . . . Reichhart, J. M. (2013). big bang gene modulates gut immune tolerance in *Drosophila*. *Proc. Natl. Acad. Sci. U. S. A., 110*(8), 2957-2962. doi: 10.1073/pnas.1221910110

Brac, T. (1983). Charged sieving by the basal lamina and the distribution of anionic sites on the external surfaces of fat body cells. *Tissue Cell, 15*(3), 489-498.

Bradford, M. M. (1976). A rapid and sensitive method for the quantitation of microgram quantities of protein utilizing the principle of protein-dye binding. *Anal. Biochem., 72*, 248-254.

Buchon, N., Broderick, N. A., Chakrabarti, S., & Lemaitre, B. (2009b). Invasive and indigenous microbiota impact intestinal stem cell activity through multiple pathways in *Drosophila*. *Genes Dev., 23*(19), 2333-2344. doi: 10.1101/gad.1827009

Buchon, N., Broderick, N. A., Kuraishi, T., & Lemaitre, B. (2010). *Drosophila* EGFR pathway coordinates stem cell proliferation and gut remodeling following infection. *BMC Biol, 8*, 152. doi: 10.1186/1741-7007-8-152

Buchon, N., Broderick, N. A., Poidevin, M., Pradervand, S., & Lemaitre, B. (2009a). *Drosophila* intestinal response to bacterial infection: activation of host defense and stem cell proliferation. *Cell Host Microbe, 5*(2), 200-211. doi: 10.1016/j.chom.2009.01.003

Budatha, M., Ningshen, T. J., & Dutta-Gupta, A. (2011). Is hexamerin receptor a GPI-anchored protein in *Achaea janata* (Lepidoptera: Noctuidae)? *J Biosci, 36*(3), 545-553.

Castagnola, A., Eda, S., & Jurat-Fuentes, J. L. (2011). Monitoring stem cell proliferation and differentiation in primary midgut cell cultures from *Heliothis virescens* larvae using flow cytometry. *Differentiation, 81*(3), 192-198. doi: 10.1016/j.diff.2010.12.001

Castagnola, A. S. (2011). Comparing the midgut regenerative responses in *Bacillus thuringiensis* susceptible and resistant *Heliothis virescens* larvae.

Chakrabarti, S., Liehl, P., Buchon, N., & Lemaitre, B. (2012). Infection-induced host translational blockage inhibits immune responses and epithelial renewal in the *Drosophila* gut. *Cell Host Microbe, 12*(1), 60-70. doi: 10.1016/j.chom.2012.06.001

Chao, A. C., Koch, A. R., & Moffett, D. F. (1990). Basal membrane uptake in potassium-secreting cells of midgut of tobacco hornworm (*Manduca sexta*). *Am. J. Physiol., 258*(1 Pt 2), R112-119.

Chapman, R. F. (1982). *The insects : structure and function* (3rd ed.). Cambridge, Mass.: Harvard University Press.

Chatterjee, M., & Ip, Y. T. (2009). Pathogenic stimulation of intestinal stem cell response in Drosophila. *J. Cell. Physiol., 220*(3), 664-671. doi: 10.1002/jcp.21808

Chen, W. J., Hsieh, F. C., Hsu, F. C., Tasy, Y. F., Liu, J. R., & Shih, M. C. (2014). Characterization of an insecticidal toxin and pathogenicity of *Pseudomonas taiwanensis* against insects. *PLoS Pathog, 10*(8), e1004288. doi: 10.1371/journal.ppat.1004288

Chiang, A. S., Yen, D. F., & Peng, W. K. (1986). Defense reaction of midgut epithelial cells in the rice moth larva (Corcyra cephalonica) infected with Bacillus thuringiensis. *J. Invertebr. Pathol., 47*(3), 333-339. doi: http://dx.doi.org/10.1016/0022-2011(86)90104-7

Cho, M. Y., Choi, H. W., Moon, G. Y., Kim, M. H., Kwon, T. H., Homma, K., . . . Lee, B. L. (1999). An 86 kDa diapause protein 1-like protein is a component of early-staged encapsulation-relating proteins in coleopteran insect, *Tenebrio molitor* larvae. *FEBS Lett., 451*(3), 303-307.

Cho, M. Y., Lee, H. S., Lee, K. M., Homma, K., Natori, S., & Lee, B. L. (1999). Molecular cloning and functional properties of two early-stage encapsulation-relating proteins from the coleopteran insect, Tenebrio molitor larvae. *Eur. J. Biochem., 262*(3), 737-744.

Choi, N. H., Kim, J. G., Yang, D. J., Kim, Y. S., & Yoo, M. A. (2008). Age-related changes in Drosophila midgut are associated with PVF2, a PDGF/VEGF-like growth factor. *Aging Cell, 7*(3), 318-334. doi: 10.1111/j.1474-9726.2008.00380.x

Cordero, J. B., & Sansom, O. J. (2012). Wnt signalling and its role in stem cell-driven intestinal regeneration and hyperplasia. *Acta Physiol (Oxf), 204*(1), 137-143. doi: 10.1111/j.1748-1716.2011.02288.x

Cordero, J. B., Stefanatos, R. K., Scopelliti, A., Vidal, M., & Sansom, O. J. (2012). Inducible progenitor-derived Wingless regulates adult midgut regeneration in *Drosophila*. *EMBO J, 31*(19), 3901-3917. doi: 10.1038/emboj.2012.248

Cronin, S. J., Nehme, N. T., Limmer, S., Liegeois, S., Pospisilik, J. A., Schramek, D., . . . Penninger, J. M. (2009). Genome-wide RNAi screen identifies genes involved in intestinal pathogenic bacterial infection. *Science, 325*(5938), 340-343. doi: 10.1126/science.1173164

Crooks, G. M., & Weinberg, K. (2006). The unpredictable stem cell. *Nat. Immunol., 7*(11), 1129-1130. doi: 10.1038/ni1106-1129

Dai, P., Akimaru, H., & Ishii, S. (2003). A hedgehog-responsive region in the *Drosophila* wing disc is defined by debra-mediated ubiquitination and lysosomal degradation of Ci. *Dev. Cell, 4*(6), 917-928.

Davis, R. J. (2000). Signal transduction by the JNK group of MAP kinases. *Cell, 103*(2), 239-252.

De Kort, C., & Koopmanschap, A. (1987). Isolation and characterization of a larval hemolymph protein in *Locusta migratoria*. *Arch. Insect Biochem. Physiol., 4*(3), 191-203.

de Navascues, J., Perdigoto, C. N., Bian, Y., Schneider, M. H., Bardin, A. J., Martinez-Arias, A., & Simons, B. D. (2012). *Drosophila* midgut homeostasis involves neutral competition between symmetrically dividing intestinal stem cells. *EMBO J, 31*(11), 2473-2485. doi: 10.1038/emboj.2012.106

Debray, H., Decout, D., Strecker, G., Spik, G., & Montreuil, J. (1981). Specificity of twelve lectins towards oligosaccharides and glycopeptides related to N- glycosylproteins. *Eur. J. Biochem., 117*(1), 41-51.

Demetriou, M., Binkert, C., Sukhu, B., Tenenbaum, H. C., & Dennis, J. W. (1996). Fetuin/alpha2-HS glycoprotein is a transforming growth factor-beta type II receptor mimic and cytokine antagonist. *J. Biol. Chem., 271*(22), 12755-12761.

Dow, J. A., & Harvey, W. R. (1988). Role of midgut electrogenic K+ pump potential difference in regulating lumen K+ and pH in larval Lepidoptera. *J. Exp. Biol., 140*(1), 455-463.

Duhamel, R., & Kunkel, J. (1983). Cockroach larval-specific protein, a tyrosine-rich serum protein. *J. Biol. Chem., 258*(23), 14461-14465.

Dussaubat, C., Brunet, J. L., Higes, M., Colbourne, J. K., Lopez, J., Choi, J. H., . . . Alaux, C. (2012). Gut pathology and responses to the microsporidium *Nosema ceranae* in the honey bee *Apis mellifera*. *PLoS One, 7*(5), e37017. doi: 10.1371/journal.pone.0037017

Eguchi, M., Itoh, M., Chou, L.-Y., & Nishino, K. (1993). Purification and characterization of a fungal protease specific protein inhibitor (FPI-F) in the silkworm haemolymph. *Comparative Biochemistry and Physiology Part B: Comparative Biochemistry, 104*(3), 537-543.

Elkind, M. M., & Sutton, H. (1960). Radiation response of mammalian cells grown in culture. 1. Repair of X-ray damage in surviving Chinese hamster cells. *Radiat. Res., 13*, 556-593.

Endo, Y., & Nishiitsutsuji-Uwo, J. (1980). Mode of action of *Bacillus thuringiensis* δ-endotoxin: Histopathological changes in the silkworm midgut. *J. Invertebr. Pathol., 36*(1), 90-103. doi: http://dx.doi.org/10.1016/0022-2011(80)90140-8

Ferkovich, S. M., & Oberlander, H. (1991). Growth factors in invertebrate *in vitro* culture. *In Vitro Cell Dev Biol, 27A*(6), 483-486.

Fernandez, L. E., Aimanova, K. G., Gill, S. S., Bravo, A., & Soberon, M. (2006). A GPI-anchored alkaline phosphatase is a functional midgut receptor of Cry11Aa toxin in *Aedes aegypti* larvae. *Biochem. J., 394*(Pt 1), 77-84. doi: 10.1042/BJ20051517

Fire, A., Xu, S., Montgomery, M. K., Kostas, S. A., Driver, S. E., & Mello, C. C. (1998). Potent and specific genetic interference by double-stranded RNA in *Caenorhabditis elegans*. *Nature, 391*(6669), 806-811. doi: 10.1038/35888

Flores-Escobar, B., Rodriguez-Magadan, H., Bravo, A., Soberon, M., & Gomez, I. (2013). Differential role of *Manduca sexta* aminopeptidase-N and alkaline phosphatase in the mode of action of Cry1Aa, Cry1Ab, and Cry1Ac toxins from *Bacillus thuringiensis*. *Appl. Environ. Microbiol., 79*(15), 4543-4550. doi: 10.1128/AEM.01062-13

Forcada, C., Alcacer, E., Garcera, M. D., Tato, A., & Martinez, R. (1999). Resistance to *Bacillus thuringiensis* Cry1Ac toxin in three strains of *Heliothis virescens*: proteolytic and SEM study of the larval midgut. *Arch. Insect Biochem. Physiol., 42*(1), 51-63. doi: 10.1002/(SICI)1520-6327(199909)42:1<51::AID-ARCH6>3.0.CO;2-6

Freitak, D., Wheat, C. W., Heckel, D. G., & Vogel, H. (2007). Immune system responses and fitness costs associated with consumption of bacteria in larvae of *Trichoplusia ni*. *BMC Biol, 5*, 56. doi: 10.1186/1741-7007-5-56

Friedrich, M. V., Schneider, M., Timpl, R., & Baumgartner, S. (2000). Perlecan domain V of *Drosophila melanogaster*. Sequence, recombinant analysis and tissue expression. *Eur. J. Biochem., 267*(11), 3149-3159.

Fujita, T., Kanno, T., & Kobayashi, S. (1988). *The paraneuron*: Springer-Verlag Tokyo.

Fujita, T., & Kobayashi, S. (1977). Structure and function of gut endocrine cells. *Int Rev Cytol Suppl*(6), 187-233.

Garcia-Gonzalo, F. R., & Izpisua Belmonte, J. C. (2008). Albumin-associated lipids regulate human embryonic stem cell self-renewal. *PLoS One, 3*(1), e1384. doi: 10.1371/journal.pone.0001384

Gilbert, M. M., Weaver, B. K., Gergen, J. P., & Reich, N. C. (2005). A novel functional activator of the *Drosophila* JAK/STAT pathway, unpaired2, is revealed by an *in vivo* reporter of pathway activation. *Mech. Dev., 122*(7-8), 939-948. doi: 10.1016/j.mod.2005.03.004

Gomez, I., Sanchez, J., Miranda, R., Bravo, A., & Soberon, M. (2002). Cadherin-like receptor binding facilitates proteolytic cleavage of helix alpha-1 in domain I and oligomer pre-pore formation of *Bacillus thuringiensis* Cry1Ab toxin. *FEBS Lett., 513*(2-3), 242-246.

Gomez, I., Sanchez, J., Munoz-Garay, C., Matus, V., Gill, S. S., Soberon, M., & Bravo, A. (2014). *Bacillus thuringiensis* Cry1A toxins are versatile proteins with multiple modes of action: two distinct pre-pores are involved in toxicity. *Biochem. J., 459*(2), 383-396. doi: 10.1042/BJ20131408

Gordadze, A. V., Korochkina, S. E., Zakharkin, S. O., Norton, A. L., & Benes, H. (1999). Molecular cloning and expression of two hexamerin cDNAs from the mosquito, *Aedes aegypti*. *Insect Mol. Biol., 8*(1), 55-66.

Goto, S., Loeb, M. J., & Takeda, M. (2005). Bombyxin stimulates proliferation of cultured stem cells derived from *Heliothis virescens* and *Mamestra brassicae* larvae1. *In Vitro Cell. Dev. Biol. Anim., 41*(1-2), 38-42. doi: 10.1290/0312092.1

Goto, S., Takeda, M., Loeb, M. J., & Hakim, R. S. (2001). Immunohistochemical detection of a putative insect cytokine, midgut differentiation factor 1 (MDF-1) in midgut columnar cells of *Heliothis virescens*. *Invertebr. Reprod. Dev., 40*(2-3), 117-124.

Goulas, S., Conder, R., & Knoblich, J. A. (2012). The Par complex and integrins direct asymmetric cell division in adult intestinal stem cells. *Cell Stem Cell, 11*(4), 529-540. doi: 10.1016/j.stem.2012.06.017

Grieneisen, M. L., Warren, J. T., & Gilbert, L. I. (1993). Early steps in ecdysteroid biosynthesis: Evidence for the involvement of cytochrome P-450 enzymes. *Insect Biochem. Mol. Biol., 23*(1), 13-23.

Guo, Z., Driver, I., & Ohlstein, B. (2013). Injury-induced BMP signaling negatively regulates *Drosophila* midgut homeostasis. *J. Cell Biol., 201*(6), 945-961. doi: 10.1083/jcb.201302049

Ha, E. M., Oh, C. T., Bae, Y. S., & Lee, W. J. (2005b). A direct role for dual oxidase in *Drosophila* gut immunity. *Science, 310*(5749), 847-850. doi: 10.1126/science.1117311

Ha, E. M., Oh, C. T., Ryu, J. H., Bae, Y. S., Kang, S. W., Jang, I. H., . . . Lee, W. J. (2005a). An antioxidant system required for host protection against gut infection in *Drosophila*. *Dev. Cell, 8*(1), 125-132. doi: 10.1016/j.devcel.2004.11.007

Hakim, R. S., Baldwin, K., & Smagghe, G. (2010). Regulation of midgut growth, development, and metamorphosis. *Annu. Rev. Entomol., 55*, 593-608. doi: 10.1146/annurev-ento-112408-085450

Hakim, R. S., Baldwin, K. M., & Bayer, P. E. (1988). Cell differentiation in the embryonic midgut of the tobacco hornworm, *Manduca sexta*. *Tissue Cell, 20*(1), 51-62.

Hakim, R. S., Baldwin, K. M., & Loeb, M. (2001). The role of stem cells in midgut growth and regeneration. *In Vitro Cellular & Developmental Biology-Animal, 37*(6), 338-342.

Hakim, R. S., Blackburn, M. B., Corti, P., Gelman, D. B., Goodman, C., Elsen, K., . . . Smagghe, G. (2007). Growth and mitogenic effects of arylphorin *in vivo* and *in vitro*. *Arch. Insect Biochem. Physiol., 64*(2), 63-73. doi: 10.1002/arch.20155

Hanozet, G. M., Giordana, B., & Sacchi, V. F. (1980). K+-dependent phenylalanine uptake in membrane vesicels isolated from the midgut of *Philosamia cynthia* larvae. *Biochim. Biophys. Acta, 596*(3), 481-486.

Harrison, D. A., McCoon, P. E., Binari, R., Gilman, M., & Perrimon, N. (1998). *Drosophila unpaired* encodes a secreted protein that activates the JAK signaling pathway. *Genes Dev., 12*(20), 3252-3263.

Haunerland, N. H. (1996). Insect storage proteins: Gene families and receptors. *Insect Biochem. Mol. Biol., 26*(8-9), 755-765.

Haunerland, N. H., & Bowers, W. S. (1986). Arylphorin from the corn earworm, *Heliothis zea*. *Insect Biochem., 16*(4), 617-625.

Hayakawa, Y. (1994). Cellular immunosuppressive protein in the plasma of parasitized insect larvae. *J. Biol. Chem., 269*(20), 14536-14540.

Hayakawa, Y., & Ohnishi, A. (1998). Cell growth activity of growth-blocking peptide. *Biochem. Biophys. Res. Commun., 250*(2), 194-199. doi: 10.1006/bbrc.1998.8959

Hecker, H. (1977). Structure and function of midgut epithelial cells in *Culicidae* mosquitoes (Insecta, Diptera). *Cell Tissue Res., 184*(3), 321-341.

Hennings, H., Michael, D., Cheng, C., Steinert, P., Holbrook, K., & Yuspa, S. H. (1980). Calcium regulation of growth and differentiation of mouse epidermal cells in culture. *Cell, 19*(1), 245-254.

Hernandez-Martinez, P., Navarro-Cerrillo, G., Caccia, S., de Maagd, R. A., Moar, W. J., Ferre, J., . . . Herrero, S. (2010). Constitutive activation of the midgut response to *Bacillus thuringiensis* in Bt-resistant *Spodoptera exigua*. *PLoS One, 5*(9). doi: 10.1371/journal.pone.0012795

Hernández-Rodríguez, C. S., Hernández-Martínez, P., Van Rie, J., Escriche, B., & Ferré, J. (2012). Specific binding of radiolabeled Cry1Fa insecticidal protein from *Bacillus thuringiensis* to midgut sites in lepidopteran species. *Appl. Environ. Microbiol., 78*(11), 4048-4050.

Hofmann, C., Lüthy, P., Hütter, R., & Pliska, V. (1988). Binding of the delta endotoxin from *Bacillus thuringiensis* to brush- border membrane vesicles of the cabbage butterfly (*Pieris brassicae*). *Eur. J. Biochem., 173*(1), 85-91.

Hombria, J. C., Brown, S., Hader, S., & Zeidler, M. P. (2005). Characterisation of Upd2, a *Drosophila* JAK/STAT pathway ligand. *Dev. Biol., 288*(2), 420-433. doi: 10.1016/j.ydbio.2005.09.040

Hoover, K., Washburn, J. O., & Volkman, L. E. (2000). Midgut-based resistance of Heliothis virescens to baculovirus infection mediated by phytochemicals in cotton. *Journal of insect physiology, 46*(6), 999-1007.

Hoover, K., Washburn, J. O., & Volkman, L. E. (2000). Midgut-based resistance of *Heliothis virescens* to baculovirus infection mediated by phytochemicals in cotton. *J. Insect Physiol., 46*(6), 999-1007.

Hou, Y., Li, J., Li, Y., Dong, Z., Xia, Q., & Yuan, Y. A. (2014). Crystal structure of *Bombyx mori* arylphorins reveals a 3:3 heterohexamer with multiple papain cleavage sites. *Protein Sci., 23*(6), 735-746. doi: 10.1002/pro.2457

Hua, G., Zhang, R., Bayyareddy, K., & Adang, M. J. (2009). *Anopheles gambiae* alkaline phosphatase is a functional receptor of *Bacillus thuringiensis jegathesan* Cry11Ba toxin. *Biochemistry, 48*(41), 9785-9793. doi: 10.1021/bi9014538

Illa-Bochaca, I., & Montuenga, L. M. (2006). The regenerative nidi of the locust midgut as a model to study epithelial cell differentiation from stem cells. *J. Exp. Biol., 209*(Pt 11), 2215-2223. doi: 10.1242/jeb.02249

Ishizaki, H., Mizoguchi, A., Suzuki, A., Moriya, I., O'oka, H., Kataoka, H., . . . Tamura, S. (1983). Species Specificity of the Insect Prothoracicotropic Hormone (PITH): the Presence of *Bombyx*- and *Samia*- Specific PTTHs in the Brain of *Bombyx mori*. *Dev. Growth Differ., 25*(6), 593-600.

James, C. (2010). *Global status of commercialized biotech/GM crops: 2010*: International Service for the Acquisition of Agri-biotech Applications (ISAAA) Ithaca, NY, USA.

Jiang, H., & Edgar, B. A. (2009a). EGFR signaling regulates the proliferation of *Drosophila* adult midgut progenitors. *Development, 136*(3), 483-493. doi: 10.1242/dev.026955

Jiang, H., Grenley, M. O., Bravo, M. J., Blumhagen, R. Z., & Edgar, B. A. (2011). EGFR/Ras/MAPK signaling mediates adult midgut epithelial homeostasis and regeneration in Drosophila. *Cell Stem Cell, 8*(1), 84-95. doi: 10.1016/j.stem.2010.11.026

Jiang, H., & Kanost, M. R. (1997). Characterization and functional analysis of 12 naturally occurring reactive site variants of serpin-1 from *Manduca sexta*. *J. Biol. Chem., 272*(2), 1082-1087.

Jiang, H., Patel, P. H., Kohlmaier, A., Grenley, M. O., McEwen, D. G., & Edgar, B. A. (2009b). Cytokine/Jak/Stat signaling mediates regeneration and homeostasis in the *Drosophila* midgut. *Cell, 137*(7), 1343-1355. doi: 10.1016/j.cell.2009.05.014

Jones, D. T., Taylor, W. R., & Thornton, J. M. (1992). The rapid generation of mutation data matrices from protein sequences. *Comput Appl Biosci, 8*(3), 275-282.

Jones, R. M., Luo, L., Ardita, C. S., Richardson, A. N., Kwon, Y. M., Mercante, J. W., . . . Neish, A. S. (2013). Symbiotic lactobacilli stimulate gut epithelial proliferation *via* Nox-mediated generation of reactive oxygen species. *EMBO (Eur. Mol. Biol. Organ.) J., 32*(23), 3017-3028. doi: 10.1038/emboj.2013.224

Jurat-Fuentes, J. L., & Adang, M. J. (2004). Characterization of a Cry1Ac-receptor alkaline phosphatase in susceptible and resistant Heliothis virescens larvae. *Eur J Biochem, 271*(15), 3127-3135. doi: 10.1111/j.1432-1033.2004.04238.x

Jurat-Fuentes, J. L., Gould, F. L., & Adang, M. J. (2002). Altered Glycosylation of 63- and 68-kilodalton microvillar proteins in *Heliothis virescens* correlates with reduced Cry1 toxin binding, decreased pore formation, and increased resistance to *Bacillus thuringiensis* Cry1 toxins. *Appl. Environ. Microbiol., 68*(11), 5711-5717.

Jurat-Fuentes, J. L., Karumbaiah, L., Jakka, S. R., Ning, C., Liu, C., Wu, K., . . . Adang, M. (2011). Reduced levels of membrane-bound alkaline phosphatase are common to lepidopteran strains resistant to Cry toxins from Bacillus thuringiensis. *PLoS One, 6*(3), e17606. doi: 10.1371/journal.pone.0017606

Kappler, C., Kabbouh, M., Hetru, C., Durst, F., & Hoffmann, J. A. (1988). Characterization of three hydroxylases involved in the final steps of biosynthesis of the steroid hormone ecdysone in *Locusta migratoria* (Insecta, Orthoptera). *J. Steroid Biochem. Mol. Biol., 31*(6), 891-898.

Kayser, H., Mann, K., Machaidze, G., Nimtz, M., Ringler, P., Muller, S. A., & Aebi, U. (2009). Isolation, characterisation and molecular imaging of a high-molecular-weight insect biliprotein, a member of the hexameric arylphorin protein family. *J. Mol. Biol., 389*(1), 74-89. doi: 10.1016/j.jmb.2009.03.075

Kim, S., Hwang, S. K., Dwek, R. A., Rudd, P. M., Ahn, Y. H., Kim, E. H., . . . Lee, S. M. (2003). Structural determination of the N-glycans of a lepidopteran arylphorin reveals the presence of a monoglucosylated oligosaccharide in the storage protein. *Glycobiology, 13*(3), 147-157. doi: 10.1093/glycob/cwg023

Kim, Y. (2005). Identification of host translation inhibitory factor of *Campoletis sonorensis* ichnovirus on the tobacco budworm, *Heliothis virescens*. *Arch. Insect Biochem. Physiol., 59*(4), 230-244. doi: 10.1002/arch.20074

Kirkpatrick, B. A., Washburn, J. O., & Volkman, L. E. (1998). AcMNPV pathogenesis and developmental resistance in fifth instar Heliothis virescens. *Journal of invertebrate pathology, 72*(1), 63-72. doi: 10.1006/jipa.1997.4752

Knight, P. J., Crickmore, N., & Ellar, D. J. (1994). The receptor for *Bacillus thuringiensis* CrylA(c) delta-endotoxin in the brush border membrane of the lepidopteran *Manduca sexta* is aminopeptidase N. *Mol. Microbiol., 11*(3), 429-436.

Koch, U., Lehal, R., & Radtke, F. (2013). Stem cells living with a Notch. *Development, 140*(4), 689-704. doi: 10.1242/dev.080614

Kramer, S. J., Mundall, E. C., & Law, J. H. (1980). Purification and properties of manducin, an amino acid storage protein of the hemolymph of larval and pupal *Manduca sexta*. *Insect Biochem., 10*(3), 279-288.

Krishnamoorthy, M., Jurat-Fuentes, J. L., McNall, R. J., Andacht, T., & Adang, M. J. (2007). Identification of novel Cry1Ac binding proteins in midgut membranes from *Heliothis virescens* using proteomic analyses. *Insect Biochem. Mol. Biol., 37*(3), 189-201. doi: 10.1016/j.ibmb.2006.10.004

Kumar, P., Pandit, S. S., & Baldwin, I. T. (2012). Tobacco rattle virus vector: A rapid and transient means of silencing *Manduca sexta* genes by plant mediated RNA interference. *PLoS One, 7*(2), e31347. doi: 10.1371/journal.pone.0031347

Kunkel, J. G., & Lawler, D. M. (1974). Larval-specific serum protein in the order Dictyoptera—I. immunologic characterization in larval *Blattella germanica* and cross-reaction throughout the order. *Comp. Biochem. Physiol. B Comp. Biochem., 47*(3), 697-710.
Leclerc, R. F., & Miller, S. G. (1990). Identification and molecular analysis of storage proteins from *Heliothis virescens*. *Arch. Insect Biochem. Physiol., 14*(3), 131-150. doi: 10.1002/arch.940140303
Lee, H. O., Davidson, J. M., & Duronio, R. J. (2009). Endoreplication: polyploidy with purpose. *Genes Dev., 23*(21), 2461-2477. doi: 10.1101/gad.1829209
Lee, W. C., Beebe, K., Sudmeier, L., & Micchelli, C. A. (2009). *Adenomatous polyposis coli* regulates *Drosophila* intestinal stem cell proliferation. *Development, 136*(13), 2255-2264. doi: 10.1242/dev.035196
Lee, W. J. (2009). Bacterial-modulated host immunity and stem cell activation for gut homeostasis. *Genes Dev., 23*(19), 2260-2265. doi: 10.1101/gad.1858709
Lehane, M. J., & Billingsley, P. F. (1996). *Biology of the Insect Midgut* (1st ed.). London: Chapman and Hall.
Lemaitre, B., & Miguel-Aliaga, I. (2013). The digestive tract of Drosophila melanogaster. *Annu. Rev. Genet., 47*, 377-404. doi: 10.1146/annurev-genet-111212-133343
Levenbook, L. (1985). Insect storage proteins. *Comprehensive insect physiology, biochemistry and pharmacology, 10*, 307-346.
Levenbook, L., & Bauer, A. C. (1984). The fate of the larval storage protein calliphorin during adult development of *Calliphora vicina*. *Insect Biochem., 14*(1), 77-86.
Li, Z., Guo, Y., Han, L., Zhang, Y., Shi, L., Huang, X., & Lin, X. (2014). Debra-mediated ci degradation controls tissue homeostasis in *Drosophila* adult midgut. *Stem Cell Reports, 2*(2), 135-144. doi: 10.1016/j.stemcr.2013.12.011
Li, Z., Zhang, Y., Han, L., Shi, L., & Lin, X. (2013). Trachea-derived Dpp controls adult midgut homeostasis in *Drosophila*. *Dev. Cell, 24*(2), 133-143. doi: 10.1016/j.devcel.2012.12.010
Limmer, S., Haller, S., Drenkard, E., Lee, J., Yu, S., Kocks, C., . . . Ferrandon, D. (2011). *Pseudomonas aeruginosa* RhlR is required to neutralize the cellular immune response in a *Drosophila melanogaster* oral infection model. *Proc. Natl. Acad. Sci. U. S. A., 108*(42), 17378-17383. doi: 10.1073/pnas.1114907108
Lin, G., Xu, N., & Xi, R. (2008). Paracrine Wingless signalling controls self-renewal of *Drosophila* intestinal stem cells. *Nature, 455*(7216), 1119-1123. doi: 10.1038/nature07329
Lin, G., Zhang, X., Ren, J., Pang, Z., Wang, C., Xu, N., & Xi, R. (2013). Integrin signaling is required for maintenance and proliferation of intestinal stem cells in *Drosophila*. *Dev. Biol., 377*(1), 177-187. doi: 10.1016/j.ydbio.2013.01.032
Liu, H., Sadygov, R. G., & Yates, J. R., 3rd. (2004). A model for random sampling and estimation of relative protein abundance in shotgun proteomics. *Anal. Chem., 76*(14), 4193-4201. doi: 10.1021/ac0498563
Liu, J., Swevers, L., Iatrou, K., Huvenne, H., & Smagghe, G. (2012). *Bombyx mori* DNA/RNA non-specific nuclease: expression of isoforms in insect culture cells, subcellular localization and functional assays. *J. Insect Physiol., 58*(8), 1166-1176. doi: 10.1016/j.jinsphys.2012.05.016
Liu, W., Singh, S. R., & Hou, S. X. (2010). JAK-STAT is restrained by Notch to control cell proliferation of the *Drosophila* intestinal stem cells. *J. Cell. Biochem., 109*(5), 992-999. doi: 10.1002/jcb.22482
Lockart, R. Z., Jr., Elkind, M. M., & Moses, W. B. (1961). Radiation response of mammalian cells grown in culture. II. Survival and recovery characteristics of several subcultures of HeLa S3 cells after x-irradiation. *J. Natl. Cancer Inst. (Bethesda), 27*, 1393-1404.

Loeb, M. J. (2005). Altering the fate of stem cells from midgut of Heliothis virescens:the effect of calcium ions. *Arch Insect Biochem Physiol, 59*(4), 202-210. doi: 10.1002/arch.20060
Loeb, M. J. (2006). Role of integrin beta1-like protein in proliferation and differentiation of cultured stem cells from midgut of Heliothis virescens. *Arch Insect Biochem Physiol, 61*(2), 55-64. doi: 10.1002/arch.20097
Loeb, M. J., Clark, E. A., Blackburn, M., Hakim, R. S., Elsen, K., & Smagghe, G. (2003). Stem cells from midguts of lepidopteran larvae: Clues to the regulation of stem cell fate. *Arch. Insect Biochem. Physiol., 53*(4), 186-198. doi: 10.1002/arch.10098
Loeb, M. J., Coronel, N., Natsukawa, D., & Takeda, M. (2004). Implications for the functions of the four known midgut differentiation factors: An immunohistologic study of *Heliothis virescens* midgut. *Arch. Insect Biochem. Physiol., 56*(1), 7-20. doi: 10.1002/arch.10140
Loeb, M. J., & Hakim, R. S. (1996). Insect midgut epithelium in vitro: an insect stem cell system. *J. Insect Physiol., 42*(11), 1103-1111.
Loeb, M. J., & Hakim, R. S. (1999). Cultured midgut cells of *Heliothis virescens* (Lepidoptera): fibronectin and integrin β1, immunoreactivity during differentiation *in vitro*. *Invertebr. Reprod. Dev., 35*(2), 95-102.
Loeb, M. J., Hakim, R. S., Martin, P., Narang, N., Goto, S., & Takeda, M. (2000). Apoptosis in cultured midgut cells from heliothis virescens larvae exposed to various conditions. *Arch. Insect Biochem. Physiol., 45*(1), 12-23. doi: 10.1002/1520-6327(200009)45:1<12::AID-ARCH2>3.0.CO;2-P
Loeb, M. J., & Jaffe, H. (2002). Peptides that elicit midgut stem cell differentiation isolated from chymotryptic digests of hemolymph from *Lymantria dispar* pupae. *Arch. Insect Biochem. Physiol., 50*(2), 85-96. doi: 10.1002/arch.10033
Loeb, M. J., Jaffe, H., Gelman, D. B., & Hakim, R. S. (1999). Two polypeptide factors that promote differentiation of insect midgut stem cells *in vitro*. *Arch. Insect Biochem. Physiol., 40*(3), 129-140. doi: 10.1002/(SICI)1520-6327(1999)40:3<129::AID-ARCH2>3.0.CO;2-B
Loeb, M. J., Martin, P. A., Hakim, R. S., Goto, S., & Takeda, M. (2001). Regeneration of cultured midgut cells after exposure to sublethal doses of toxin from two strains of *Bacillus thuringiensis*. *J. Insect Physiol., 47*(6), 599-606.
Loeb, M. J., Martin, P. A., Narang, N., Hakim, R. S., Goto, S., & Takeda, M. (2001). Control of life, death, and differentiation in cultured midgut cells of the lepidopteran, *Heliothis virescens*. *In Vitro Cell. Dev. Biol. Anim., 37*(6), 348-352. doi: 10.1007/BF02577569
Luo, K., Sangadala, S., Masson, L., Mazza, A., Brousseau, R., & Adang, M. J. (1997). The *Heliothis virescens* 170 kDa aminopeptidase functions as "receptor A" by mediating specific *Bacillus thuringiensis* Cry1A delta-endotoxin binding and pore formation. *Insect Biochem. Mol. Biol., 27*(8-9), 735-743.
Ma, G., Rahman, M. M., Grant, W., Schmidt, O., & Asgari, S. (2012). Insect tolerance to the crystal toxins Cry1Ac and Cry2Ab is mediated by the binding of monomeric toxin to lipophorin glycolipids causing oligomerization and sequestration reactions. *Dev Comp Immunol, 37*(1), 184-192. doi: 10.1016/j.dci.2011.08.017
Ma, G., Roberts, H., Sarjan, M., Featherstone, N., Lahnstein, J., Akhurst, R., & Schmidt, O. (2005). Is the mature endotoxin Cry1Ac from Bacillus thuringiensis inactivated by a coagulation reaction in the gut lumen of resistant Helicoverpa armigera larvae? *Insect Biochem Mol Biol, 35*(7), 729-739. doi: 10.1016/j.ibmb.2005.02.011
Maeda, K., Takemura, M., Umemori, M., & Adachi-Yamada, T. (2008). E-cadherin prolongs the moment for interaction between intestinal stem cell and its progenitor cell to ensure Notch signaling in adult Drosophila midgut. *Genes Cells, 13*(12), 1219-1227. doi: 10.1111/j.1365-2443.2008.01239.x

Mao, Y. B., Cai, W. J., Wang, J. W., Hong, G. J., Tao, X. Y., Wang, L. J., . . . Chen, X. Y. (2007). Silencing a cotton bollworm P450 monooxygenase gene by plant-mediated RNAi impairs larval tolerance of gossypol. *Nat. Biotechnol., 25*(11), 1307-1313. doi: 10.1038/nbt1352

Martinez-Ramirez, A. C., Gould, F., & Ferre, J. (1999). Histopathological effects and growth reduction in a susceptible and a resistant strain of *Heliothis virescens* (Lepidoptera : Noctuidae) caused by sublethal doses of pure Cry1A crystal proteins from *Bacillus thuringiensis*. *Biocontrol Sci. Technol., 9*(2), 239-246.

Martins, E. S., Monnerat, R. G., Queiroz, P. R., Dumas, V. F., Braz, S. V., de Souza Aguiar, R. W., . . . Ribeiro, B. M. (2010). Midgut GPI-anchored proteins with alkaline phosphatase activity from the cotton boll weevil (*Anthonomus grandis*) are putative receptors for the Cry1B protein of *Bacillus thuringiensis*. *Insect Biochem. Mol. Biol., 40*(2), 138-145. doi: 10.1016/j.ibmb.2010.01.005

Masumura, M., Satake, S., Saegusa, H., & Mizoguchi, A. (2000). Glucose stimulates the release of bombyxin, an insulin-related peptide of the silkworm *Bombyx mori*. *Gen. Comp. Endocrinol., 118*(3), 393-399. doi: 10.1006/gcen.1999.7438

Mathur, D., Bost, A., Driver, I., & Ohlstein, B. (2010). A transient niche regulates the specification of *Drosophila* intestinal stem cells. *Science, 327*(5962), 210-213. doi: 10.1126/science.1181958

McNall, R. J., & Adang, M. J. (2003). Identification of novel *Bacillus thuringiensis* Cry1Ac binding proteins in *Manduca sexta* midgut through proteomic analysis. *Insect Biochem. Mol. Biol., 33*(10), 999-1010.

Mehrabadi, M., & Bandani, A. R. (2011). Secretion and formation of perimicrovillar membrane in the digestive system of the Sunn pest, Eurygaster integriceps (Hemiptera: Scutelleridae) in response to feeding. *Arch. Insect Biochem. Physiol., 78*(4), 190-200. doi: 10.1002/arch.20452

Micchelli, C. A., & Perrimon, N. (2006). Evidence that stem cells reside in the adult *Drosophila* midgut epithelium. *Nature, 439*(7075), 475-479. doi: 10.1038/nature04371

Micchelli, C. A., Sudmeier, L., Perrimon, N., Tang, S., & Beehler-Evans, R. (2011). Identification of adult midgut precursors in *Drosophila*. *Gene Expr. Patterns, 11*(1-2), 12-21. doi: 10.1016/j.gep.2010.08.005

Nagasawa, H., Kataoka, H., Hori, Y., Isogai, A., Tamura, S., Suzuki, A., . . . et al. (1984). Isolation and some characterization of the prothoracicotropic hormone from *Bombyx mori*. *Gen. Comp. Endocrinol., 53*(1), 143-152.

Ning, C., Wu, K., Liu, C., Gao, Y., Jurat-Fuentes, J. L., & Gao, X. (2010). Characterization of a Cry1Ac toxin-binding alkaline phosphatase in the midgut from *Helicoverpa armigera* (Hubner) larvae. *J. Insect Physiol., 56*(6), 666-672. doi: 10.1016/j.jinsphys.2010.02.003

Nishiitsutsujiuwo, J., & Endo, Y. (1981). Mode of action of *Bacillus thuringiensis* delta-endotoxin - Effect on *Galleria Mellonella* (Lepidoptera, Pyralidae). *Appl. Entomol. Zool., 16*(2), 79-87.

O'Brien, L. E., Soliman, S. S., Li, X., & Bilder, D. (2011). Altered modes of stem cell division drive adaptive intestinal growth. *Cell, 147*(3), 603-614. doi: 10.1016/j.cell.2011.08.048

Ohlstein, B., & Spradling, A. (2006). The adult Drosophila posterior midgut is maintained by pluripotent stem cells. *Nature, 439*(7075), 470-474. doi: 10.1038/nature04333

Ohlstein, B., & Spradling, A. (2007). Multipotent *Drosophila* intestinal stem cells specify daughter cell fates by differential Notch signaling. *Science, 315*(5814), 988-992. doi: 10.1126/science.1136606

Ohnishi, A., Hayakawa, Y., Matsuda, Y., Kwon, K. W., Takahashi, T. A., & Sekiguchi, S. (1995). Growth-blocking peptide titer during larval development of parasitized and cold-stressed armyworm. *Insect Biochem. Mol. Biol., 25*(10), 1121-1127.

Okumura, T., Takeda, K., Taniguchi, K., & Adachi-Yamada, T. (2014). βv integrin inhibits chronic and high level activation of JNK to repress senescence phenotypes in *Drosophila* adult midgut. *PLoS One, 9*(2), e89387. doi: 10.1371/journal.pone.0089387

Osman, D., Buchon, N., Chakrabarti, S., Huang, Y. T., Su, W. C., Poidevin, M., . . . Lemaitre, B. (2012). Autocrine and paracrine unpaired signaling regulate intestinal stem cell maintenance and division. *J. Cell Sci., 125*(Pt 24), 5944-5949. doi: 10.1242/jcs.113100

Palli, S. R., Ladd, T. R., Ricci, A. R., Primavera, M., Mungrue, I. N., Pang, A. S., & Retnakaran, A. (1998). Synthesis of the same two proteins prior to larval diapause and pupation in the spruce budworm, *Choristoneura fumiferana*. *J. Insect Physiol., 44*(5-6), 509-524.

Palli, S. R., & Locke, M. (1987a). Purification and characterization of three major hemolymph proteins of an insect, *Calpodes ethlius* (Lepidoptera, Hesperiidae). *Archives of Insect Biochemistry and Physiology, 5*(4), 233-244.

Palli, S. R., & Locke, M. (1987c). The synthesis of hemolymph proteins by the larval midgut of an insect *Calpodes ethlius* (Lepidoptera: Hesperiidae). *Insect Biochem., 17*(4), 561-572.

Park, J. S., Yim, Y. S., Park, S. Y., & Yoo, M. A. (2003). Expression of the *Drosophila* p38b gene promoter during development and in the immune response. *Korean J. Genet., 25*(3), 243-250.

Parthasarathy, R., & Palli, S. R. (2008). Proliferation and differentiation of intestinal stem cells during metamorphosis of the red flour beetle, *Tribolium castaneum*. *Dev. Dyn., 237*(4), 893-908. doi: Doi 10.1002/Dvdy.21475

Pauchet, Y., Muck, A., Svatos, A., Heckel, D. G., & Preiss, S. (2008). Mapping the larval midgut lumen proteome of *Helicoverpa armigera*, a generalist herbivorous insect. *J. Proteome Res., 7*(4), 1629-1639. doi: 10.1021/pr7006208

Pedersen, K. O. (1944). Fetuin, a new globulin isolated from serum. *Nature, 154*(3914), 575-575.

Penton, A., Chen, Y., Staehling-Hampton, K., Wrana, J. L., Attisano, L., Szidonya, J., . . . Hoffmann, F. M. (1994). Identification of two bone morphogenetic protein type I receptors in *Drosophila* and evidence that Brk25D is a Decapentaplegic receptor. *Cell, 78*(2), 239-250.

Perdigoto, C. N., Schweisguth, F., & Bardin, A. J. (2011). Distinct levels of Notch activity for commitment and terminal differentiation of stem cells in the adult fly intestine. *Development, 138*(21), 4585-4595. doi: 10.1242/dev.065292

Perera, O. P., Willis, J. D., Adang, M. J., & Jurat-Fuentes, J. L. (2009). Cloning and characterization of the Cry1Ac-binding alkaline phosphatase (HvALP) from Heliothis virescens. *Insect Biochem. Mol. Biol., 39*(4), 294-302. doi: 10.1016/j.ibmb.2009.01.006

Pfaffl, M. W. (2001). A new mathematical model for relative quantification in real-time RT-PCR. *Nucleic Acids Res., 29*(9), e45.

Pryor, A., & Boelen, M. (1987). A double-stranded RNA mycovirus from the maize rust Puccinia sorghi. *Can. J. Bot., 65*(11), 2380-2383.

Quan, G. X., Kim, I., Komoto, N., Sezutsu, H., Ote, M., Shimada, T., . . . Tamura, T. (2002). Characterization of the kynurenine 3-monooxygenase gene corresponding to the white egg 1 mutant in the silkworm Bombyx mori. *Mol Genet Genomics, 267*(1), 1-9. doi: 10.1007/s00438-001-0629-2

Radford, S. V., & Misch, D. W. (1971). The cytological effect of ecdysterone on the midgut cells of the flesh-fly *Sarcophaga bullata*. *J. Cell Biol., 49*(3), 702-711.

Ragab, A., Buechling, T., Gesellchen, V., Spirohn, K., Boettcher, A. L., & Boutros, M. (2011). *Drosophila* Ras/MAPK signalling regulates innate immune responses in immune and intestinal stem cells. *EMBO (Eur. Mol. Biol. Organ.) J., 30*(6), 1123-1136. doi: 10.1038/emboj.2011.4

Rahman, M. M., Roberts, H. L., Sarjan, M., Asgari, S., & Schmidt, O. (2004). Induction and transmission of *Bacillus thuringiensis* tolerance in the flour moth *Ephestia kuehniella*. *Proc. Natl. Acad. Sci. U. S. A., 101*(9), 2696-2699. doi: 10.1073/pnas.0306669101

Reddy, J. T., & Locke, M. (1990). The size limited penetration of gold particles through insect basal laminae. *J. Insect Physiol., 36*(6), 397-407.

Ren, F., Wang, B., Yue, T., Yun, E. Y., Ip, Y. T., & Jiang, J. (2010). Hippo signaling regulates *Drosophila* intestine stem cell proliferation through multiple pathways. *Proc. Natl. Acad. Sci. U. S. A., 107*(49), 21064-21069. doi: 10.1073/pnas.1012759107

Riddiford, L. M. (1994). Cellular and molecular actions of juvenile hormone. I. General considerations and premetamorphic actions. *Adv. Insect Physiol.*

Riddiford, L. M., Cherbas, P., & Truman, J. W. (2000). Ecdysone receptors and their biological actions. *Vitam Horm, 60*, 1-73.

Rosell, R. C., Davidson, E. W., Jancovich, J. K., Hendrix, D. L., & Brown, J. K. (2003). Size limitations in the filter chamber and digestive tract of nymphal and adult *Bemisia tabaci* whiteflies (Hemiptera: Aleyrodidae). *Ann. Entomol. Soc. Am., 96*(4), 544-552.

Rost, M. M. (2006). Comparative studies on regeneration of the midgut epithelium in *Lepisma saccharina* and *Thermobia domestica*. *Ann. Entomol. Soc. Am., 99*(5), 910-916. doi: Doi 10.1603/0013-8746(2006)99[910:Csorot]2.0.Co;2

Ryan, R. O., Anderson, D. R., Grimes, W. J., & Law, J. H. (1985). Arylphorin from Manduca sexta: carbohydrate structure and immunological studies. *Arch. Biochem. Biophys., 243*(1), 115-124.

Sadrud-Din, S., Loeb, M., & Hakim, R. (1996). *In vitro* differentiation of isolated stem cells from the midgut of *Manduca sexta* larvae. *J. Exp. Biol., 199*(Pt 2), 319-325.

Sadruddin, S. Y., Hakim, R. S., & Loeb, M. (1994). Proliferation and differentiation of midgut epithelial cells from *Manduca sexta*, *in vitro*. *Invertebr. Reprod. Dev., 26*(3), 197-204. doi: Doi 10.1080/07924259.1994.9672418

Satake, S., Masumura, M., Ishizaki, H., Nagata, K., Kataoka, H., Suzuki, A., & Mizoguchi, A. (1997). Bombyxin, an insulin-related peptide of insects, reduces the major storage carbohydrates in the silkworm *Bombyx mori*. *Comp. Biochem. Physiol. Part B Biochem. Mol. Biol., 118*(2), 349-357.

Scott, J. G., Michel, K., Bartholomay, L. C., Siegfried, B. D., Hunter, W. B., Smagghe, G., . . . Douglas, A. E. (2013). Towards the elements of successful insect RNAi. *J. Insect Physiol., 59*(12), 1212-1221. doi: 10.1016/j.jinsphys.2013.08.014

Shelby, K. S., & Popham, H. J. (2008). Cloning and characterization of the secreted hemocytic prophenoloxidases of Heliothis virescens. *Arch. Insect Biochem. Physiol., 69*(3), 127-142. doi: 10.1002/arch.20274

Shelby, K. S., & Webb, B. A. (1994). Polydnavirus infection inhibits synthesis of an insect plasma protein, arylphorin. *J. Gen. Virol., 75 (Pt 9)*, 2285-2292.

Shelby, K. S., & Webb, B. A. (1997). Polydnavirus infection inhibits translation of specific growth-associated host proteins. *Insect Biochem. Mol. Biol., 27*(3), 263-270.

Sheppard, C. A., & Loeb, M. J. (1992). ATP- dependent Ca2+ transport and Ca2+- ATPase activities in an enriched plasma membrane fraction from gypsy moth larval midgut tissue. *Arch. Insect Biochem. Physiol., 21*(3), 179-193.

Shivdasani, R. A., & Orkin, S. H. (1996). The transcriptional control of hematopoiesis. *Blood, 87*(10), 4025-4039.

Sievers, F., Wilm, A., Dineen, D., Gibson, T. J., Karplus, K., Li, W., . . . Söding, J. (2011). Fast, scalable generation of high- quality protein multiple sequence alignments using Clustal Omega. *Molecular systems biology, 7*(1).

Slaoui, M., & Fiette, L. (2011). Histopathology procedures: from tissue sampling to histopathological evaluation. *Methods Mol. Biol., 691*, 69-82. doi: 10.1007/978-1-60761-849-2_4

Smagghe, G. (2009). *Ecdysone: structures and functions*: Springer.

Smagghe, G., Vanhassel, W., Moeremans, C., De Wilde, D., Goto, S., Loeb, M. J., . . . Hakim, R. S. (2005a). Stimulation of midgut stem cell proliferation and differentiation by insect hormones and peptides. *Ann. N. Y. Acad. Sci., 1040*, 472-475. doi: 10.1196/annals.1327.094

Smagghe, G., Vanhassel, W., Moeremans, C., De Wilde, D., Goto, S., Loeb, M. J., . . . Hakim, R. S. (2005b). Stimulation of midgut stem cell proliferation and differentiation by insect hormones and peptides. *Ann N Y Acad Sci, 1040*, 472-475. doi: 10.1196/annals.1327.094

Smagghe, G. J., Elsen, K., Loeb, M. J., Gelman, D. B., & Blackburn, M. (2003). Effects of a fat body extract on larval midgut cells and growth of Lepidoptera. *In Vitro Cell. Dev. Biol. Anim., 39*(1-2), 8-12. doi: 10.1290/1543-706X(2003)039<0008:EOAFBE>2.0.CO;2

Smith, A. V., & Orr-Weaver, T. L. (1991). The regulation of the cell cycle during Drosophila embryogenesis: the transition to polyteny. *Development, 112*(4), 997-1008.

Sparks, M. E., Blackburn, M. B., Kuhar, D., & Gundersen-Rindal, D. E. (2013). Transcriptome of the *Lymantria dispar* (gypsy moth) larval midgut in response to infection by *Bacillus thuringiensis*. *PLoS One, 8*(5), e61190. doi: 10.1371/journal.pone.0061190

Spies, A. G., & Spence, K. D. (1985). Effect of sublethal *Bacillus thuringiensis* crystal endotoxin treatment on the larval midgut of a moth, *Manduca*: SEM study. *Tissue Cell, 17*(3), 379-394.

Spring, J., Paine-Saunders, S. E., Hynes, R. O., & Bernfield, M. (1994). *Drosophila* syndecan: conservation of a cell-surface heparan sulfate proteoglycan. *Proc. Natl. Acad. Sci. U. S. A., 91*(8), 3334-3338.

Staley, B. K., & Irvine, K. D. (2010). Warts and Yorkie mediate intestinal regeneration by influencing stem cell proliferation. *Curr. Biol., 20*(17), 1580-1587. doi: 10.1016/j.cub.2010.07.041

Takeda, M., Sakai, T., Fujisawa, Y., Narita, M., Iwabuchi, K., & Loeb, M. J. (2001). Cockroach midgut peptides that regulate cell proliferation, differentiation, and death *in vitro*. *In Vitro Cell. Dev. Biol. Anim., 37*(6), 343-347. doi: 10.1007/BF02577568

Tamura, K., Stecher, G., Peterson, D., Filipski, A., & Kumar, S. (2013). MEGA6: Molecular Evolutionary Genetics Analysis version 6.0. *Mol. Biol. Evol., 30*(12), 2725-2729. doi: 10.1093/molbev/mst197

Tanaka, S., Miyamoto, K., Noda, H., Jurat-Fuentes, J. L., Yoshizawa, Y., Endo, H., & Sato, R. (2013). The ATP-binding cassette transporter subfamily C member 2 in *Bombyx mori* larvae is a functional receptor for Cry toxins from *Bacillus thuringiensis*. *FEBS J., 280*(8), 1782-1794. doi: 10.1111/febs.12200

Tanaka, Y., & Yukuhiro, F. (1999). Ecdysone has an effect on the regeneration of midgut epithelial cells that is distinct from 20-hydroxyecdysone in the silkworm *Bombyx mori*. *Gen. Comp. Endocrinol., 116*(3), 382-395. doi: 10.1006/gcen.1999.7374

Telfer, W. H., Keim, P. S., & Law, J. H. (1983). Arylphorin, a new protein from *Hyalophora cecropia*: Comparisons with calliphorin and manducin. *Insect Biochem., 13*(6), 601-613.

Telfer, W. H., & Kunkel, J. G. (1991). The function and evolution of insect storage hexamers. *Annu. Rev. Entomol., 36*, 205-228. doi: 10.1146/annurev.en.36.010191.001225

Terenius, O., Papanicolaou, A., Garbutt, J. S., Eleftherianos, I., Huvenne, H., Kanginakudru, S., . . . Smagghe, G. (2011). RNA interference in Lepidoptera: an overview of successful and unsuccessful studies and implications for experimental design. *J. Insect Physiol., 57*(2), 231-245. doi: 10.1016/j.jinsphys.2010.11.006

Tojo, S., Liu, Y., & Zheng, Y. (2012). Dynamics of Storage Proteins in Lepidoptera. *Hemolymph Proteins and Functional Peptides: Recent Advances in Insects and Other Arthropods, 1*, 32.

Tojo, S., Nagata, M., & Kobayashi, M. (1980). Storage proteins in the silkworm, *Bombyx mori*. *Insect Biochem., 10*(3), 289-303.

Untergasser, A., Cutcutache, I., Koressaar, T., Ye, J., Faircloth, B. C., Remm, M., & Rozen, S. G. (2012). Primer3--new capabilities and interfaces. *Nucleic Acids Res., 40*(15), e115. doi: 10.1093/nar/gks596

Vilcinskas, A., & Wedde, M. (1997). Inhibition of *Beauveria bassiana* proteases and fungal development by inducible protease inhibitors in the haemolymph of *Galleria mellonella* larvae. *Biocontrol Sci. Technol., 7*(4), 591-602.

Wang, Z., Hang, S., Purdy, A. E., & Watnick, P. I. (2013). Mutations in the IMD pathway and mustard counter *Vibrio cholerae* suppression of intestinal stem cell division in *Drosophila*. *MBio, 4*(3), e00337-00313. doi: 10.1128/mBio.00337-13

Weston, C. R., & Davis, R. J. (2002). The JNK signal transduction pathway. *Curr. Opin. Genet. Dev., 12*(1), 14-21.

Wieczorek, H., Weerth, S., Schindlbeck, M., & Klein, U. (1989). A Vacuolar-Type Proton Pump in a Vesicle Fraction Enriched with Potassium Transporting Plasma-Membranes from Tobacco Hornworm Midgut. *Journal of Biological Chemistry, 264*(19), 11143-11148.

Wigglesworth, V. B. (1939). *The Principles of Insect Physiology*. London,: Methuen & co.

Wolfersberger, M., Luethy, P., Maurer, A., Parenti, P., Sacchi, F., Giordana, B., & Hanozet, G. (1987). Preparation and partial characterization of amino acid transporting brush border membrane vesicles from the larval midgut of the cabbage butterfly (Pieris brassicae). *Comparative Biochemistry and Physiology Part A: Physiology, 86*(2), 301-308.

Wood, J. L., & Harvey, W. R. (1976). Active transport of calcium across the isolated midgut of *Hyalophora cecropia*. *J. Exp. Biol., 65*(2), 347-360.

Xu, N., Wang, S. Q., Tan, D., Gao, Y., Lin, G., & Xi, R. (2011a). EGFR, Wingless and JAK/STAT signaling cooperatively maintain Drosophila intestinal stem cells. *Dev. Biol., 354*(1), 31-43. doi: 10.1016/j.ydbio.2011.03.018

Xu, N., Wang, S. Q., Tan, D., Gao, Y., Lin, G., & Xi, R. (2011b). EGFR, Wingless and JAK/STAT signaling cooperatively maintain *Drosophila* intestinal stem cells. *Dev. Biol., 354*(1), 31-43. doi: 10.1016/j.ydbio.2011.03.018

Yan, R., Small, S., Desplan, C., Dearolf, C. R., & Darnell, J. E., Jr. (1996). Identification of a *Stat* gene that functions in *Drosophila* development. *Cell, 84*(3), 421-430.

You, J., Zhang, Y., Li, Z., Lou, Z., Jin, L., & Lin, X. (2014). *Drosophila* Perlecan Regulates Intestinal Stem Cell Activity via Cell-Matrix Attachment. *Stem Cell Reports, 2*(6), 761-769. doi: 10.1016/j.stemcr.2014.04.007

Zhang, C. R., Zhang, S., Xia, J., Li, F. F., Xia, W. Q., Liu, S. S., & Wang, X. W. (2014). The immune strategy and stress response of the Mediterranean species of the *Bemisia tabaci* complex to an orally delivered bacterial pathogen. *PLoS One, 9*(4), e94477. doi: 10.1371/journal.pone.0094477

Zhang, X., Candas, M., Griko, N. B., Taussig, R., & Bulla, L. A., Jr. (2006). A mechanism of cell death involving an adenylyl cyclase/PKA signaling pathway is induced by the Cry1Ab toxin of *Bacillus thuringiensis*. *Proc. Natl. Acad. Sci. U. S. A., 103*(26), 9897-9902. doi: 10.1073/pnas.0604017103

Zhou, F., Rasmussen, A., Lee, S., & Agaisse, H. (2013). The UPD3 cytokine couples environmental challenge and intestinal stem cell division through modulation of JAK/STAT signaling in the stem cell microenvironment. *Dev. Biol., 373*(2), 383-393. doi: 10.1016/j.ydbio.2012.10.023

Zhou, X., Oi, F. M., & Scharf, M. E. (2006). Social exploitation of hexamerin: RNAi reveals a major caste-regulatory factor in termites. *Proc. Natl. Acad. Sci. U. S. A., 103*(12), 4499-4504. doi: 10.1073/pnas.0508866103

Zhou, X., Tarver, M. R., Bennett, G. W., Oi, F. M., & Scharf, M. E. (2006). Two hexamerin genes from the termite *Reticulitermes flavipes*: Sequence, expression, and proposed functions in caste regulation. *Gene 376*(1), 47-58. doi: 10.1016/j.gene.2006.02.002

Zhu, Y. C., Muthukrishnan, S., & Kramer, K. J. (2002). cDNA sequences and mRNA levels of two hexamerin storage proteins PinSP1 and PinSP2 from the Indianmeal moth, *Plodia interpunctella*. *Insect Biochem. Mol. Biol., 32*(5), 525-536.

Zhuang, M., Oltean, D. I., Gomez, I., Pullikuth, A. K., Soberon, M., Bravo, A., & Gill, S. S. (2002). *Heliothis virescens* and *Manduca sexta* lipid rafts are involved in Cry1A toxin binding to the midgut epithelium and subsequent pore formation. *J. Biol. Chem., 277*(16), 13863-13872. doi: 10.1074/jbc.M110057200

Žitňan, D., Šauman, I., & Sehnal, F. (1993). Peptidergic innervation and endocrine cells of insect midgut. *Arch. Insect Biochem. Physiol., 22*(1-2), 113-132. doi: 10.1002/arch.940220110

Appendix 1

Development of an RNA interference protocol for silencing gene expression in *Heliothis virescens*

Abstract

Heliothis virescens, belonging to the order Lepidoptera, is one of the most destructive agriculturally important pests worldwide. *H. virescens* eggs are deposited on the blossoms and fruit structures of preferred host plants, which allows emerging neonate larvae to begin feeding immediately. The continuous feeding pattern during larval development, results in extensive crop damage and significant monetary loss world-wide. The Cry1Ac toxin produced by the bacterium *Bacillus thuringiensis* is the most active Cry toxin against *Heliothis virescens*, our insect model to study the Cry1Ac mode of toxicity.

RNAi-mediated gene silencing has rapidly emerged as an efficacious technique that allows for sequence-specific down-regulation of target protein expression in several organisms. Upon the detection of cytosolic double-stranded RNA (dsRNA), the ribonuclease Dicer cleaves dsRNA molecules into short 20-25 base-pair duplexes and initiates the formation of the RNA-Induced Silencing Complex (RISC). The assembled RISC uses one strand of the dsRNA duplex as a guide to locate and degrade the complementary mRNA, resulting in the reduced translation of the target protein. The primary objective of this research is to develop an RNAi protocol to investigate the significance of *Heliothis virescens* midgut alkaline phosphatase (HvmALP) as a functional receptor in the Cry1Ac toxin mode of action, by, first, investigating the effectiveness of physiologically different dsRNA delivery strategies. Second, we will make direct correlations between reduced expression of HvmALP and resistance to Cry1Ac exposure. It is our expectation that dsRNA targeting HvmALP *in vivo* will result in increased resistance to Cry1Ac, thereby reinforcing the role of HvmALP as a Cry1Ac receptor. These results will enhance our understanding of the Cry1Ac intoxication process and evaluate the effectiveness of dsRNA delivery strategies for RNAi-based insect pest control in the next generation of transgenic crop technologies.

A1.1 Introduction

Genes encoding Insecticidal crystal (Cry) toxins produced by the bacterium *Bacillus thuringiensis* (Bt) are the most effective traits in genetically engineered crops used to control insect pests worldwide (James 2010). It is generally accepted that the Cry toxin mode of action begins with crystal ingestion by susceptible insects, followed by solubilization and proteolytic activation in the alkaline conditions of the host midgut (Gomez et al. 2014; Hofmann et al. 1988). In the most commonly proposed Bt mechanism of toxicity, activated toxin monomers traverse the peritrophic matrix and bind to cadherin proteins localized on the apical brush border membrane of the intestinal epithelium, resulting in proteolytic cleavage of helix α-1 from domain I and monomer oligomerization into pre-pore structures (Gomez et al. 2002). Toxin oligomers then bind with high-affinity to GPI-anchored aminopeptidase-N (APN) (Luo et al. 1997), or membrane alkaline phosphatase (HvmALP) (Jurat-Fuentes and Adang 2004) concentrated on membrane lipid rafts. Binding with these receptors facilitates membrane insertion of the toxin oligomers, resulting in death by osmotic shock (Zhuang et al. 2002). In an alternative mechanism, Cry toxins monomers binding to cadherin activates adenylyl cyclase/PKA – dependent intracellular signaling resulting in cell death, characterized by cellular features commonly associated with oncosis (Zhang et al. 2006). More recently, ATP-binding cassette transporter subfamily C2 (ABCC2) proteins has been proposed as Cry toxin receptors (Tanaka et al. 2013), although the mechanistic role of Cry-ABCC2 interactions in enterocyte death has not been resolved to date .

To date, mALP has been reported as a Cry toxin receptor in Lepidoptera (Krishnamoorthy et al. 2007; McNall and Adang 2003; Ning et al. 2010), Diptera (Fernandez et al. 2006; Hua et al. 2009), and Coleoptera (Martins et al. 2010). Furthermore, Cry toxin resistant *H. virescens* strains have been reported to express reduced levels of HvmALP (Jurat-Fuentes, Karumbaiah et al. 2011), supporting that hypothesis that HvmALP is important for

susceptibility to Cry toxins.

To further investigate the role of HvmALP in the Cry toxin mode of action in *H. virescens*, we sought to develop a protocol using RNA interference (RNAi) to post-transcriptionally silence *H. virescens* mALP (HvmALP) in susceptible larvae. RNAi-mediated gene silencing relies on the delivery of double-stranded RNA (dsRNA) duplexes into the cytoplasm of target cells and the subsequent degradation of their complementary mRNA mediated by the ribonuclease, Dicer, the RNA-induced silencing complex (RISC), and RISC-associated argonaute (Fire et al. 1998). To date, RNAi-mediated gene silencing has been successfully utilized to investigate gene functionality in a number of lepidopteran insects (Terenius et al. 2011). Conversely, attempts to induce gene silencing using RNAi in *H.* virescens have been met with limited success. Using invasive and non-invasive delivery strategies, we demonstrated that RNAi can significantly reduce levels of HvmALP in *H. virescens* larvae and, furthermore, that variable target gene expression plays a critical role in consistently achieving significant degrees of gene silencing.

A1.2 Materials and methods

A1.2.1 Insects

H. virescens eggs were purchased from Benzon Research Inc. (Carlisle, PA). After hatching, larvae were maintained on artificial diet (BioServ, Frenchtown, NJ) under standard rearing conditions of a 16-h light 8-h dark photoperiod at 26°

A1.2.2 Bacterial toxin purification

Bacillus thuringiensis var. *kurstaki* strain HD73 producing Cry1Ac toxin was obtained from the *Bacillus* Genetic Stock Center (BGSC, Columbus, OH). Bacterial inoculation, toxin purification, activation and verification were performed as previously described (Perera, Willis et

al. 2009). Purified activated toxin was quantified by the method of Bradford (Bradford 1976), using the Coomassie Plus Protein Assay (Pierce) with BSA as the standard.

A1.2.3 Preparation of double stranded RNA (dsRNA)

A 539 bp conserved internal region of five *H. virescens* midgut alkaline phosphatase (HvmALP) transcripts (accession numbers: FJ416470.1, FJ416471.1, FJ416472.1, FJ416473.1, EF531619.1) was amplified from *H. virescens* midgut cDNA with the primers T7ALP1 and T7ALP2 (Table 4) using Platinum® Blue PCR SuperMix (Invitrogen™). After 1% agarose gel electrophoresis of the PCR product, the band was excised and purified with the QIAquick Gel Extraction Kit (Qiagen, Valencia, CA) according to the manufacturer's instructions. The cDNA template for *in vitro* transcription of HvmALP was generated from the purified PCR product using gene-specific primers (Table 4) flanked on the 5' ends by the T7 RNA polymerase promoter sequence. A 441 bp region of cycle 3 green fluorescent protein (GFP) was amplified from pIZT/V5-His (Invitrogen™) with the primers T7GFPF and T7GFPR and used as a negative control template. Double stranded RNA (dsRNA) was prepared with the TranscriptAid T7 High Yield Transcription Kit (Thermo Scientific, Kalamazoo, MI) according to the manufacturer's instructions. Following transcription, 2 μL of DNase I (Thermo Scientific) was added directly to each reaction and the tubes were incubated at 37°C for an additional 15 minutes. DNase I was deactivated by adding 2 μL of 0.5 M EDTA pH 8.0 (Thermo Scientific) and incubating at 65°C for 10 minutes. DsRNA duplexes were precipitated with 7.5 M lithium chloride precipitation solution (Ambion) according to the manufacturer instructions and solubilized in 0.1% DEPC-treated deionized water. An aliquot of each dsRNA preparation was diluted 300-fold and measured with a NanoDrop 2000 spectrophotometer (Thermo Scientific) to determine 260/280 absorbance ratios and concentration. To confirm the structural integrity of the dsRNA duplexes, we subjected an aliquot of each construct to RNase A degradation in Saline-Sodium Citrate

buffer (SSC) as previously described (Pryor and Boelen 1987). Purified dsRNAs were stored at -70°C until they were used in insect bioassays.

A1.2.4 RNA interference (RNAi) of alkaline phosphatase (HvmALP)

For RNAi silencing bioassays by feeding, 100 μL of artificial diet (tobacco budworm diet, BioServ) was dispensed into the wells of polystyrene flat bottom 96-well plates (Fisher Scientific) using a multichannel pipette. After diet solidification, 10 μL of a 2.5 μg/μL dilution of dsGFP, or dsALP was applied on the surface using a pipette and allowed to dry in a laminar flow cabinet. Upon drying, a single neonate larva was placed in each well, and the wells were covered with polyurethane gas-permeable Breath-Easy® Membranes (MIDSCI, St. Louis, MO). Larvae were then allowed to feed on diet containing dsRNA for five days under standard rearing conditions. After five days, larvae were flash frozen in liquid nitrogen (LN_2) or transferred to freshly prepared artificial diet that had been overlaid with 75 μL of activated Cry1Ac toxin (45 $\mu g/cm^2$) or control diet overlaid with buffer. The numbers of dead and surviving larvae were monitored for seven days.

For microinjection of dsRNAs, 3rd instar *H. virescens* larvae received an intrahemocoelic injection of 1.0 or 3.0 μg of purified dsRNA duplexes targeting GFP (dsGFP) or HvmALP (dsALP). After injection, a single larva was placed in each well of a 128-well bioassay tray (Bio-Serv, Flemington, NJ) containing artificial diet and maintained under standard rearing conditions for two days. After two days, individual midguts were dissected and flash frozen in liquid nitrogen (LN_2) and stored at -70°C.

A1.2.5 Preparation of midgut total RNA (tRNA) and protein

Total midgut protein was prepared from individual larvae microinjected with control diethylpyrocarbonate (DEPC) ddH_20, (dsGFP) and experimental (dsALP) treatments using

TRI® Reagent (MRC, Cincinnati, OH) and quantified using the 2D Quant Kit (GE Healthcare Bio-Sciences, Pittsburgh, PA).

A1.2.6 Preparation of brush border membrane vesicles (BBMV)

Pooled larvae were used for BBMV preparation by the $MgCl_2$ precipitation method (Wolfersberger, Luethy et al. 1987). Larvae were homogenized in 500 μL SET buffer (250 mM sucrose, 5 mM EGTA, 17 mM Tris-HCL pH 7.5) with Complete protease inhibitors (Pierce) for 30 seconds with a Brinkmann Polytron PT-2100 homogenizer (Kinematica Inc., Bohemia, NY). An equivalent volume of ice-cold 24 mM $MgCl_2$ 250 mM sucrose was added to the homogenate, followed by incubation on ice for 15 minutes. Homogenates were centrifuged at 4,600 rpm for 15 minutes at 4°C to pellet debris. Supernatants were collected and centrifuged at maximum speed in a microcentrifuge for 20 minutes at 4°C. BBMV pellets were re-suspended in 30-40 μL phosphate buffered saline (PBS) pH 7.5 with protease inhibitors and quantified by the method of Bradford.

A1.2.7 Electrophoresis and Western blotting

Total midgut (30 μg) and BBMV proteins were resolved by SDS-10% PAGE and electrotransfered overnight at 4°C to PVDF Immobilon-P filters (Millipore) using 20 mV constant voltage. Filters were blocked by incubating in blocking buffer (PBS pH 7.4, 0.1% Tween-20, 3% BSA) for one hour at room temperature, and then probed with rabbit antisera (1:10,000 dilution in blocking buffer) against *Anopheles gambiae* (mosquito) midgut alkaline phosphatase (accession number XM308522). After washing filters 6 times (10 min per wash) in washing buffer (PBS pH 7.4, 0.1% Tween-20, 0.1% BSA), they were probed with a 1:20,000 dilution of anti-rabbit antisera conjugated to horseradish peroxidase (HRP) in washing buffer for one hour. Filters were then washed as previously and developed using the SuperSignal™ West Pico

chemiluminescence substrate (Pierce) followed by exposure to photographic film.

A1.2.8 Real-time quantitative PCR (RT-qPCR)

Total midgut RNA was prepared from individual larvae from control (dsGFP) and experimental (dsALP) treatment groups using TRIzol® Reagent (Ambion), according to the manufacturer instructions. Total RNAs were incubated at 37°C for 15 minutes in 1X DNase buffer (10 mM Tris-HCL pH 7.5, 2.5 mM $MgCl_2$, 0.1 mM $CaCl_2$) containing one unit of DNase I (Thermo Scientific) to remove contaminating genomic DNA. After inactivation of DNase I with 31 mM, 0.5 M EDTA, pH 8.0 (Thermo Scientific) and incubating at 65°C for 10 minutes, total RNAs were precipitated with 7.5 M lithium chloride (Ambion) and then solubilized in 0.1 % DEPC-treated deionized water. Upon quantification in a NanoDrop spectrophotometer, total RNA from individual larvae (50 ng) was used for first strand cDNA synthesis with the High Capacity cDNA Reverse Transcription Kit (Applied Biosystems), according to the manufacturer instructions. The resulting cDNAs were quantified with a NanoDrop spectrophotometer.

Relative quantities of target and reference gene transcripts in individual templates were measured in a 7900HT Fast Real-Time PCR System (Applied Biosystems) in standard mode using SDS 2.3 and SDS RQ manager software to collect threshold cycle (C_t) values for individual templates using the Power SYBR® Green PCR Master Mix. All primers used in RT-qPCR are listed in Table 4. A multiple sequence alignment was constructed and degenerate primers targeting the GPI-anchor region of five HvmALP isoforms were designed using MEGA version 6.06 (Tamura, Stecher et al. 2013). A *H. virescens* α-tubulin transcript from the transcriptome, exhibiting a high degree of similarity to *Xestia cnigrum* α-tubulin (accession number EU100015), was used as a reference gene in the relative quantification calculations. The target gene fold expression level in each template was calculated with triplicate threshold cycle (C_t) values normalized to a reference gene (α-tubulin) according to the method of Pfaffl

(Pfaffl 2001).

A1.3 Results

A1.3.1 RNAi reduces HvmALP expression in *H. virescens* larvae but not Cry1Ac toxicity.

Since feeding dsRNA is non-invasive and relevant to the potential development of future technologies utilizing the expression of coleopteran (Baum et al. 2007) and lepidopteran (Mao et al. 2007) specific dsRNAs in transgenic plants, we tested whether feeding on high dsRNA dosages (25 μg) of dsALP would be potent enough to induce gene silencing in newly emerged neonates (Fig. 13). Ingesting dsALP significantly reduced detection of alkaline phosphatase in dsALP pool #3 (Lane 6, Fig. 13), relative to dsGFP treated controls (Fig. 13, Lanes 2-3) and *H. virescens* BBMV used as a positive control (Fig. 13, Lane 1). These results support that oral delivery of high dsRNA dosages is able to induce silencing target genes in the *H virescens* midgut epithelium, albeit at a low rate of success.

Since reduced expression of mALP has been observed in Cry toxin resistant *H. virescens*, *H. armigera* and *Spodoptera frugiperda* (fall armyworm) strains (Jurat-Fuentes, Karumbaiah et al. 2011), and silencing of *M. sexta* alkaline phosphatase significantly reduced toxicity of Cry1Aa, Cry1Ab, and Cry1Ac (Flores-Escobar et al. 2013), we sought to test the effects of silencing HvmALP would have on susceptibility to Cry1Ac in *H. virescens* larvae. We observed no significant increase in the percentage of dsALP-treated larvae that survived on diet coated with Cry1Ac relative to dsGFP-treated larvae, suggesting that the RNAi mechanism was not induced or that silencing HvmALP was not sufficient to reduce the toxic effects of Cry1Ac on the midgut epithelium (Fig 14, top panel).

Similarly, because arylphorins have been associated with the immune response to Cry intoxication (Castagnola 2011; Hernandez-Martinez, Navarro-Cerrillo et al. 2010), we tested the effects of α-arylphorin silencing on susceptibility toCry1Ac in *H. virescens*. No significant

changes in larval susceptibility to Cry1Ac were observed for silenced larvae relative to controls, suggesting again that silencing of α-arylphorin was not induced by ingesting dsRNA or that silencing was induced but insufficient to cause significant changes in Cry1Ac susceptibility (Fig. 14, bottom panel).

A1.3.2 Quantification of HvmALP expression in *H. virescens*

In order to determine if ingesting dsRNA targeting HvmALP induced gene silencing without affecting Cry1Ac resistance in *H. virescens* larvae, total RNA was extracted from dsGFP (control) and dsALP treated larvae feeding on diet coated with buffer and used to prepare cDNA for analysis of HvmALP transcript abundance. RT-qPCR analysis showed no significant difference in HvmALP expression in dsALP-treated larvae relative to control larvae treated with dsGFP, suggesting that feeding on dsALP did not induce silencing of HvmALP at the time of analysis (Fig. 15).

A1.3.3 Microinjection of dsALP reduces HvmALP expression in *H. virescens*

An alternative mechanism of inducing RNAi-mediated gene silencing that we tested utilized microinjection of dsRNA duplexes into the hemocoel of 3rd instar larvae. In support of this technique, the first reports of gene silencing by RNAi in Lepidoptera utilized microinjection of dsRNA duplexes in *Bombyx mori* (silkworm) larvae (Quan et al. 2002) and *Hyalophora cecropia* (cecropia moth) pupae (Bettencourt et al. 2002). To test the efficacy of systemic RNAi, we performed intrahemocoelic injections of dsALP duplexes (1 or 3 μg) into 3rd instar *H. virescens*. After 48 hours, we extracted total RNA and protein. Total RNA was stored and -70°C and proteins were prepared for Western blot analysis.

A significant and dose-dependent reduction in HvmALP was detected in Western blots of total midgut protein from individual larvae (Fig. 16). Relative to the control group (DEPC

microinjected), HvmALP was drastically reduced in the midguts of larvae injected with 1 μg and 3 μg of dsALP after 48 hours suggesting that the systemic method of inducing RNAi was highly effective in silencing target genes expressed in the *H. virescens* midgut. Antisera to HvmALP also detected a band of approximately 45-kDa, which we believe to represent mild protein degradation resulting from the phenol-based protein extraction protocol.

A1.3.4 Discussion

RNAi-based strategies of transiently silencing target gene expression in numerous model insect systems have rapidly emerged as go-to reverse genetic approaches of elucidating gene functionality (Terenius, Papanicolaou et al. 2011). Moreover, the sequence-specific silencing induced by RNAi makes it an attractive feature to incorporate in the next generation of transgenic technologies for insect pest management. It has already been shown that corn genetically modified to express dsRNA targeting *Diabrotica virgifera virgifera* (western corn rootworm, WCR) vacuolar-ATPase (V-ATPase) significantly reduces WCR feeding damage (Baum, Bogaert et al. 2007). Similarly, *M. sexta* CYP6B46 dsRNAs expressed in *Nicotiana attenuata* (coyote tobacco) suppressed expression in larval midguts upon ingestion of plant material (Kumar et al. 2012). In this study, we tested the efficacy of different dsRNA delivery methods to induce silencing of *H. virescens* HvmALP and arylphorin, proteins with a putative role in Cry intoxication in that insect. Our results suggest that the RNAi mechanism can be used to induce transient silencing of target genes in *H. virescens*.

Inducing gene silencing through the ingestion of dsRNA duplexes is a preferred method for examining the efficacy of RNAi-mediated silencing, due to a lack of invasiveness and a resemblance to natural feeding behaviors of insects. However, there are physiological differences in gut morphology across lepidopteran species as well as unique traits, including the production of dsRNA-degrading enzymes (Arimatsu et al. 2007; Liu et al. 2012) that potentially

attenuate the gene silencing potency of ingested dsRNAs (Terenius, Papanicolaou et al. 2011). Utilizing a high-dosage approach, we allowed *H. virescens* neonates to feed on 25 μg of dsALP for five days, before assessing knockdown of HvmALP in BBMV. Significant repression of HvmALP expression was only observed in a fraction of samples analyzed (approximately 33%). However, within the samples exhibiting knockdown, there was usually a significant reduction in HvmALP.

Ingesting dsALP or dsArylphorin prior to exposure to diet coated with Cry1Ac did not increase resistance of larvae to Cry1Ac. Given the low percentage of knockdown obtained in feeding assays, results from the toxicity assay support that HvmALP may have only been reduced in a small a percentage of larvae. It is plausible that functional redundancy among Cry toxin receptors may have masked any RNAi-induced repression of HvmALP, thereby resulting in toxicity in the absence of the down-regulated protein. Cry1Aa has been shown to exhibit similar dependencies on *M. sexta* APN and ALP (MsAPN and msALP) (Flores-Escobar, Rodriguez-Magadan et al. 2013). It was expected that knockdown of α-arylphorin would potentially accelerate the onset of Cry1Ac toxicity, given it's role in midgut healing. However, we did not observe any significant differences in the mortality rates among treatment groups. We may have observed a significantly different effect between treatment groups if we had temporarily exposed the insects to Cry1Ac, then allowed them to recover on untreated diet. Under these circumstances, a reduction in α-arylphorin may have lead to a slower rate of epithelial healing relative to controls. Analysis of HvmALP transcript abundance in dsGFP and dsALP treated larvae placed on control diet in our toxicity bioassays strongly supports variable expression levels within the susceptible *H. virescen*s stain used for our studies. It cannot be ruled out at this time that the high-dose strategy for delivering large quantities of dsRNA during feeding bioassays actually elicits an immune response that upregulates HvmALP expression relative to controls.

Despite the potential of eliciting an immune while penetrating the insect body, microinjection techniques have been the most frequently used techniques for inducing RNAi-mediated gene silencing (Scott et al. 2013). In our microinjection experiments, we detected the greatest reduction in HvmALP expression, while using a much smaller dsRNA dosage, suggesting that hemocoelic delivering of dsRNAs is the most efficient method for silencing target genes in *H. virescens*. Future work should test the effect of silencing by injection of HvmALP and arylphorin on susceptibility to Cry1Ac toxin.

In this work, we have demonstrated a potential for exploiting the RNAi mechanism in *H. virescens*, an insect many consider refractory to this method of post-transcriptional gene silencing. In doing so, we were also able to probe the role of HvmALP in the Cry toxin mode of action using two of the most commonly employed strategies for activating the RNAi response. While our data on the HvmALP role in Cry1Ac toxicity is inconclusive, our limited success inducing an RNAi response in *H. virescens* strongly suggests that optimization of dsRNA delivery protocols in the future will require precise dosage and length of dsRNA treatment. Anatomical and physiological barriers, such as the midgut epithelium and the biochemical environment of the lumen, likely impacted the consistency of reducing HvmALP in our feeding bioassays, but these barriers can be circumvented in future efforts that involve optimization of dosages for use with microinjections as well as performing microinjections during embryonic development rather than in insects that are midway through larval development. This will also facilitate evaluating the contribution of genes involved in the Cry toxin mode of action early during larval development.

Appendix: tables and figures

Table 4: Primers used for *in vitro* synthesis of dsALP and RT-qPCR

Name	5' --- 3' Sequence	Direction
T7GFP1	TAATACGACTCACTATAGGGGGTGAAGGTGATGCTACATA	Forward
T7GFP2	TAATACGACTCACTATAGGGCATCTTCAATGTTGTGACGA	Reverse
T7ALP1	TAATACGACTCACTATAGGGGTGTCGCTGTACAGTGCCTA	Forward
T7ALP2	TAATACGACTCACTATAGGGGCACGATACCGACATCTCGTC	Reverse
HvALP1	CASCGCGCACTTCYTTATTG	Forward
HvALP2	GTAAAATYGRKGTGAATAGAGC	Reverse
HvTub1	CGGAGTCCAGATCGGTAACG	Forward
HvTub2	GGCTGGATTCCATGCTCAAG	Reverse

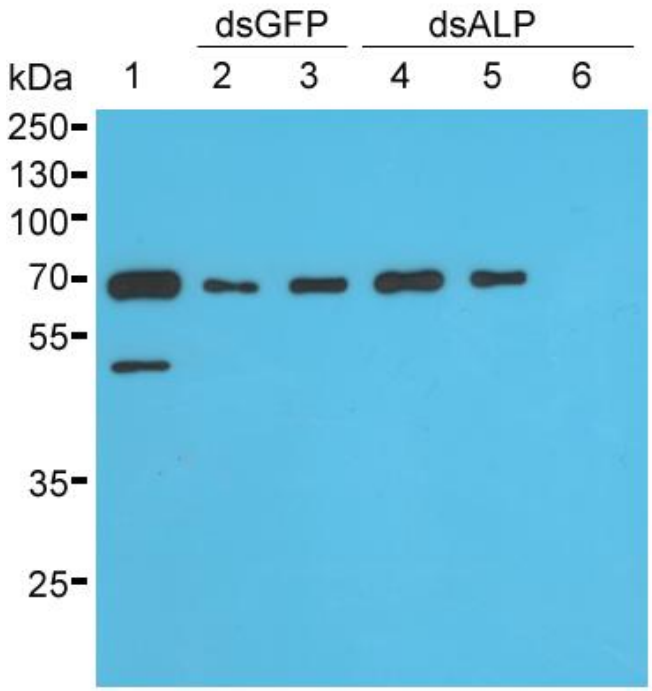
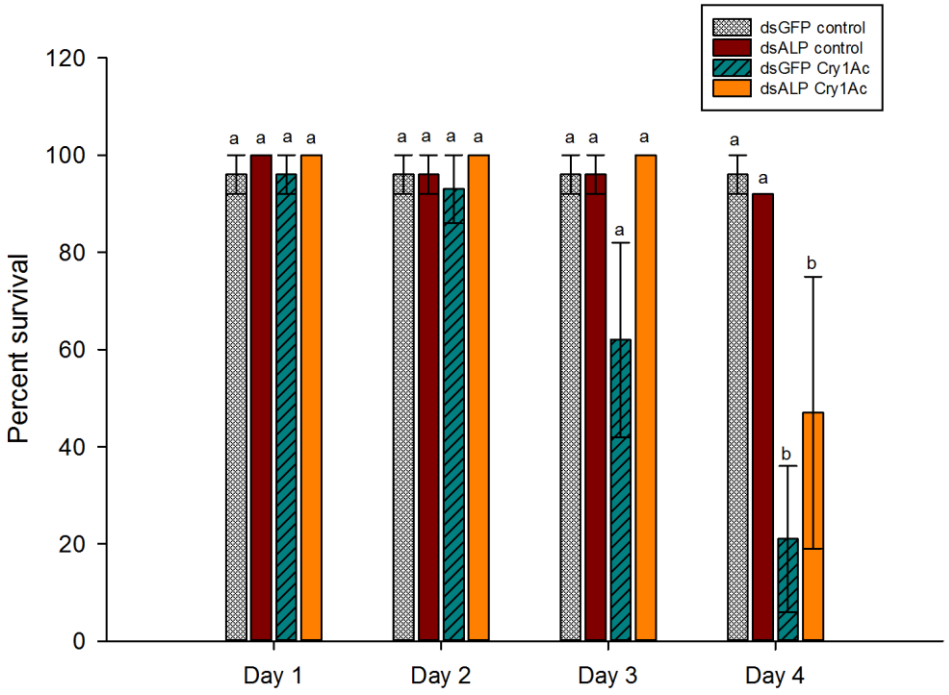


Figure 13: Analysis of dsALP ingestion effects on silencing expression of *H. virescens* mALP. BBMV proteins from pooled *H. virescens* larval midguts (n=4-6 guts per pool) were resolved by electrophoresis and transferred to PVDF Immobilon-P filters. Lane: (1) 2 μg positive control *H. virescens* BBMV, (2) 2 μg dsGFP pool #1, (3) 2 μg dsGFP pool #2, (4) 2 μg dsALP pool #1, (5) 2 μg dsALP pool #2, (6) 2 μg dsALP pool #3. To detect HvmALP, filters were incubated with αALP against *A. gambiae* (accession number XM308522).

Figure 14: Testing the effects of feeding dsALP or dsArylphorin on Cry1Ac toxicity in *H. virescens*. *H. virescens* larvae fed dsGFP (control), dsALP, or dsArylphorin for 5 days were next split into two groups. One group was transferred to diet coated with 0.5 $\mu g/cm^2$ Cry1Ac and the other group was transferred to control diet coated with buffer. Bars denote standard error of the mean for each treatment of 5-15 larvae from two (dsGFP and dsArylphorin) or three (dsGFP and dsALP) bioassay replicates; statistically significant differences between treatment groups are denoted by different letters for each column ($P < 0.05$, One-way ANOVA).



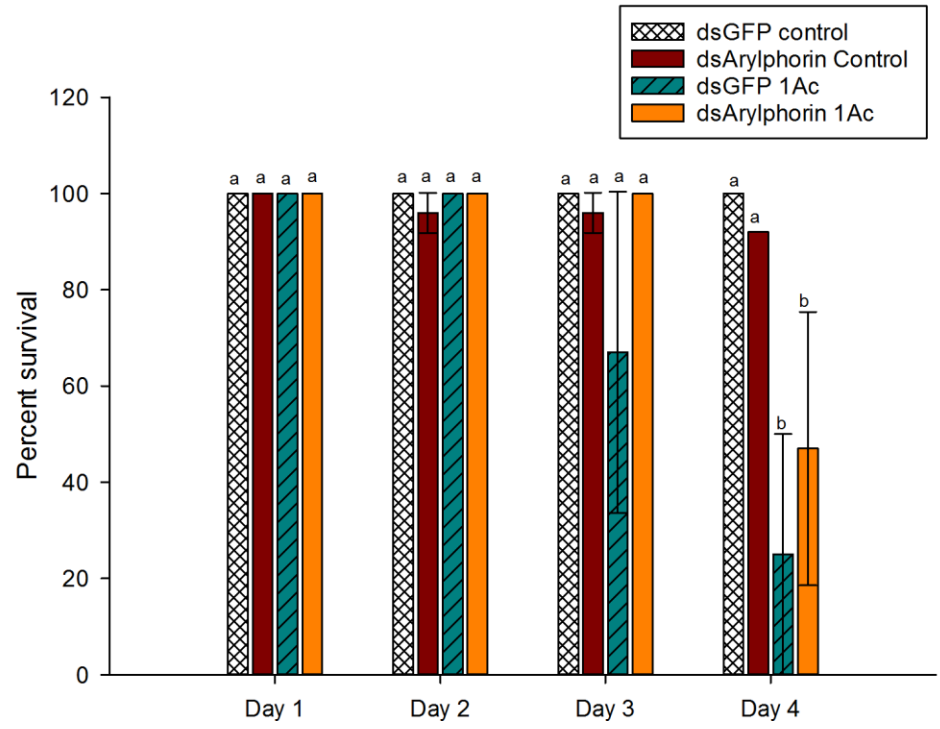


Figure 14 continued

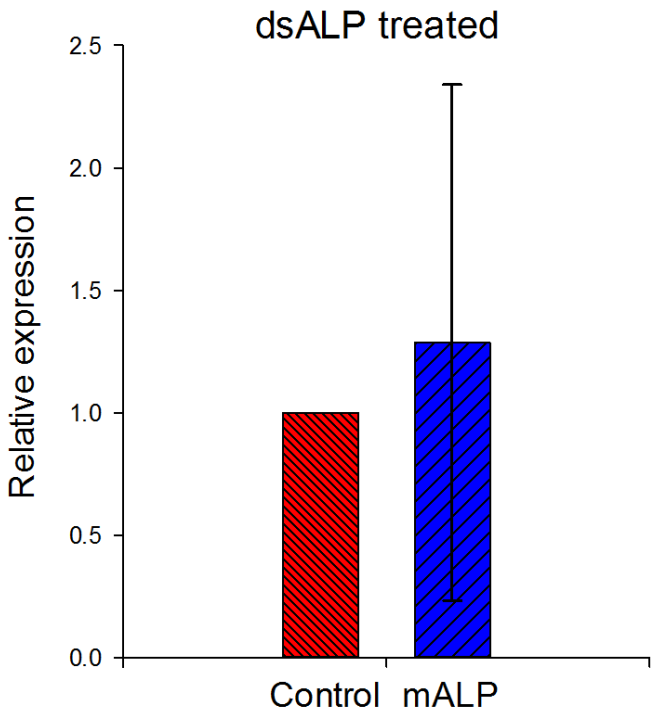


Figure 15: Analysis of HvALP transcript levels in larvae fed control and dsALP. *H. virescens* larvae were fed on diet coated with 25 μg dsALP or dsGFP for 5 days before being transferred to control diet. Bars represent standard error of the mean for n= 10 (dsGFP), and n=12 (dsALP) individual midguts.

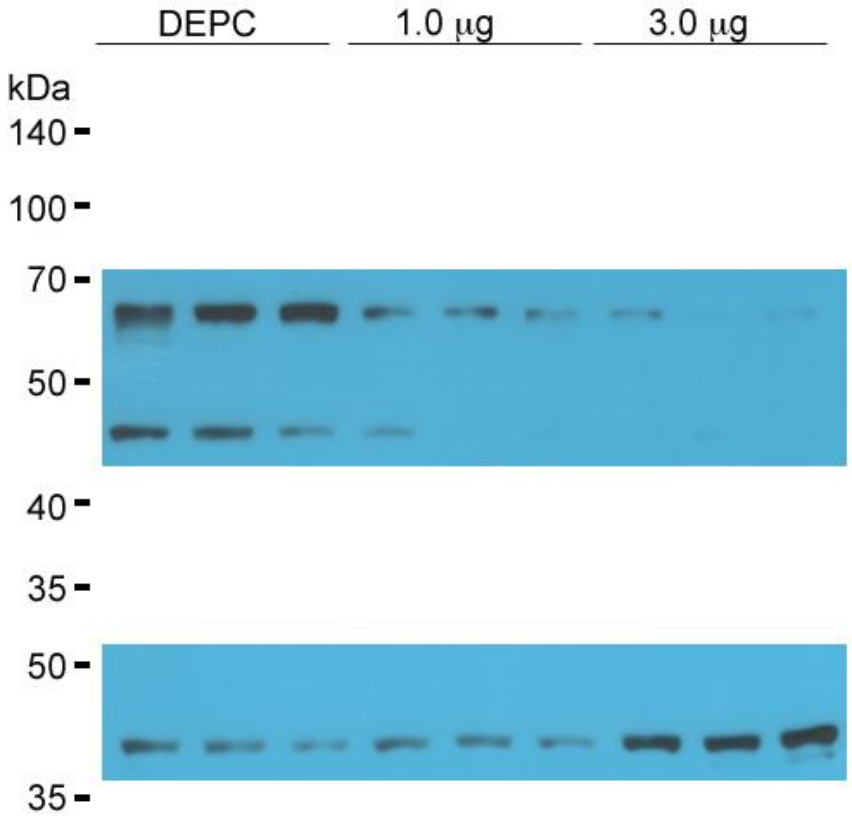


Figure 16: Microinjection of dsALP causes reduction in HvmALP expression in *H. virescens*. Western blot of total protein (30 μg) from individual 3rd instar *H. virescens* larvae microinjected with DEPC water (Lanes 1-3), 1 μg dsALP (Lanes 4-6), or 3 μg of dsALP (lanes 7-9). As a loading control, filters were probed with actin antisera.

Vita

Jerreme Jamael Jackson was born on March 30, 1980, in Lawrence, Kansas. After graduating from Lawrence High School in 1998, he received an academic scholarship and an invited walk-on position on the men's' varsity track and field team at the University of Kansas (KU) also located in Lawrence. For the first two years, he studied chemical engineering, but during his junior year he decided to major in biology. It was also during his junior year that his 9th place finish in the men's' long jump at the Big XII Track and Field Championships earned him an athletic scholarship. In 2002, he graduated from KU with a Bachelors of Science in Biology with a concentration in genetics. Following graduation, Jerreme spent six years working in the biotechnology industry, first characterizing cytochrome P450 activity in primary and immortalized hepatocytes for Xenotech L.L.C in Lenexa (KS), and then characterizing differential *in vitro* gene and protein expression in canine and feline cells lines in a genomic and proteomic laboratory at the Hill's Pet Nutrition Pet Nutrition Center in Topeka, KS. After receiving extensive hands-on laboratory training, Jerreme's interest in the scientific research was piqued, and he decided to enroll in the Genome Science and Technology graduate program at the University of Tennessee, Knoxville, in the fall of 2008. In the summer of 2009, Jerreme joined the laboratory of Dr. Juan Luis Jurat-Fuentes in the Entomology & Plant Pathology Department and studied stem cell-mediated enhanced regeneration of the intestinal epithelium of *Heliothis virescens.* In the winter of 2015, Jerreme completed his doctoral degree and currently plans on obtaining postdoctoral research experience that will expand the breadth of his training and ultimately better equip him to answer challenging scientific questions and contribute, as a tenure-track professor, to undergraduate and graduate student education.